THE DIFFUSION MECHANISM OF HYDROCARBONS IN ZEOLITES

by

Jirong Xiao
B.S., East China Institute of Chemical Technology
(1982)

Submitted to the Department of
Chemical Engineering
in Partial Fulfillment of the Requirements
for the Degree of

DOCTOR OF SCIENCE

at the

Massachusetts Institute of Technology
April, 1990

Signature of Author_____
Department of Chemical Engineering
April, 1990

Certified by_____
Professor James Wei
Thesis Supervisor

Accepted by_____
Professor William Deen
Committee for Graduate Students

THE DIFFUSION MECHANISM OF HYDROCARBONS IN ZEOLITES

by

JIRONG XIAO

Submitted to the Department of Chemical Engineering
on April 26, 1990 in partial fulfillment of the
requirements for the Degree of Doctor of Science in
Chemical Engineering

ABSTRACT

The properties of single component diffusion of hydrocarbons in zeolites, especially its dependence on temperature and concentration, are studied using both theoretical and experimental approaches. The effects of the molecule-zeolite interactions and the molecule-molecule interactions on these properties are probed. The molecule-zeolite interactions dominantly determine the orders of magnitude of the diffusivity, whereas the molecule-molecule interactions could alter the concentration dependence of the diffusivity.

The mode of translational motion of molecules in zeolites is proposed to be bounded by two extreme cases characterized by two models: (1) the Gas Translation (GT) model: molecules within the lattice retain their entity and their gaseous velocity, although the movement of molecules becomes restricted due to the energy barrier imposed by the channel system; (2) the Solid Vibration (SV) model: molecules within the lattice lose their gaseous characteristics due to the strong interactions between the zeolite framework and the molecules so that they vibrate with their host lattice before accumulating enough energy to jump. Based upon the information of zeolite structure and molecular properties, the estimation of the diffusivity can be made with no fitting parameters.

The first-order correlation function method based on a Markov stochastic model for single-file diffusion is used to analyze the concentration dependence of the diffusivity. If the interaction between molecules inside the lattice is negligible and double-occupancy of a site is excluded, a constant Fick's law diffusivity results. The isotherm under this condition is of Langmuir type. If the interaction between molecules is significant at a double-occupied site and the interaction is repulsive, a rising trend of apparent diffusivity is expected. The Langmuir parameter is of a decreasing trend.

The effects of microscopic properties of molecule-zeolite systems on the macroscopic diffusional behavior and equilibrium properties are experimentally investigated in a systematic manner. The model compounds are 19 different hydrocarbons, including paraffins, aromatics and naphthene. Zeolites include two types of ZSM-5, and 5A. The activation energy for diffusion reflects the complicated

interplay between the guest molecule and host lattice, and is mainly responsible for the different diffusivities of various compounds in ZSM-5. For some molecules in 5A, the intracrystalline partitioning is important. The diffusion coefficients of benzene, toluene, and 2-methylbutane in ZSM-5 are not dramatically influenced by the concentration up to about 4 molecules/unit cell. The isotherms are of the Langmuir type. At higher concentration, the diffusivities show strong concentration dependent trends. The Langmuir adsorption isotherm can no longer describe the equilibrium data. The rising trend of diffusivity is also observed for heptane diffusion in 5A where one cage can host two molecules.

The predictions of the proposed mechanistic models agree, in general, with the experimental results of the diffusion measurements by this study on both the orders of magnitude and the concentration dependence. The good agreement is also found between the theoretical predictions and a set of the literature data for 5A.

Thesis Supervisor: Professor James Wei
Title: Warren K. Lewis Professor of Chemical Engineering

ACKNOWLEDGMENT

I am deeply grateful to my thesis advisor, Professor James Wei, for his guidance, support, encouragement, and trust. I have benefitted from his high standard of accomplishment, his philosophy of research, his open-minded approach to new ideas, and will continue to do so in the years to come.

I would like to express my appreciation to my thesis committee members, Professor Charles N. Satterfield and Professor Adel F. Sarofim, for their valuable discussions and helpful suggestions; and to Professor Sarofim for his advice as my academic advisor during my first year at MIT.

Thanks to my colleagues and friends in our research group: Tom Mo, Waqar Qureshi, Joy Mendoza, Gordon Smith, Kirk Limbach, Barbara Smith, and Xinjin Zhao for the help they have given and the discussions we have had on research, sports, culture, politics and everything else. They have enriched my educational experience. Special thanks to Joy Mendoza for reading and commenting on part of this thesis. And thanks to Jean Bueche, Arline Benford, and Linda Mousseau for their help.

I very much appreciate the discussions on the various subjects with Zhiyou Du of Mechanical Engineering, and the comments on Chapter 2 of my thesis by Longqing Chen of Materials Science and Engineering.

Thanks also to Xiaoling and Tong Chen, Joan and Jimmy Hsia, Glen Ko, Ling Ma, Fennie Mui, and Guozhong Xie and many other friends for making my stay in Boston so enjoyable and worthwhile. It has been a lot of fun.

At the East China Institute of Chemical Technology, Shanghai, I am indebted to Professors Minheng Chen, Weikang Yuan and many others in the Department of Chemical Engineering. I am grateful to Professors Shanqiong Zhou and Rifang Pan for encouraging me to chose chemical engineering, and to Professor Weikang Yuan for recommending me to MIT.

Financial support from the Shiah Fellowship of MIT, and the National Fellowship of the Chinese Education Ministry are gratefully acknowledged.

Special thanks to Professors Guohui Qian and Zaixiang Chu of Harbin, to Mr. and Mrs. Thomas and Lily Rowen of Marblehead, and to Chao family of Summit.

Finally, and most importantly, I wish to express my deepest gratitude to my parents for their unwavering love and support, for values they have instilled in me, for their encouragement to enter the field of engineering; to my sister and her family; and to my beloved wife, Shiao-Ming, for her love, support, and motivation, to whom I dedicate this thesis.

DEDICATED TO

SHIAO-MING

TABLE OF CONTENTS

1. INTRODUCTION

1.1 Research Motivation and Objectives

Zeolites have revolutionized the chemical and the petroleum industries over the past three decades as catalysts, sorbents, and ion-exchangers. Their molecular-sized pores make it possible to engineer the industrial processes on the molecular level to achieve high selectivity of desired products in ways not observed heretofore. The development of new zeolite technology and the understanding of existing zeolite properties continue to be a challenge.

One very unique property of zeolites is their shape selectivity (Weisz and Frilette, 1960). The steric and diffusional constraints imposed by the zeolite structure can discriminate among molecules according to molecular shapes to favor the production of desirable results.

The diffusion of molecules in zeolite pores of comparable size plays an important role in the shape selective process. This still poorly understood type of diffusion has been coined "configurational diffusion" (Weisz, 1973). The selectivity of a desired product in a zeolite could be dramatically enhanced by manipulating diffusion properties and chemical kinetics (Wei, 1982). The understanding of the diffusion mechanism can thus greatly facilitate the design of zeolite catalysts.

The objective of this study is to capture the fundamentals of single component diffusion of hydrocarbons in zeolites, especially its dependence on temperature and concentration using both theoretical and experimental approaches. The specific aims

for this thesis are:

1. To propose mechanistic models capable of predicting the diffusion characteristics in zeolites based upon the understanding of the interactions between the zeolite lattice and molecules, and the interactions among molecules.

2. To examine experimentally the diffusion of hydrocarbons in zeolites, particularly in ZSM-5 and in 5A, in a systematic manner.

3. To compare the experimental results generated from this study and those reported in the literature with the predictions of the proposed models, and to delineate the diffusion characteristics in zeolites from these comparisons.

1.2 Background

Zeolites are porous, crystalline alumino-silicates. Their well-defined lattice structures contains cavities and/or channel intersections connected to each other by channels (also called windows or pores) of molecular dimensions.

1.2.1 Applications of Zeolites

Natural zeolites have been utilized in ion-exchange and sorption processes since their discovery two centuries ago by Cronstedt. The breakthrough on synthesis of zeolites thirty years ago has had a great impact on adsorption, and perhaps more importantly, catalytic process technology throughout the petroleum and chemical industries. Over the years, the utilization of synthetic zeolites has not only saved billions of dollars, but also provided a new flexibility in the design of products and

processes.

The following properties make zeolites attractive as catalysts, sorbents, and ion-exchangers (Chen, Degnan, 1988)

(1) well-defined crystalline structure

(2) high internal surface areas ($>600\ m^2/g$)

(3) uniform pores with one or more discrete sizes

(4) good thermal stability

(5) highly acidic sites when ion exchanged with protons

(6) ability to sorb and concentrate hydrocarbons.

In catalysis, the largest as well as the oldest application of zeolites is the fluidized catalytic cracking (FCC). Zeolite X was used, and soon superseded by zeolite Y due to its better catalytic stability. X,Y, and mordenite are also the most widely used zeolites for hydrocracking. ZSM-5 is used for a large number of processes. Some examples of its commercial usage are: selective cracking, dewaxing, synfuel production, xylene isomerization, toluene disproportionation, ethylbenzene synthesis, toluene alkylation with methanol, para-ethyltoluene and para-methylstyrene synthesis, and methanol-to-olefins conversion.

As adsorbents, zeolites A, X, Y, mordenite, and ZSM-5 are widely used in processes such as air separation, linear paraffin separation, drying of cracked gas, pressure swing H_2 purification, xylene separation, and removal of organics from water (Ruthven 1984).

Ion-exchange application is mainly in industrial and domestic water softening (Flanigen, 1984).

1.2.2 Shape Selectivity

The success of the above mentioned processes can be at least partially attributed in one way or another to the shape selectivity of zeolites. Three types of shape selectivity are exhibited by zeolites, as shown in Figure 1.1: reactant selectivity by discrimination among molecules according to their sizes and shapes; transition state selectivity by constraints the zeolite channel structure imposes on forming molecules during the transition stage; and product selectivity by discrimination among molecules that can leave the zeolite. Based upon these principles, some specially designed zeolites can do catalysis and separation in one step. Thus, zeolites as catalysts have opened a new avenue to direct dramatically the selectivity of catalysts by varying the geometry of the zeolite cavities and channel dimensions. The concept of "molecular engineering" in catalyst design was born (Chen, Weisz, 1967).

One typical example of a molecularly engineered catalytic process is toluene disproportionation over ZSM-5. The chemical equilibrium concentration of xylene isomers is typically about 25% para-xylene, 50% meta-xylene, and 25% ortho-xylene. Para-xylene is the most valuable product. Since the diffusivity of p-xylene is about 1000 times faster than its isomers, the production of p-xylene is then favored in the diffusion limited regime where the diffusion process of products is the rate limiting step. By the use of catalyst modifiers such as magnesium and phosphorous to block partially the entrance of zeolite pores, ZSM-5 functions not only as a catalyst, but also as a product selector. Due to the product shape selectivity, the selectivity of p-xylene can be enhanced to over 97% out of total xylene (Wei, 1982). More such examples can be found in Chen and Garwood (1986), and Chen and Degnan(1988).

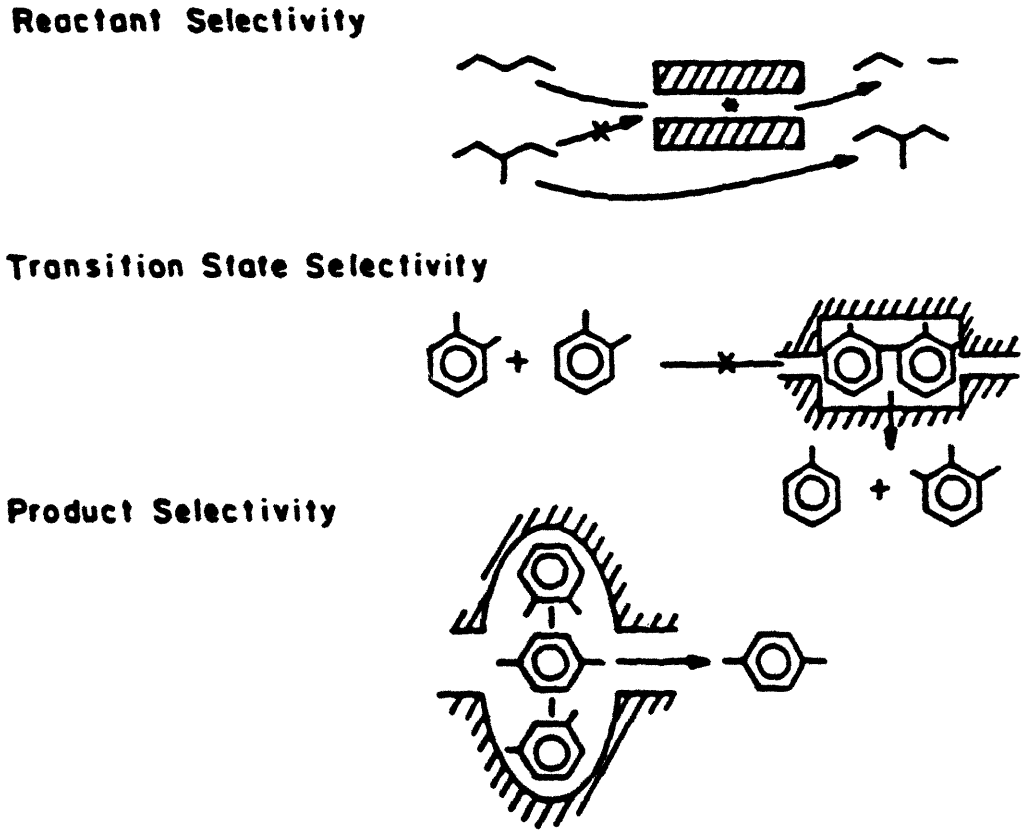

Figure 1.1 Classification of Shape-Selective Catalysis in Zeolite

1.2.3 Zeolite Structure

The primary building block of the zeolite structure is a tetrahedron of four oxygen atoms surrounding a central silicon atom. The tetrahedrons are bonded together via shared oxygen atoms to form a variety of secondary building units, which in turn generate a wide range of polyhedra. The combination of secondary building units and polyhedra forms the infinitely extended frameworks of various zeolite structures, as shown in Figure 1.2. About 60 different structures or topologies are known (Vaughan 1988). Detailed reviews on zeolite structures have been given by Breck (1974), and Barrer (1978).

The general formula to describe zeolites in terms of its unit cell is given by:

$$M_xD_y(Al_{x+2y}\ Si_{n-(x+2y)}\ O_{2n})\ MH_2O$$

where M and D respectively designate a mono- or a divalent cation to compensate the negative charge born by AlO_4^-, which determines the acidity of zeolites.

Zeolites can be classified into several groups based on channel size: 12-membered oxygen ring, large pore zeolites, such as X and Y; 10-membered ring, intermediate pore zeolites, such as ZSM-5; 8-membered ring, small pore zeolites, such as A, erionite, and chabazite; and 6-membered rings, such as solidate. The discovery of aluminophosphate materials has opened a new dimension in molecular sieves (Flanigen et al, 1986, 1988). Recently, a new aluminophosphate material with 18-membered rings has been successfully synthesized (Davis et al, 1988).

This study has selected zeolite ZSM-5 and, to a lesser extent, zeolite 5-A as the model zeolites.

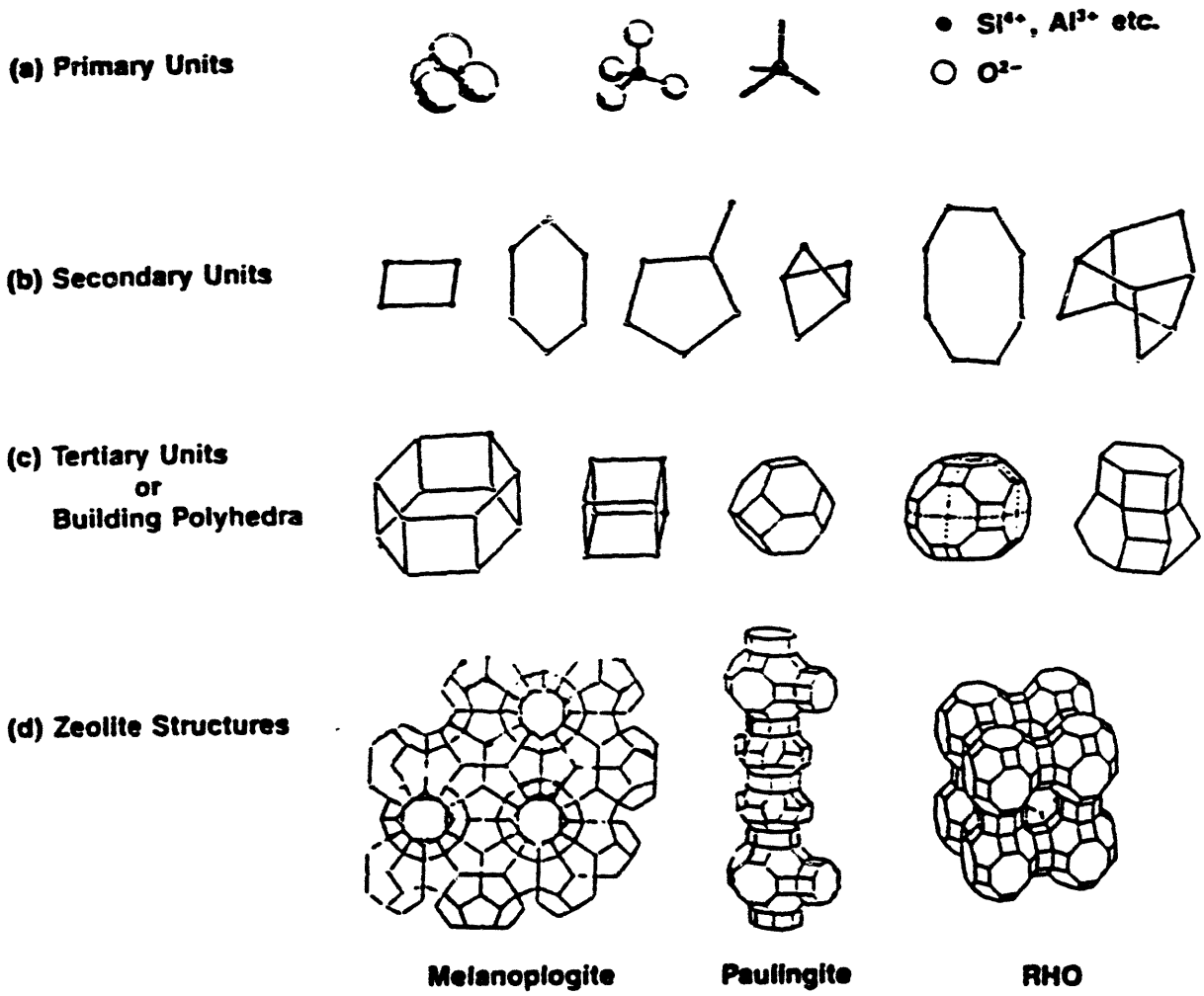

Figure 1.2 Formation of Zeolite Structures (Vaughan, 1988)

ZSM-5, patented by Argauer and Landolt (1972), is a 10-membered ring zeolite with two distinct sets of intersecting channels. Near circular sinusoidal channels with a free cross section of 5.4 ± 0.2 Å are parallel to the a-axis or [100]. Elliptical straight channels with a free cross section of 5.7-5.8 x 5.1-5.2 Å are parallel to the b-axis or [010]. The calculated free cross section assumes that oxygen ions have a radius of 1.3 Å (Flanigen et al 1978). Figures 1.3a and 1.3b shows these two types of channels generated from the combinations of the secondary building unit for ZSM-5. The intersecting channels form a three-dimensional framework with a coordination number of 4; each intersection connects to four other neighboring intersections by channels. The size of these intersections is about 9 Å in diameter (Nowak et al, 1987). The distances between intersections are about 10.0 Å for straight channels and 12.6 Å for sinusoidal channels respectively (Richards and Rees, 1987). Figure 1.4 is a schematic of the ZSM-5 channel system.

The ZSM-5 unit cell contains 96 T (= Si or Al) atoms and 192 oxygen atoms with lattice constants a=20.1, b=19.9, and c=13.4 Å (Kokotailo et al, 1978). There are four intersections per unit cell. The Si/Al ratio is typically above 10. ZSM-5 with Si/Al ratio above 500 is sometimes referred to as silicalite.

Each unit cell of zeolite A contains 24 tetrahedral (AlO_2 or SiO_2) units to form a cubic structure with a lattice constant a=12.32 Å. As shown in Figure 1.5, in the center of the unit cell is a large cage about 11.4 Å in diameter, which is connected to six like cages by the 8-membered oxygen windows. The window size can vary from its free diameter of about 4.2 Å for 5-A (Ca^{2+}, or Mg^{2+} form) to 3.5 Å for 4-A (Na^+ form) or 3.2 Å for 3-A (K^+ form). The framework of zeolite A is three dimensional with a coordination number of 6. The Si/Al ratio in zeolite A is always close to one (Breck 1956; Walker et al 1966).

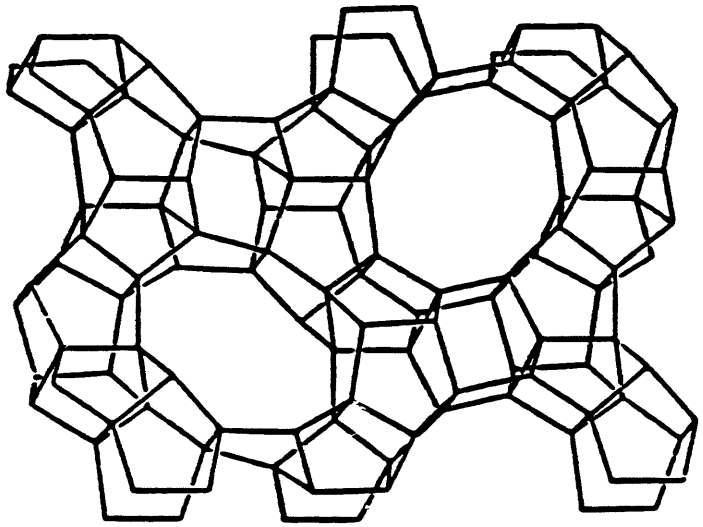

Figure 1.3a The b-face of the unit cell. The axis is horizontal, and the c-axis vertical. The 10-membered ring apertures are the elliptical entrances to the straight channels which run parallel to the b-axis (adapted from Kokotailo et al, 1978).

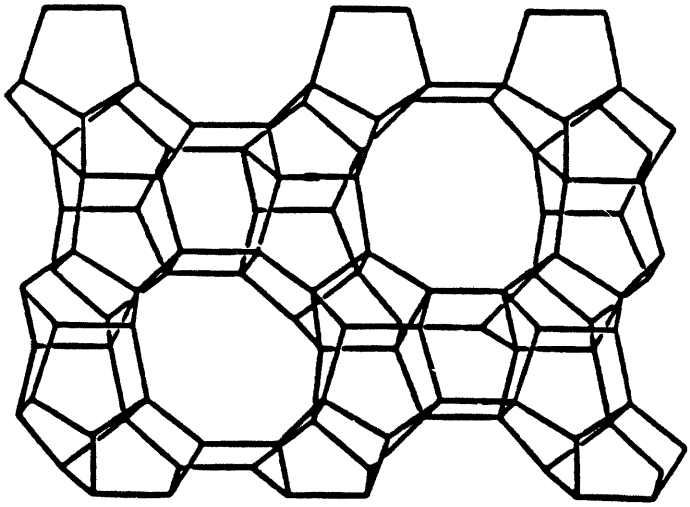

Figure 1.3b The a-face of the unit cell. The b-axis is horizontal, and the c-axis vertical. The 10-membered ring aperture are near circular entrances to the sinusoidal channels which run parallel to the a-axis (adapted from Kokotailo et al, 1978).

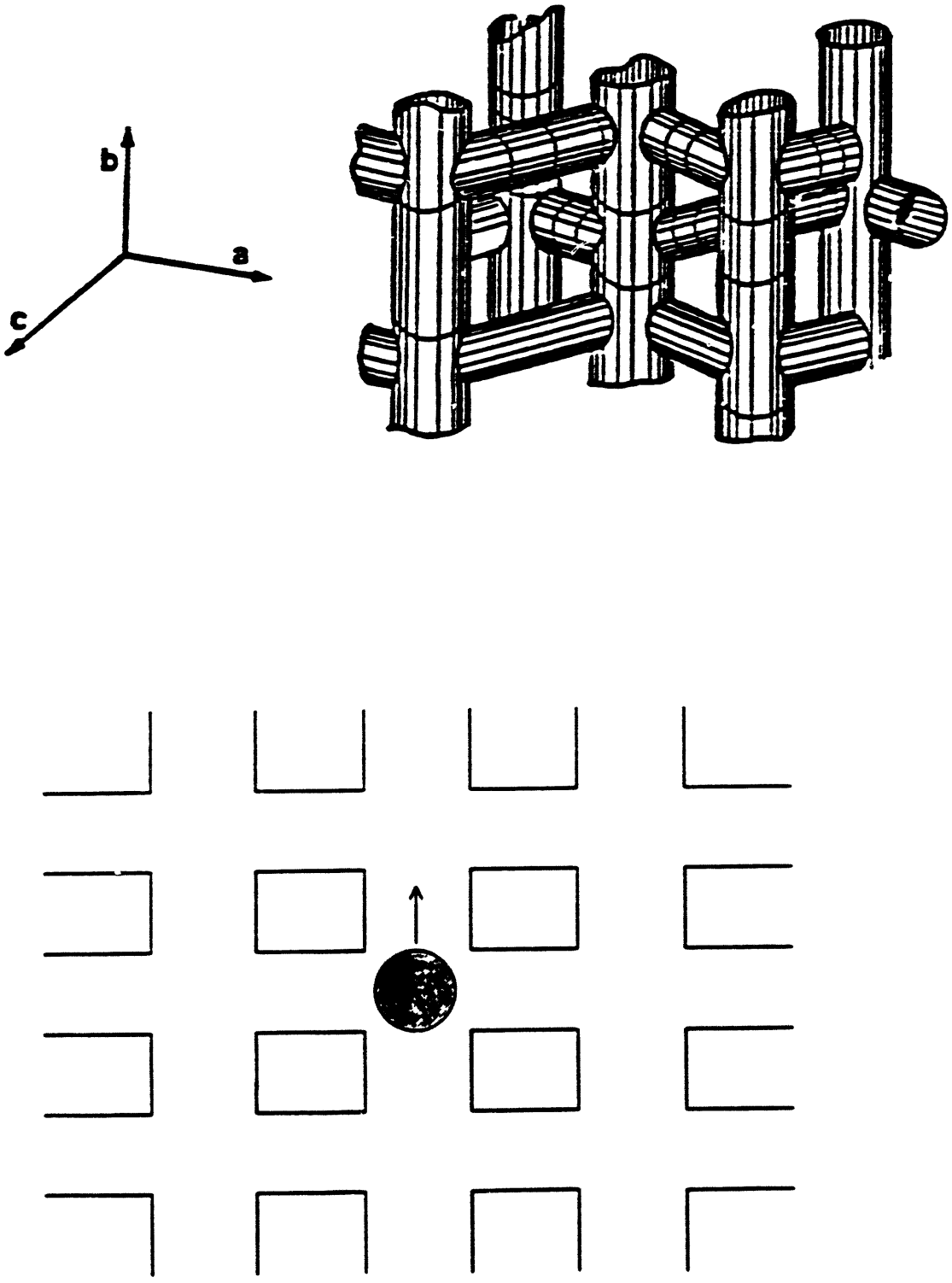

Figure 1.4 Schematic of ZSM-5 Channel System

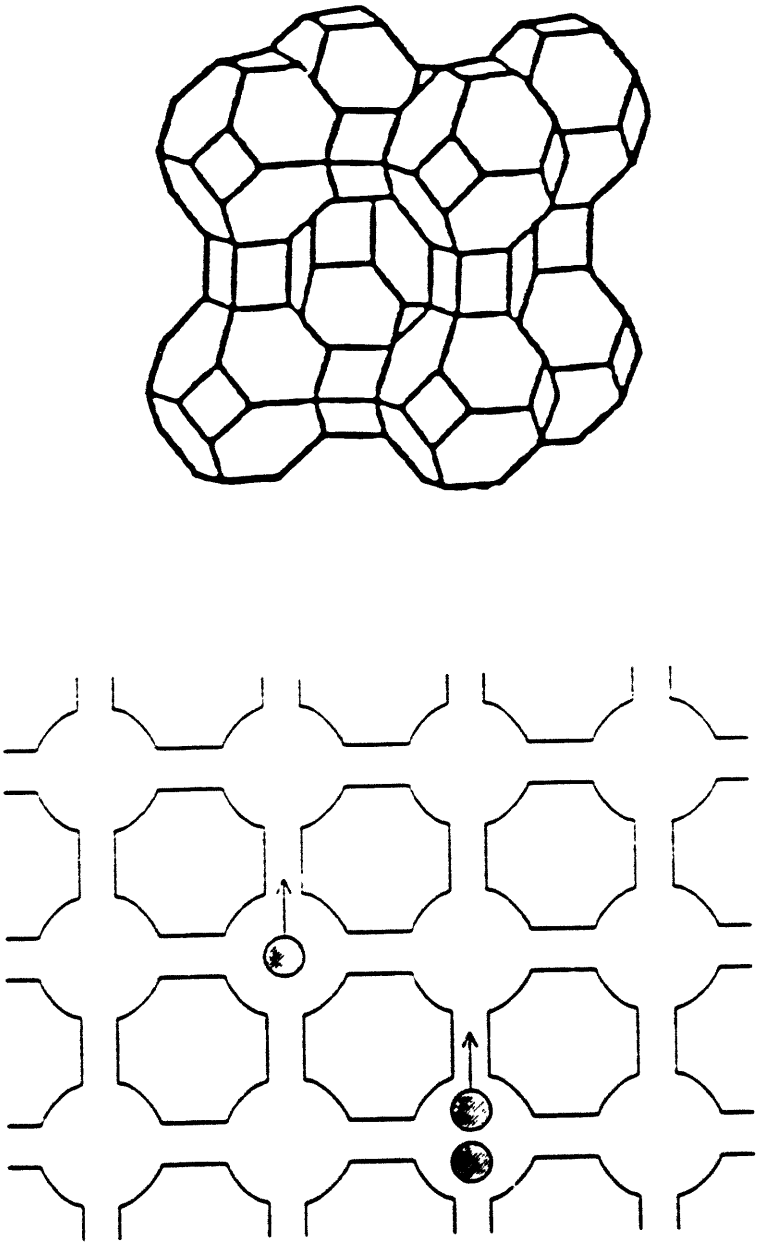

Figure 1.5 Schematic of Zeolite A Channel System

1.2.4 Molecular and Pore Diameters

There are at least two ways to characterize the size of zeolite channels (Breck, 1974; Barrer, 1978; Ruthven, 1984). The free diameter of a zeolite channel can be calculated from the structural model of the oxygen rings forming the channel openings, by assuming a diameter for the oxygen atom. This method gives the most often quoted zeolite pore sizes: 2.8 Å for 6-membered rings; 4.2 Å for 8-membered rings; 5.7 Å for 10-membered rings; and 7 to 7.4 Å for 12-membered rings. In these calculations, a radius of 1.4 Å for oxygen was used (Ruthven, 1984). The channel size of a zeolite can also be characterized by the occlusion of guest molecules. The so-called effective diameter of the zeolite channel is determined experimentally by subjecting a zeolite to guest molecules with different kinetic diameters. For the unobstructed 8-, 10-, and 12-membered ring zeolites, the effective sizes are approximately 4.5, 6.0, and 8.5 Å (Ruthven, 1984).

In the study of a guest molecule in a zeolite, the molecular diameter is often characterized by either the minimum kinetic diameter of the molecule, d_m, (Breck, 1974) or the Lennard-Jones length constant, σ_m, (or its corresponding van der Waals diameter, σ_o, where $\sigma_o = 2^{1/6}\sigma_m$) (Ruthven, 1984). The minimum kinetic diameter can be calculated from the minimum equilibrium cross-sectional diameter, and is often used to characterize how difficult it is for a molecule to penetrate through a zeolite channel (Breck, 1974). The value of the Lennard-Jones length constant can be determined either from transport properties (viscosity, thermal conductivity) or from detailed measurements of the deviations from the ideal gas law (second virial coefficients) (Reid et al, 1977). This method gives a spherical representation of the molecule. When a molecule is within a cage (or intersection) of a zeolite, this potential length constant may give some indication of the interaction between the

molecule and the surrounding oxygen ions.

Molecules should not be viewed as rigid spheres, nor should zeolite channels be viewed as rigid walls. For the case where molecular diameter is close to but still smaller than the zeolite channel diameter, molecules might experience a net attraction when passing through the channels. If molecular diameter is slightly larger than the zeolite channel diameter, molecules might experience a net repulsive force instead. If molecular diameter is much larger than channel diameter, molecules can no longer enter the zeolite due to the strong repulsive force from the channels.

Neither zeolite channel diameter nor molecular diameter can be described by a well-defined number. The diameter of an atom, such as oxygen, is difficult to define explicitly. In the electron cloud model of the atom, the probability density distribution theoretically reaches zero only at infinity. The electron density, however, falls off so rapidly at a short distance from the nucleus that some approximation of size can be made. In the case of zeolites, different radii of oxygen, such as 1.3 Å (Flanigen, 1978), 1.35 Å (Olson et al, 1981), 1.4 Å (Ruthven, 1984), were used. The calculation of free diameter of a zeolite channel is also slightly dependent on the choice of diametrically opposing oxygens (Flanigen, 1978). The vibration of the crystal lattice and the possible distortions of both molecule and zeolite when the molecule penetrates through the lattice make it even more difficult to assess the "true" diameter of either molecule or zeolite pore. Furthermore, it is over-simplified to characterize a molecule, especially a non-spherical one, by either a minimum diameter or a potential constant. The free diameter of the zeolite channel, the minimum diameter of the molecule and the potential constant mentioned above have nevertheless given some characteristic descriptions on channel and molecule size, which will be used in this thesis.

Figure 1.6 lists the minimum diameters of some hydrocarbons (Breck, 1974) and the pore sizes of three zeolites. The ratio between these two sizes is defined as λ. Hydrocarbons of interest in this thesis are normal-paraffins, single- and double-branched paraffins, aromatics, such as benzene and toluene, and cyclohexane. Model zeolites, as mentioned before, are ZSM-5 and 5A. Table 1.1 lists the Lennard-Jones potential length constants for some hydrocarbons determined by Wilke-Lee method (Reid et al, 1977).

1.3 Literature Review: Experimental Results

Barrer and his co-workers pioneered the diffusion study of zeolites more than forty years ago (e.g. Barrer, and Ibbitson, 1944). Over the decades, many research groups have engaged in probing the diffusional behavior in natural and synthetic zeolites by various techniques (e.g. Ruthven, 1984; Bülow et al, 1980; Kärger and Pfeifer, 1987; Hayhurst and Paravar, 1988). Here a brief summary on the experimental techniques and the results will be presented. An excellent review on the subject was recently published by Kärger and Ruthven (1989).

1.3.1 Experimental Methods

The measurements of the diffusivity in zeolites have been made by both macroscopic and microscopic methods (Kärger and Ruthven, 1989).

The macroscopic methods mainly include the transient methods, such as gravimetric or volumetric uptake, frequency response, chromatographic measurements, and tracer exchange, and the steady-state or quasi steady-state methods, such as the Wicke-Kallenbach method, and effectiveness factor calculation

MOLECULAR AND PORE DIAMETERS

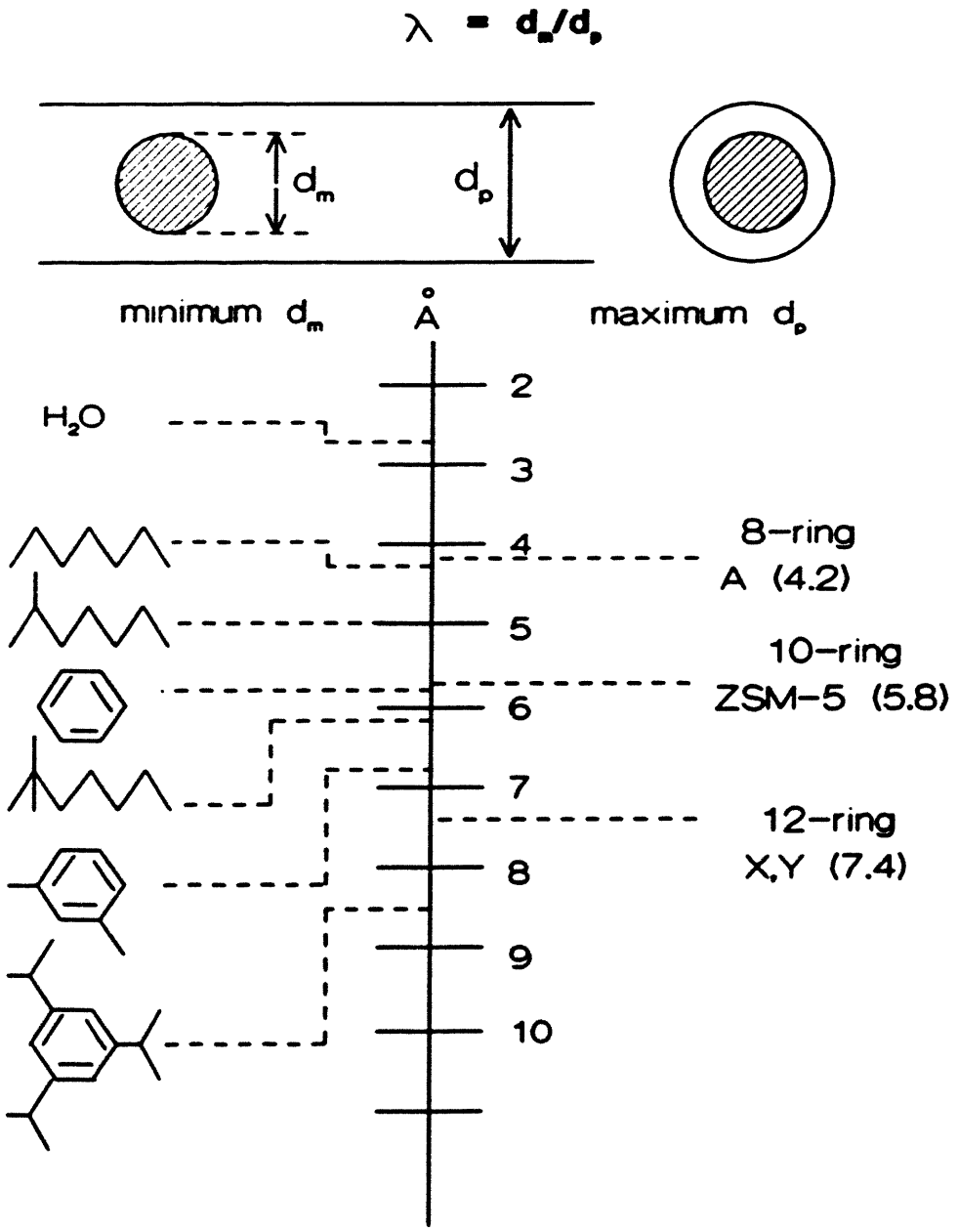

Figure 1.6 Molecular and Pore Diameters

Table 1.1 Dimensions for Various Molecules

Molecule	d_m (Å)	σ_m (Å)	ϵ_m/R (°K)
methane	3.8	3.65	128
ethane		4.40	212
propane	4.3	4.95	266
n-butane	4.3	5.41	314
n-pentane		5.79	356
n-hexane		6.14	393
n-heptane		6.44	427
n-octane		6.72	459
n-nonane		6.98	488
n-decane		7.22	514
2-methylbutane	5.0	5.79	346
2-methylpentane		6.14	384
2,2-dimethylbutane	6.2	6.14	371
2,3-dimethylbutane		6.14	381
cyclohexane	6.0	5.79	407
benzene	5.85	5.40	406
carbon tetrafluorine	4.7	4.34	167

* values of d_m from Breck (1974).

** values of σ_m and ϵ_m/R estimated by Wilke-Lee method (Reid et al, 1977):

$$\sigma_m = 1.18\ V_m^{1/3}, \text{ and } \epsilon_m/R = 1.15\ T_b$$

where V_b = Le Bas volume

T_b = normal boiling point, °K.

under reaction condition. The flux into or through a zeolite crystal (or an assemblage of crystals) under well-defined boundary conditions is measured. The diffusivity is then calculated by matching the experimental flux or uptake rate to the appropriate theoretical solution derived from the Fick's law of diffusion (e.g. Ruthven, 1984). In the chromatographic method, the diffusional time constant is determined from the dynamic response of a packed column to a change in sorbate concentration. In the effectiveness factor method, diffusivity can be derived from the results of simultaneous catalysis and diffusion under diffusion limited conditions over catalysts of different diameters (Haag et al, 1981).

The uptake methods are experimentally simple and straightforward, they are however unreliable for fast processes (e.g. practical limit $D/r_p^2 < 0.01\ s^{-1}$ for gravimetric or volumetric method). In the chromatographic method, axial dispersion and intercrystalline diffusion are difficult to eliminate or estimate with confidence. The Wicke-Kallenbach technique needs large crystals which are not easy to synthesize. The advantage of the effectiveness factor method is that the measurement is made at the reaction condition. The requirement of using at least two sets of zeolite catalysts with the identical activity but different sizes is not easy to meet in practice.

All of these measurements are subject to possible limitations from external heat and mass transfer resistance, although to varying degrees. A small amount of contaminants on the catalyst surface can also change significantly the measured diffusivity. It is therefore very important to confirm experimentally the absence of such effects under experimental conditions. This may be achieved by varying the size of the zeolite crystals and the configuration of the sample, by checking the conformity of the shape of the uptake curves to the diffusion model, by varying the nature and

flow rate of the carrier gas (or carrier liquid) in the case where carrier is used, and by carefully eliminating possible sources of contaminants.

The microscopic methods are based on n.m.r. or neutron-scattering measurements (e.g. Kärger et al 1980a, 1980b; Egelstaff et al 1968). These techniques measure the self-diffusivity, by determining the average time between molecular jumps indirectly (n.m.r. relaxation, neutron scattering), or directly (n.m.r. PFG method). The n.m.r. PFG method allows direct determination of the probability distribution of the lengths of the diffusion paths (typically of the order of a micron or more) during a known observation time (typically of a few milliseconds). Both the intracrystalline diffusivity and the extracrystalline diffusivity may be determined, depending on the ratio between the r.m.s. displacement and the mean crystal radius. This method is, however, only suitable for rapid processes (in practice, for diffusivities larger than 10^{-8} cm^2/s). The method has also been extended to measure the rate of interchange of molecules between the adsorbed phase and the surrounding gas. The indirect methods all suffer from the disadvantage that the estimated diffusivity depends on an assumed jump length.

1.3.2 Experimental Observations

A picture of zeolite diffusion emerges from past studies. Configurational diffusion can be characterized by the following distinct experimental observations:
(a) very small diffusivities, typically between 10^{-6} to 10^{-14} cm^2/s (Weisz, 1973);
(b) a strong dependence on the size and the shape of the guest molecules (up to 1000 times difference between p-xylene and o-xylene; Wei, 1982);
(c) high activation energy (3 to 14 kcal/mol for paraffins in 4A and 5A; Ruthven, 1984);

(d) a strong concentration dependence, which may increase or decrease by as much as two orders of magnitude (Barrer, 1953; Doetsch et al, 1974);
(e) a slow rate of counter-diffusion in comparison to that of a single component diffusion (Satterfield and Katzer, 1971; Qureshi and Wei, 1988).

The experimental observations reported in the literature, however, are not conclusive and sometimes even contradictory on how the microscopic properties of a molecule-zeolite system affect the macroscopic behavior.

For example, the discrepancy of the diffusivities measured by different research groups, and/or by different methods for the same system under apparently similar conditions can be as large as several orders of magnitude. More careful studies showed that some of the reported data were significantly affected by external heat and mass transfer resistances (e.g. Ruthven et al, 1980, 1981). In more recent studies, larger and often unaggregated crystals were used in the uptake measurements so that the intrusion of rate-limiting steps other than intracrystalline diffusion could be eliminated. The good agreements for some systems were found not only between the results for the same system by different macroscopic methods, but also by macroscopic and microscopic methods. Kärger and Ruthven (1989) listed some of these systems: CH_4/4A; C_3H_8, nC_4, CF_4/5A; TEA/NaX. The systems where macro/micro data disagree include: nC_4, Benzene, xylenes/NaX; C_3H_8/silicalite. In these cases, the macro diffusivity are smaller. Among these systems, C_3H_8 is unique since it shows agreement between n.m.r.PFG and uptake method (square wave) data, whereas the other macro techniques also yield consistent but much lower diffusivity values.

Many of the earlier uptake studies were carried out with small commercial

zeolite crystals, or even with pelleted material. The effects of heat and mass transfer resistance and existence of contaminants in these samples could be severe. The difference in the reported diffusivities for the same system might also be the result of using different techniques, in which different assumptions are involved. In the chromatographic method, a model of dispersion and diffusion is needed, and the intracrystalline diffusivity is calculated after considerable deconvolution of the data. And in some of the microscopic methods mentioned above, a jump length must be assumed. Furthermore, in some cases, two different dynamic events might be monitored due to the time scale difference of the measurements (Kärger and Ruthven, 1989). The time scale of an n.m.r. (PFG) experiment is of the order of a few milliseconds, whereas the time scale of most macroscopic sorption rate measurements is of the order of seconds, minutes, or even hours. The results by the macroscopic, short-time scale square-wave measurements are consistent with those by n.m.r., but not with those by other longer-time scale macroscopic methods. If there are two types of molecules inside the zeolite lattice: one is mobile while the other is relatively immobile, different methods with different time scales might just measure different diffusion processes. This hypothesis, however, needs further experimental support.

Diffusion in zeolites is often found to be an activated process. The apparent activation energy of normal-paraffins in zeolites 4A and 5A increases with the van der Waals diameter of the diffusant (Ruthven, 1984). No other systematic study on this aspect of the different zeolite systems has been carried out.

There are four types of concentration dependence of uptake diffusivity which have been observed to date: type I, diffusivity, D, increases monitonically with increasing concentration, c; type II, D is independent of c; type III, D decreases

monitonically with c; type IV, D decreases and then increases with c. Ruthven and co-workers (e.g. 1971a, 1971b, 1972, 1973a, 1973b, 1975b, 1976a, 1976b, 1982) found that the parameter λ, defined in section 1.2.4, is critical to the observed diffusion types. For 8- and 12-membered ring zeolites, they observed type I or II for most of the systems with λ greater than one, and type III or IV with λ less than one. Ruthven and Lee (1981) later showed that some of the type III and IV results might be inaccurate due to heat and bed diffusion effects. Type I or II was also observed for systems with λ greater than one by Habgood (1958), Barrer et al (1971), Eagan et al (1975), Quig et al (1976), Bülow et al (1982), Choudhary et al (1986), Tsikoyiannis (1986), Zikanova et al (1987), Shah et al (1988), Qureshi and Wei (1988). In contrast, Barrer and co-workers (1948, 1953, 1974) observed type III in several experiments, even though all λ's were greater than one.

The reported concentration dependent trends of diffusivities for a given system are sometimes not consistent with each other. For the diffusion of benzene in ZSM-5, for example, Tsikoyiannis (1986) observed a thirty-fold increase in diffusivity as concentration rises from about 0.5 molecule/unit cell to about 4 molecules/unit cell. The results of Zikanova et al (1987) showed a roughly concentration independent trend of diffusivity over the same concentration range, after converting the corrected diffusion coefficients presented in the paper to uptake diffusion coefficient. Qureshi (1989) reported no dramatic effect of occupancy on the diffusion coefficient for concentrations less than about 3 molecules/unit cell.

The lack of reliable data on diffusivity and its dependence on the temperature and concentration has therefore limited the quantitative understanding of zeolite diffusion, which has in turn hindered the development of a comprehensive diffusion theory for zeolites. A systematic experimental study on these subjects can greatly

advance the better understanding of this important diffusional phenomenon.

1.4 Literature Review: Existing Theories

There are two main approaches to modeling diffusion in zeolites. These are the microscopic approach, where kinetic properties of guest molecules are explicitly considered, and macroscopic approach, where the molecule-zeolite system is viewed as a continuous medium and kinetic properties of guest molecules are ignored.

The macroscopic model, also known as the irreversible thermodynamics model, is mainly used to explain the concentration dependence of diffusivities for one-component and two-component diffusion in zeolites. This model can explain some data of types I and II described in the previous section. The reason for the success and failure of the model is, however, not clear since the model is established on phenomenological ground and the detailed descriptions of molecule motion are ignored. This model is not capable of predicting the order of magnitude of the diffusivity. The macroscopic model can, therefore, at most be used as a correlative model. The microscopic model, on the other hand, can incorporate a variety of assumptions in regard to individual particle motion, the interaction between the guest molecule and its host zeolite, and the interaction among molecules themselves. Through these assumptions, one should be able to predict and explain not only the concentration dependence of the diffusivity but also its magnitude. Only limited success has been achieved to date by this approach, mainly due to the difficulty of making appropriate assumptions and verifying these assumptions. With the recent emerging experimental results reported on the motion of molecules inside the zeolite lattice by different techniques, this obstacle might soon be overcome.

Before proceeding further to detailed discussions on these two approaches, it would be helpful to review briefly the definitions of diffusivity, particularly those in zeolites.

1.4.1 Definitions of Diffusivity

Bird et al (1960) presented the relations among the fluxes with respect to stationary axes as follows:

$$n_A = j_A + \rho_A u_m \tag{1.1}$$

where n_A is the mass flux of species A,

$$n_A = \rho_A u_A \tag{1.2}$$

and ρ_A is the mass concentration of A (for example: g of A/cm^3 of solution), u_m is the mass average velocity, defined by

$$u_m = \omega_A u_A + \omega_B u_B \tag{1.3}$$

In the above equation, ω_i ($=\rho_i/\rho$) is the mass fraction of species i (i = A, B), and u_i is the velocity of species i relative to stationary coordinates.

For diffusion in zeolites, component B (zeolite) is stationary ($u_B = 0$). The mass of component A (guest molecule) is negligible in comparison to the total mass of zeolite crystal and molecules ($\rho_A \ll \rho$). The right hand side of Eq. (1.3) is therefore approximately equal to zero. Equation (1.1) can thus be simplified to

$$n_A = j_A \tag{1.4}$$

The mass transfer process inside of zeolites is therefore a pseudo-one-component

diffusive process if there only one type of guest molecules presents. The corresponding Fick's first law is of form:

$$J = -D \nabla c \tag{1.5}$$

where J is the molar flux of guest molecules relative to stationary coordinates, and D is the diffusion coefficient, or the diffusivity.

It should be noted that the diffusivity is defined here in relation to the concentration gradient of a targeting species INSIDE the zeolite lattice. If the partitioning of molecules between gas phase and zeolite can be described by Henry's law:

$$c = K_H c_g \tag{1.6}$$

where K_H is the Henry's law constant, and if the flux is expressed in terms of gaseous concentration, a different diffusivity is then introduced:

$$J = -D_g \nabla c_g \tag{1.7}$$

where

$$D = \frac{D_g}{K_H} \tag{1.8}$$

If the partitioning between two phases is of Langmuir type and gas phase is ideal, then we have:

$$D = \frac{D_g}{c_s RTK(1-\frac{c}{c_s})^2} \tag{1.9}$$

where c_s is the saturation concentration in zeolite , and K is the Langmuir parameter, defined by

$$K = \frac{c}{P(c_s - c)} \tag{1.10}$$

where P is the corresponding gaseous phase pressure.

The differences in the definitions of diffusivity can therefore lead to different values of diffusivity, different activation energies, and different concentration dependent trends of diffusivity. The mobile species and the immobile species presented in the adsorption process can add even more complications into the definition of diffusivity (Haynes, 1988; Garcia and Weisz, 1990). One thus needs to specify the conditions under which a diffusion experiment was conducted, and the procedures and the methods used in obtaining the diffusivity. Care should be taken if the diffusivities by different research groups and/or by different techniques are compared.

For this thesis, the aim is to investigate how the interaction between the molecule and the lattice, and the interaction between molecules inside the zeolite can affect the diffusional behavior. The experimental diffusivity is obtained by the uptake method in which a concentration gradient inside the lattice drives the uptake process. The diffusivity defined by Equation 1.5 is therefore used in both theoretical

and experimental analysis.

1.4.2 Macroscopic Approach

This approach is based on the general theory of irreversible thermodynamics. The theory was presented by Onsager (1931) and later by Casimir (1945), Prigogine (1967), de Groot and Mazer (1969). The fluxes, J_i, the time derivatives of appropriate variables, are related to the "thermodynamic force", X_j, by the expression

$$J_i = \sum_j L_{ij} X_j \tag{1.11}$$

The force, X_j, arises from the tendency of a nonequilibrium system to return to equilibrium conditions.

An irreversible thermodynamics theory of diffusion in zeolites has been developed by Barrer and Jost (1949), Ash and Barrer (1967), Ruthven et al (1971a), and Kärger (1973, 1975). When the "true driving force for diffusion", the gradient of the chemical potential, is represented in terms of a concentration gradient, the formulation of the diffusion equation leads to

$$J_x = -RTBc\frac{\partial lnP}{\partial x} \tag{1.12}$$

$$= -D_c\frac{\partial lnP}{\partial lnc}\frac{\partial c}{\partial x} \tag{1.13}$$

where B is the mobility, and D_c is the "corrected diffusivity", defined by

$$D_c = RTB \tag{1.14}$$

Comparing Eq. (1.13) with Eq. (1.5), we have:

$$D = D_c \frac{\partial lnP}{\partial lnc} \tag{1.15}$$

Equation (1.15) is commonly known as Darken's equation. The relation $\partial \ln P / \partial \ln c$ can be obtained from the adsorption isotherm. Utilizing the Langmuir isotherm gives

$$D = \frac{D_c}{1 - \theta} \tag{1.16}$$

where the occupancy, θ, is simply c/c_s. An order of magnitude increase in diffusivity should be observed if θ rises from about zero to about 0.9 for the case where D_c is a constant.

Habgood (1958) extended the irreversible thermodynamics concept to two-component systems. The same concept was also used in the studies of self-diffusion (Barrer and Fender, 1961; Kärger, 1976).

Experimentally, it has been observed that for a number of molecule/zeolite systems the concentration dependence of diffusivity can be correlated by using Darken's equation with a concentration-independent D_c. This approach, however, gives no mechanistic reason why it happens and when it should fail since the details of molecular motions were ignored in the formulation of this correlation. There is also no theoretical basis why a term of concentration, c, should be included in Eq. (1.12).

1.4.3 Microscopic Approach

A first attempt to model the diffusion in zeolites by kinetic theory was made almost an half of century ago by Barrer (1941). The diffusion rate of a molecule with sufficient energy to jump from one site to another depends on the chance of finding a vacant site. The probability of a site being occupied by a molecule, θ, the vibration frequency, ν, the lattice constant, α, and the activation energy, E, were related to the apparent diffusivity, D_{app}, by

$$D_{app} = D\,(1-\theta) \tag{1.17}$$

and

$$D = \frac{1}{6}\alpha^2 \nu e^{-\frac{E}{RT}} \tag{1.18}$$

Barrer and Jost (1949) modified the above equations by superimposing the effect of equilibrium isotherm into the formulation. For the Langmuir isotherm, the effect of finding a vacant neighboring site, $(1-\theta)$, and the effect of the chemical potential, $1/(1-\theta)$, compensated exactly, and a constant diffusivity results. They also assumed that the activation energy persisted long enough for an n-fold molecular jump in a straight line, which led to different types of concentration dependence of diffusivity. There is no experimental evidence, however, as to whether such a multi-step jump actually occurs.

Riekert (1970) used a lattice model to conclude that single-component diffusion in zeolites gives a concentration-independent diffusivity, similar to Eq. (1.18). The effect of the decrease in the average jumping frequency of the targeting particle with increasing occupancy cancels out in the expression. For binary diffusion,

the apparent diffusivity decreases with the concentration, proportional to $(1-\theta)$.

Palekar and Rajadhyaksha (1984) modelled a zeolite lattice with one-dimensional, parallel, non-intersecting channel system as tanks-in-series. An activated molecule was assumed to jump to its neighboring site unless both of the adjacent sites were occupied. This leads to the concentration dependence of diffusivity being $(1-\theta^2)$. Based upon the same assumption, they (1985a, 1985b, 1986a) later carried out Monte-Carlo simulations to model one- and two-component diffusion in the same type of zeolite lattice. A rising trend of apparent diffusivity was observed for the single-component diffusion. Aust et al (1989) extended the work of Palekar and Rajadhyaksha to the two-dimensional lattice by similar Monte Carlo simulations. They reported a rising trend of diffusivity under the assumption that a molecule would jump if it could. An almost concentration-independent trend was observed when the assumption was changed so that the molecule would not leave the site if the first assigned direction led to an unsuccessful jump.

Theodorou and Wei (1983) developed a Monte Carlo model, in which the movement of molecules within zeolites was assumed to be a random walk from intersection to intersection in a finite two-dimensional square lattice. A molecule was randomly activated, and one of four neighboring sites was randomly selectived. If the site was unoccupied, the activated molecule "jumped" to the new site. If the site was already occupied by another molecule, then both molecules remained where they were. A decreasing trend in self-diffusivity with increasing concentration was predicted due to the exclusion of double occupancy of the sites. The blockages of the interior diffusion path and the pore entrance could also cause a decrease in diffusivity.

Tsikoyiannis (1986) has further extended this study by the theory of Markov Pure Jump Processes (Hoel et al, 1972). Zeolitic sorption, diffusion, and reaction were modelled as a sequence of elementary jump events taking place in a finite periodic lattice. The Master equation was derived, and Monte Carlo simulations were used. Approximate analytic solutions were presented, based on first order correlation functions where only the sites immediately adjacent to the targeting site were considered. Assuming exclusion of double occupancy of the lattice sites and non-interacting molecules, the single-component uptake diffusivity was found to be independent of occupancy. In contrast, self-diffusivity decreased with occupancy. These results are the same as those from Riekert (1970). The first order correlation was also applied to the case where the weak attractive or repulsive interparticle interaction existed.

The advantage of the above models is their flexibility in incorporating a variety of assumptions in regard to individual particle motion on a microscopic scale. The macroscopic diffusional behavior of the system can then be derived. The first-order correlation function method can even give an approximate, easy-to-use analytic solution. The assumption of weak interaction between molecules needs further justification. The experimental results in the literature (e.g. Ruthven, 1984) suggested that an increasing trend in diffusivity occurred at the same time as a decreasing trend in Langmuir parameter was observed. The attraction between molecules, according to the model, could result in a rising trend in diffusivity with occupancy. And a rising trend in the Langmuir parameter, defined by Eq. (1.10), with occupancy was also expected under this condition. The repulsion between molecules, on the other hand, could result in a decreasing trend in diffusivity and Langmuir parameter. The theoretical predictions mentioned are, therefore, not consistent with the experimental observations. A further modification on the theory

needs to be advanced.

The above discussions mainly concern the concentration dependence of the diffusivity. Another important issue is the estimation of the order of magnitude of the diffusivity. Equation (1.18) is one of those attempts based upon the view that zeolitic diffusion is similar to atomic diffusion in solid.

Ruthven and Derrah (1972) applied transition state theory to estimate the "corrected diffusivity", defined by Eqs. (1.13) and (1.14):

$$D_c = \frac{kT\alpha^2}{6h}\frac{f_c}{f_i}\, e^{-\frac{\Phi_c-\Phi_i}{kT}} \qquad (1.19)$$

where k is Boltzmann's constant, h is Planck's constant, f_c and f_i are the partition functions at the channel (pore) and at the intersection (cage) respectively, and Φ_c-Φ_i is the molecule potential difference between the channel and the intersection. Utilizing Henry's law, they related D_c to the ratio of the partition function at the channel and that of the gaseous phase, the pre-exponential term of Henry's law constant (K_H^o), the molecule potential difference between the gaseous phase and the channel, and the heat of the adsorption. The values of K_H^o and the heat of adsorption might be found from equilibrium data. The potential difference may be calculated from potential theory. And the ratio of the partition functions may be estimated from theoretical considerations. Kärger et al (1980) extended this method on the estimation of the ratio of the partition functions.

In using this model, two parameters, K_H^o and the heat of adsorption, need to be experimentally determined. Furthermore, in the derivation of the transition state theory, the species at the transition state is assumed to be weakly bound and

vibrate with a frequency, ν_{rc}, along the "reaction" coordinate. It is also assumed that $h\nu_{rc}$ is much less than kT. These assumptions lead to the pre-exponential term expressed in Eq. (1.19). This picture might not describe diffusion in zeolites. Molecules reside preferably at the intersection for most of the time due to the attractive force from the framework. When a molecule is slightly larger in size than the channel size, such as the case of normal-paraffins/5A, the molecule might experience a soft repulsive force while passing through the channel. It is very unlikely that this molecule would be "bound" at the channel (the "transition state" of the zeolitic diffusion). The effective vibrational frequency, ν_e, of simple molecules within a zeolite lattice was estimated to be about the order of 10^{12} s^{-1} (Barrer, 1978). This frequency would give the ratio of ($h\nu$/kT) a value of the order of 0.1 at 300K. Even though ν_{rc} could be smaller than ν_e due to the weak "bonding" (assuming the existence of such a "bonding"), it might not be safe to assume that $h\nu_{rc}$ is much smaller than kT, as required by the derivation of the transition state theory.

Derouane (1986) described the interactions between molecules and the zeolite framework as a stereochemical, rather than diffusional, issue. He proposed the "nest effect" image wherein a molecule and its direct environment tend to reciprocally optimize their van der Waals interaction. And van der Waals bonding was suggested to be proportional to the Gaussian curvature of the zeolite surface. A molecule may acquire supermobility when its dimension(s) match intimately that of the surrounding pore, a case referred to as the floating molecule. And serpentine or creeping motion of chain molecules along the channel wall should be expected in other situation. Derouane et al (1988) then applied an uptake formula based on this van der Waals model to determine the mass transfer coefficient for n-hexane in zeolites. That formula suggests that the uptake should follow an exponential function. This is mathematically equivalent to the surface barrier model proposed by Kärger and

Herman (1974) in which the uptake is assumed to be controlled by transmission through a surface skin, instead of by intracrystalline diffusion. In most of the experimental observations of diffusion in zeolites, the uptake follows Fick's law. The surface curvature effect, though it may exist, is at least not a dominant factor in most of the uptake measurements.

Choudhary and Akolekar (1989) proposed a shuttlecock-shuttlebox model. The relative penetrability and diffusivity of bulky sorbate molecules in ZSM-5 were discussed qualitatively, based on the configuration and flexibility of molecules and zeolite pores. No quantitative analysis was given.

The computer modeling based upon the principles of statistical mechanics and molecular dynamics has been applied to the study of structural, adsorptive, diffusive and catalytic properties of zeolites (e.g Kiselev et al., 1981; Ramdas et al., 1984; Nowak et al., 1987; June et al., 1988). Some interesting features of zeolites were predicted by these computation-intensive studies.

Ramdas et al. used computer graphics to depict features of zeolite structures determined by X-ray studies. They also modeled the possible zeolite intergrowths, and twinning. Dynamic simulations of interaction between organic molecules and the framework were performed by summing the atom-atom interactions.

Nowak et al. extended the above study to consider the adsorption and diffusion of benzene and toluene in the zeolites theta-1 and silicalite. A molecule was placed in a specified starting configuration, and then allowed to translate along and rotate about the molecular axis that was parallel to the channel axis. The Lennard-Jones description of the atom-atom potentials was employed. The average

interaction energy between molecule and zeolite was obtained by Boltzmann factor averaging of the position-dependent interaction energy. They predicted that a molecule is most likely to be situated in the channel center instead of at the channel wall. The calculated heat of adsorption for benzene in silicalite is about -57.3 kJ/mol. An activation energy of about 22-45 kJ/mol was estimated for the diffusion of benzene and toluene in silicalite. The movement for both benzene and toluene seems to have similar energy constraints.

For hydrocarbons in silicalite, June et al. determined Henry's law constants and isosteric heat of sorption by the evaluation of configurational integrals with a Monte Carlo integration scheme. The spatial distribution of sorbate molecules within the pore network, as well as perturbations to their conformation due to confinement in the pores, were determined via a Metropolis Monte Carlo algorithm. They concluded that the linear alkanes, such as n-butane and n-hexane, prefer to reside in the channels and bulky branched alkanes, such as 2-methylpentane, reside at more spacious channel intersection. The self-diffusivity of methane was also estimated by molecular dynamics simulations.

These kind of models seem very promising in the modeling of zeolite properties, since the structures of zeolites are well defined and more powerful computers are emerging. The bottleneck is the availability of the proper inter-atomic potential parameters for the interaction of hydrocarbon atoms with the zeolite framework. The calculation results are very sensitive to the values of these parameters, and how the interactions are modeled. For example, June et al (1989) used an "optimal value" for the oxygen van der Waals radius determined by comparing the computed Henry's law constant to a set of experimental data for methane in silicalite. This optimal oxygen radius was found to be 1.575 Å, which is

larger than the often-used values, such as 1.3 Å (Flanigen et al, 1987), 1.35 Å (Olson et al, 1981), and 1.4 Å (Ruthven, 1984). The ultimate goal for these type of approach is to determine all the parameters from an independent source, such as from quantum mechanics calculation and the structural analysis of the zeolite and molecules, and then to predict the adsorptive, diffusive and catalytic properties of a given molecule/zeolite system with no fitting parameter.

1.5 Thesis Outline

As stated at the beginning of this chapter, the objective of the thesis is to obtain a better understanding of diffusion in zeolites, particularly in relation to temperature and concentration effects.

In Chapter 2, two models (the GT model and the SV model) will be derived from the principles of statistical mechanics to bound the diffusional behavior of hydrocarbons in zeolites. The fundamental assumptions of the models will be validated by recent emerging experimental results characterizing molecular behavior inside zeolites. These two models are self-consistent models capable of predicting the diffusivity, based upon the information of molecular structure and zeolite framework, and that of the molecule-zeolite interactions. All the parameters in the models are well-defined, and can be determined independently. A Lennard-Jones potential method is used to estimate the potentials of a molecule at the channel and at the intersection. The concept of intracrystalline partitioning is introduced to account for differences in molecular rotational degree of freedom at the channel and at the intersection.

The stochastic models proposed by Theodorou and Wei (1983), and

Tsikoyiannis (1986) are extended to predict the collective behavior of molecules inside the lattice. Attempts are made to explain the concentration dependences of the diffusivity and the Langmuir parameter of the equilibrium isotherms in relation to the interactions among molecules. Molecular distributions due to the molecule-molecule interactions inside the lattice are also discussed.

In Chapter 3, the results of a systematic experimental study are presented. The diffusional and adsorptive properties of about 19 different hydrocarbons, including paraffins, aromatics and naphthene, in ZSM-5 and, to a lesser extent, in 5A are investigated. The effects of temperature, molecular diameter, molecular length, concentration, cage, Si/Al ratio, adsorption and desorption, zeolite modifier and activating process are probed. The equilibrium isotherms and adsorption capacities are reported. The objective is to generate reliable data to facilitate our understanding of zeolitic behavior, and to serve as a basis for comparison with the theoretical predictions.

In Chapter 4, the comparisons are made between the models proposed in Chapter 2 and the experimental results from Chapter 3, along with some of the experimental data in the literature which are reportedly consistent among different research groups. There are two key issues in these comparisons: the orders of magnitudes of diffusivity for a given molecule/zeolite system, and the concentration dependence of diffusivity. No fitting parameters are used in the model predictions. The good agreements between the experimental results and the theoretical predictions suggest that we might have captured the fundamentals of the diffusion in zeolites.

In Chapter 5, the results will be summarized.

2. THEORY

In this chapter, the effort will be devoted to developing a diffusion theory of hydrocarbons in zeolites. Four well-known diffusion regimes and their relationship to zeolite diffusion will be discussed first. A brief summary of the molecule-lattice interaction characterized by different techniques reported in the literature will be presented. These characteristics will lead to formulations capable of estimating the orders of magnitude of diffusivity for a given molecule/zeolite system. The interaction between molecules at high concentration will be proposed to be responsible for the concentration dependent trend of the diffusivity.

2.1 Introduction

2.1.1 Diffusion Regimes

According to Fick's first law of diffusion, the net diffusive flux of one species in a given direction is related to the gradient of the concentration of this species by a phenomenological relation:

$$J_x = -D\frac{\partial c}{\partial x} \tag{2.1}$$

where D is the diffusion coefficient or diffusivity. The minus sign means that diffusion occurs away from regions of high concentration.

There are four well-known types of diffusion: gaseous (or molecular) diffusion (Hirschfelder, 1954), Knudsen diffusion (Satterfield, 1980), liquid diffusion (Kirkaldy and Young, 1987), and atomic diffusion in solids (Kittle, 1976; Girigalco, 1973).

Figure 2.1 is a schematic of these four diffusion regimes.

In porous media exposed to a gas phase, gaseous diffusion retains its characteristics so long as the pore size is much larger than the mean free path of the molecules. Molecules collide with each other after travelling an average distance equivalent to their mean free path with the average kinetic speed determined by the Maxwell-Boltzmann distribution. When the pore size is smaller than the mean free path, collisions between molecules and the wall occur more frequently than collisions among molecules themselves. The average distance travelled before collisions approximately equals the pore diameter. Knudsen diffusion results.

In the condensed state of liquids, the diffusion process could be viewed as a gradual movement of molecules through the matrix as a result of thermal vibration and expansion. A liquid molecule would retain its kinetic energy, and the mean jump length is related to the free volume in the somewhat loosely packed structure of liquid molecules, and to the variation in free volume due to thermal expansion (Kirkaldy and Young, 1987).

For solids, an atom vibrates about its equilibrium position due to the strong bonding with neighboring atoms. The atomic vibrational mode with its frequency, ν, becomes responsible for diffusion. In one unit of time, the atom makes ν passes at the energy barrier presented by its neighbors, with a probability exp(-E/kT) of surmounting the barrier on each try. The jump length is often relatd to α, the lattice constant (Kittle, 1976).

The mathematic formulas to estimate the diffusivities of these four types of diffusion are summarized in Table 2.1. These formulas can be easily derived from

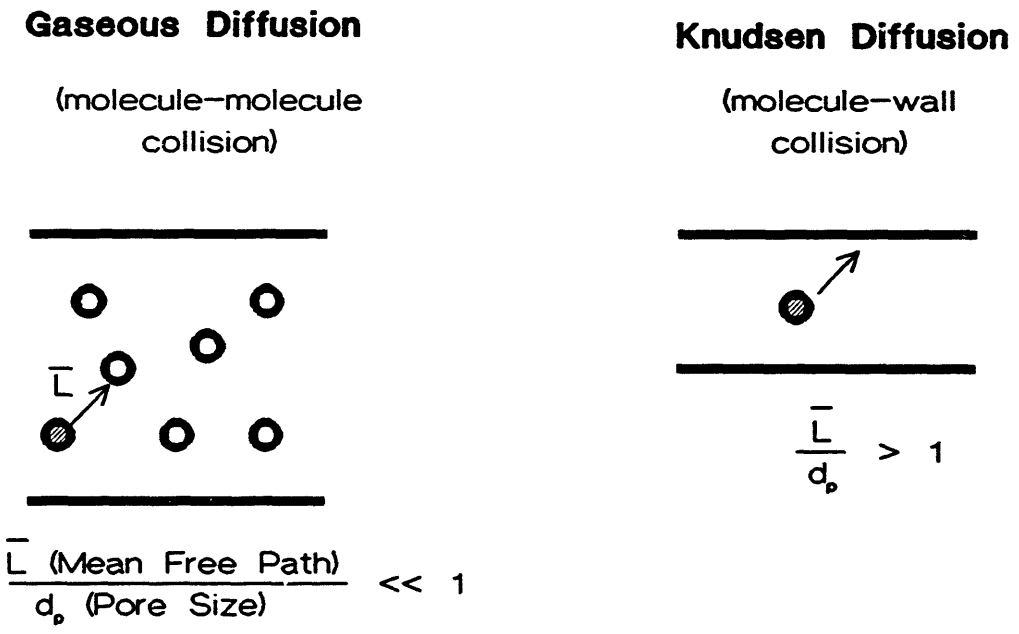

Figure 2.1 Schematic of Diffusion Regimes

$$J_x = - D \, \partial C/\partial x$$

$$D = g \; u \; L \; EXP(-E/RT)$$

	g	u	L	E
Gaseous	1/3	$(8kT/\pi m)^{1/2}$	$kT/\xi p \pi \sigma_m^2$	0
Liquid	1/3	$(8kT/\pi m)^{1/2}$	$3\alpha_T T \sigma_m$	0
Knudsen	1/3	$(8kT/\pi m)^{1/2}$	d_p	0
Solid	1/Z	$\nu \; \alpha$	α	10–90

* Z: coordination number;
  E: kcal/mol.

Table 2.1 Summary of Diffusivity Formulas (1)

their well-understood mechanisms. The diffusivities for all of these four cases can be expressed as:

$$D = g\,u\,L\,e^{-\frac{E}{RT}} \tag{2.2}$$

where u is the velocity, at which the molecule or the atom travels. L is the diffusional length (the average distance between collisions or jumps). E is the activation energy for diffusion, and g is a geometrical factor.

For gaseous, Knudsen, and liquid diffusion, the velocity is simply the averaged kinetic velocity, as stated in their mechanisms. The diffusional lengths are, respectively, the mean free path of the molecule for gaseous diffusion; the pore diameter, d_p, of the porous media for Knudsen diffusion; and the free volume length for liquid diffusion, which is related to the thermal expansion coefficient, α_T, the temperature, and the molecular size (Kirkaldy and Young, 1987). The orders of magnitude of the diffusional length at room temperature are typically about 1000 Å for gaseous diffusion, 100 Å for Knudsen diffusion, and 0.1 Å for liquid diffusion. Based on these diffusional lengths and the velocity value, the orders of magnitude of diffusivity yield 0.1 cm^2/s for gaseous diffusion, 0.01 cm^2/s for Knudsen diffusion, and 10^{-5} cm^2/s for liquid diffusion. These estimated values agree in order of magnitude with the measured diffusivities of these three diffusional regimes.

The weak temperature dependence of the diffusivities are $T^{1.5}$ for both gaseous and liquid diffusion, and $T^{0.5}$ for Knudsen diffusion. There is no activation energy for these diffusion processes. Gaseous diffusivity is inversely proportional to pressure, whereas Knudsen diffusivity is independent of pressure.

The factor of 1/3 listed in Table 2.1 as the geometry factor, g, is to indicate that those molecules moving in the y and z directions do not contribute to the diffusive flux in the x direction. In porous media, a tortuosity factor, τ, should be included in g to account for the irregular shapes of pores and the tortuous diffusion path in real pores which is greater than the distance along a straight line in the mean direction of diffusion. Values of τ are often found experimentally in the range of 2 to 7, and a value of $\tau = 4$ is recommended for estimation purposes in the absence of other information. Moreover, the diffusion flux per unit total cross section of the porous solid would be a fraction, θ_p, of the flux under similar conditions with no solid present, where θ_p is the porosity. Values of θ_p vary from about 0.3 to 0.7. In the absence of other information a value of $\theta_p = 0.5$ is recommended (Satterfield, 1980). The resulting diffusivity from considering the above effects is called the effective diffusivity, D_{eff}, defined as

$$D_{eff} = D \frac{\theta_p}{\tau} \tag{2.3}$$

The estimated effective diffusivities are, therefore, about 0.01 cm^2/s for gaseous diffusion, 10^{-3} cm^2/s for Knudsen diffusion in porous media.

It should be noted that for gaseous and Knudsen diffusion, the effective diffusivity defined above is often determined by passing two gases past opposite faces of a catalyst pellet and measuring the flux of one gas into the other (the Wicke-Kallenbach method). The concentration gradient used in the flux expression is the concentration difference in these two gaseous phases. If the concentration gradient inside porous media is to be used, a partition coefficient describing the equilibrium of molecules between gas phase and solid phase should be included in Eq. (2.3), as discussed in section 1.4.1., in the case where such a partitioning exits. There would

be significant corrections when the adsorbed concentrations are not linear with the gaseous concentrations.

Many solid solutions are interstitial, as shown in Figure 2.1, and interstitial atoms are able to move through the narrow interatomic channels. This type of diffusion is called interstitial diffusion. Furthermore all crystals contain vacancies, indicated by V in Figure 2.1. The number of vacancies increases rapidly with temperature up to about 0.01% of sites near the melting point. Even substitutional atoms near V (see Figure 2.1) can move by interchanging with the vacancies. This type of diffusion is called vacancy diffusion. The values of the characteristic atomic vibrational frequency, ν, are of the order of 10^{13} to 10^{14} s^{-1} (Kirkaldy and Young, 1987; Kittle, 1976). The lattice constant, α, is of the order of about 10 Å. Activation energy barriers that atoms have to overcome for a successful jump are about 10 to 90 kcal/mol (Kittle, 1976). Based on the above information, the upper bound for the diffusivity at room temperature is of the order of 10^{-8} cm^2/s. The temperature dependence of the diffusivity in solid is more dramatic, since diffusion in solids is an activated process. At the melting point, the diffusivities in solids may approach liquid diffusivity values (Kirkaldy and Young, 1987).

The diffusion of molecules in zeolite pores of comparable size presents us with a new diffusion regime, the "configurational regime" as coined by Weisz in 1973. As discussed in Chapter 1, the mechanism for this type of diffusion is still far from being well-understood. There is no well-accepted formula for estimating the diffusivity in this regime, in contrary to the four regimes discussed above where the mechanisms are well-understood and formulas are available for estimating the diffusivities. The objective of this chapter is, therefore, to develop a mechanistic theory for configurational diffusion, to propose a model (models) to estimate the diffusivity in

zeolites and predict the temperature as well as concentration dependence of the diffusivity.

Qualitatively, the movement of molecules in zeolites are "bounded" by two diffusional regimes: Knudsen diffusion and solid diffusion. Molecules inside zeolites, however, are not as free as in Knudsen diffusion where the effect of the potential field of the solid surface is minimal. In zeolites, molecules can never escape completely from the potential field of the lattice since the pore size is comparable to the molecular size. On the other hand, a molecule should not be bonded as strongly as an atom in the interstitials due to the existence of well-defined pore opening in zeolites. Interactions among molecules inside the lattice can further complicate the diffusional behavior. In order to understand how a molecule behaves inside zeolites, a brief summary of the molecule-lattice interaction characterized by different techniques reported in the literature will be presented in the following section. These characterization results will lead to the assumptions of our proposed diffusion models.

2.1.2 Characterization of Molecules Inside Zeolites

Recently, attempts have been made to characterize experimentally the interactions between molecules and zeolites by different techniques.

Cohen De Lara et al (1984) studied methane in 4A and 5A by IR and neutron scattering techniques. They observed that molecules inside the zeolites behaves in practically the same way as those in a liquid medium in respect to the rotational freedom. Molecules stay in the cavities for most of the time, although not at a specific site at a high temperature (> 300 K). At a lower temperature (<200 K),

molecules tend towards the surface of the wall and the mobility becomes more restricted.

Nagy et al (1983) studied the mobility of o-xylene and p-xylene in ZSM-5 at 37 °C by proton decoupled ^{13}C NMR spectroscopy. It was concluded that the spectrum of p-xylene was consistent with the rapid translational motion of molecules in all three zeolite channel directions. The p-xylene diffusion was fast on the NMR time scale, with an estimated mean time between jumps of less than 10^{-4} s. The o-xylene, however, gave a "rigid lattice" pattern, and was estimated to have a diffusion coefficient of about four orders of magnitude less than the p-xylene. The dynamics of organic molecules, such as methanol, benzene, toluene, and p-xylene, sorbed by zeolites ZSM-5, mordenite, Y and erionite were investigated by using solid-state deuterium NMR (Eckman and Vega, 1986). The results suggested that up to 150 °C, p-xylene molecules can move along the straight channels in ZSM-5, but do not move from the straight channels into the zigzag channels nor move along the zigzag channels on the NMR time scale of 10^{-5} s. The reorientation motion of toluene in ZSM-5 is less restricted than that of p-xylene. At room temperature, the toluene molecule cannot undergo a complete head-over-tail flip or complete three-dimensional diffusion. These motions become possible at higher temperatures. For benzene/ZSM-5, the motion of benzene molecules is nearly isotropic and benzene molecules rotate rapidly about the C_6 axes. Kustanovich et al (1988) demonstrated by (MASS) NMR study that the para axes of all sorbed p-xylene species are fixed in the lattice up to -70 °C. At higher temperature, p-xylene freely rotates about the molecular para axis, and reorientates the para axis by 90° to 112°. No evidence for the three-dimensional diffusion inside the channel system was found on the NMR time scale of 10^{-5} s.

Mentzen and his co-workers (1987a, b, c; 1988) probed the guest molecules, such as benzene, p-xylene, and n-hexane, adsorbed on ZSM-5 by X-ray powder profile refinements. They found that the benzene molecule appears to be present in the channel intersections, up to about 4 molecules/unit cell, with two simultaneous orientations, and free rotations about the axis. N-hexane molecules preferentially reside in the channels up to about 7 molecules/unit cell. At low concentration, p-xylene occupies the channel intersections with the methyl groups parallel to the straight channel, and at higher coverage (up to about 8 p-xylene molecules/unit cell) p-xylene appears in the sinusoidal channels, resulting in significant molecule-molecule interaction in addition to the interaction between molecules and the framework of zeolite.

Fraissard (1987) conducted an NMR study of ^{129}Xe adsorbed on zeolites Z, ZSM-5, ZSM-11, CaA, X, and Y. He found that at lower concentrations the molecule-wall collision is the dominant factor whereas at higher concentrations the molecule-molecule collision becomes important.

An IR study done by Aroson et al (1987) indicated that 2-methyl-2-propanol and 2-propanol dehydrate in ZSM-5 to form carbonium ion-like intermediates prior to desorption. Egelstaff et al (1968) examined water, methyl alcohol, methyl cycanide, and ammonia in 3A by neutron scattering. They concluded that molecules vibrate with the vibrational frequency of the zeolite lattice before they jump to a new orientation in the cage.

Some of the above observations are supported by some of the theoretical calculations. Nowak et al (1987) showed by a Lennard-Jones type of approach that benzene retains the orientational freedom, though restrictively, at the intersections

of silicalite channels. The simulations by June et al (1988) predicted that normal hexane prefers to sit in the sinusoidal pores while branched 2-methyl pentane prefers to sit at the intersections.

The experimental and the theoretical results in the literature on characterization of molecules inside zeolites are not conclusive, sometimes even contradictory. The following pictures have nevertheless emerged from these observations:

(1). Bulky molecules, such as aromatics and branched paraffins, are localized at the channel intersections of ZSM-5. Smaller molecules, such as normal paraffins, prefer to sit in the channels of ZSM-5.

(2). Above room temperature, non-polar molecules rotate as freely, if not as those in the gas phase, at least as those in the liquid phase. At very low temperatures, molecules might become more attached to the surface of the lattice.

(3). Polar molecules with strong specific interactions with the framework of zeolites, such as water and alcohol, might be adsorbed very strongly on the adsorption sites, and vibrate with the host lattice.

(4). At low concentrations, the molecule-lattice interaction is the dominant factor. The molecule-molecule interaction becomes important at high concentrations.

In the remainder of this chapter, a diffusion theory of hydrocarbons in zeolites will be proposed based on the above pictures.

2.2 Diffusivity In Zeolites: Orders of Magnitude and Temperature Effect

Based upon the experimental observations discussed above, we propose that the diffusion in zeolites is bounded by two extreme cases characterized by two models:

the Gas Translation (GT) Model:

> the molecules inside the zeolite lattice retain their gaseous characteristics, although the movement of molecules from site to site becomes restricted and has to overcome the energy barrier imposed by the channels;

the Solid Vibration (SV) Model:

> the molecules inside the zeolite lattice lose their gaseous entity because of the strong interaction between the zeolite framework and the molecules; the molecules vibrate with their host lattice before accumulating enough energy to jump to the neighboring sites.

In reality, the molecules would behave somewhere in between those two limiting cases.

2.2.1 Derivations of the GT Model and the SV Model

In this section, the mathematical expressions for the GT model and the SV model will be derived from the principles of statistical mechanics.

Considering a molecule in a potential field, V(x), of a periodic lattice, as

shown in Figure 2.2, we assume that

(1). The diffusion process in zeolites is an activated process. A molecule spends most of its time at its equilibrium position. The difference between the maximum energy, Φ_{max}, and the minimum energy, Φ_{min}, is approximately the activation barrier, E. When the molecule of mass, m, acquires an energy equal to or greater than the activation energy by thermal interaction with its surroundings, it climbs out of the well and moves over the barrier to enter a new equilibrium position adjacent to its old one.

(2). The molecule will have a mean velocity u given by classical statistical mechanics as

$$u = \sqrt{\frac{8kT}{\pi m}} \tag{2.4}$$

The assumption (1) is consistent with the experimental observations summarized in the last section that the molecules are localized in the zeolite, and that the diffusion process is an activated process. For the small molecules that preferentially reside in the channels, the equilibrium positions of the molecules are in the channels; and for the bulky molecules that preferentially reside at the channel intersections, the equilibrium positions are at the intersectons. In assumption (2), we assume that the mean velocity can still be determined by the Maxwell-Boltzmann distribution. As verified by Ross and Mazur (1961), the characteristic velocity is still Maxwellian type as long as the rate of diffusion is slower compared to the rate of collision between molecule and wall. The diffusion can only perturb the Maxwellian distribution of the speeds by, for instance, removing the molecules with kinetic energy

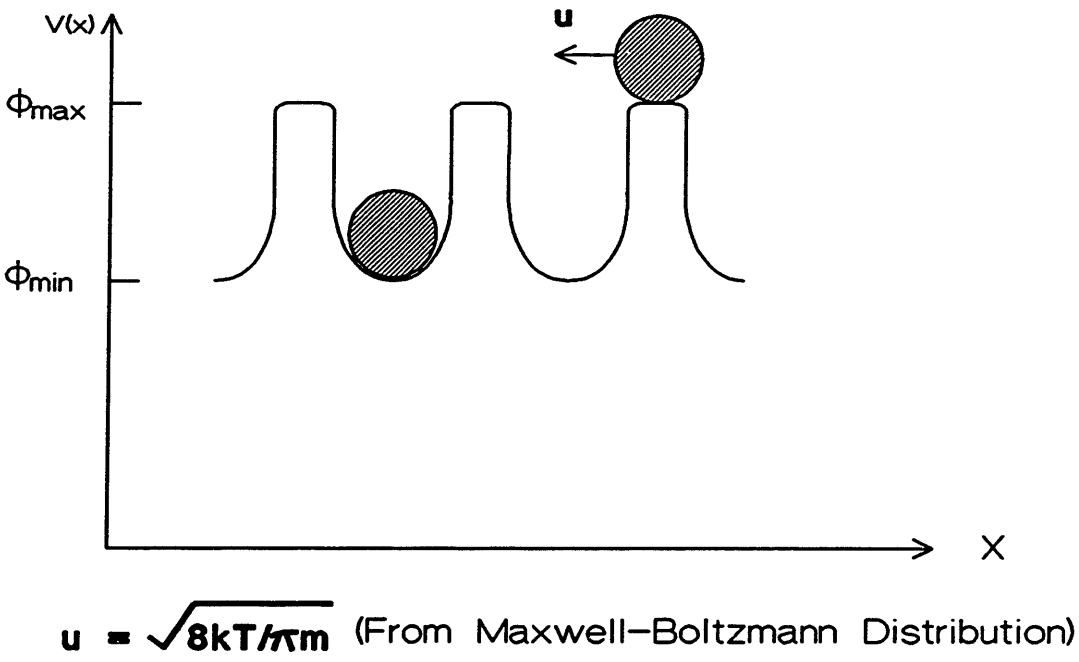

Figure 2.2 Particle in a Potential Field of Periodic Lattice

larger than the activation energy. The continuous molecule-wall interaction, however, tends to restore this distribution.

In a time interval, t, the molecule spends most of its time, t_b, near the bottom of a well, and a small amount of time, t_t, at the top of the barrier with velocity, u. The average velocity of the molecule travelling in the lattice, u_a, can be determined by

$$u_a = u \frac{t_t}{t} \tag{2.5}$$

Since a jump is relatively rare, t is very nearly equal to t_b. Thus, the above equation becomes approximately

$$u_a = u \frac{t_t}{t_b} \tag{2.6}$$

The ratio t_t/t_b can be obtained from the basic axiom of statistical mechanics that states that ensemble averages are equal to time averages. The time a system spends in any group of states is proportional to the partition function for those states. Therefore, we have

$$u_a = u \frac{\int_t e^{-V(x)/kT} dx}{\int_b e^{-V(x)/kT} dx} \tag{2.7}$$

At the top of the potential well,

$$V(x) \sim \Phi_{max} = constant \tag{2.8}$$

Therefore,

$$\int_t e^{-V(x)/kT} dx = e^{-\Phi_{max}/kT} \alpha_t \tag{2.9}$$

where α_t is the size of the well-top.

At the intersection (the bottom of the well), V(x) can be expanded in its Taylor's series as

$$V(x) = \Phi_{min} + \frac{1}{2}\frac{\partial^2 V}{\partial x^2}x^2 + O(x^3) \tag{2.10}$$

We consider two extreme cases, the flat-bottom well and the harmonic oscillator, as shown in Figure 2.3.

For the flat-bottom well case, the potential, V(x), at the bottom remains approximately constant even for a small perturbation from its equilibrium position. The following equations hold

$$\frac{\partial^2 V}{\partial x^2} \sim 0 \tag{2.11}$$

and

$$V(x) \sim \Phi_{min} \tag{2.12}$$

For the case of the harmonic oscillator, we assume that the molecule is harmonically bound to the energy minimum in accord with Hooke's law so that

the Flat-Bottom Well:

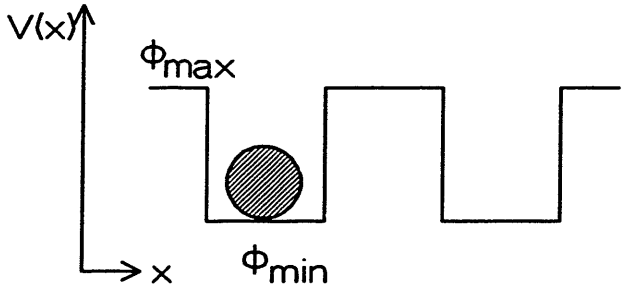

the Harmonic Oscillator:

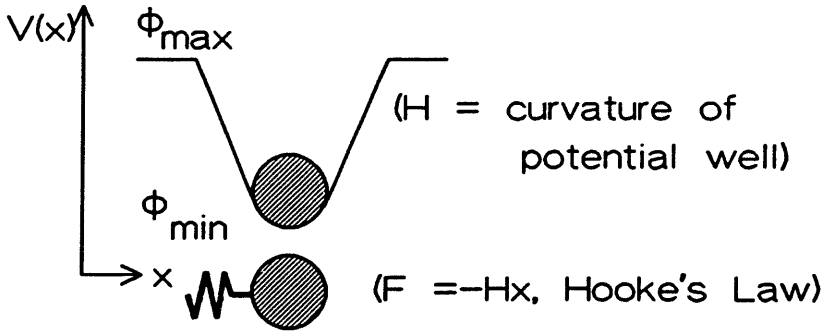

Figure 2.3 the Flat-Bottom Well and the Harmonic Oscillator

$$\frac{\partial^2 V}{\partial x^2} = H \tag{2.13}$$

and

$$V(x) \approx \Phi_{min} + \frac{1}{2}Hx^2 \tag{2.14}$$

where H is the Hooke's law constant, which is the curvature of potential well at the well bottom. Therefore, we have

$$\int_b e^{-V(x)/kT} dx \approx e^{-\Phi_{min}/kT} \alpha_b \qquad \textit{for the flat-bottom well} \tag{2.15}$$

where α_b is the length of the well bottom, and

$$\int_b e^{-V(x)/kT} dx \approx e^{-\Phi_{min}/kT} \int_{-\infty}^{+\infty} e^{-Hx^2/2kT} dx = \sqrt{\frac{2\pi kT}{H}}\, e^{-\Phi_{min}/kT} \tag{2.16}$$

for the harmonic oscillator

The integral should be taken over the bottom of the well and part way up to its wall. The above integration is, however, taken from -∞ to +∞. Only a negligible error is introduced since the exponential factor rapidly approaches zero as x becomes large.

The flat-bottom well corresponds to the GT model where molecules have no specific interaction with the lattice. The activation energy is mainly due to the structural constraints of the lattice. We call this type of the activation energy "configurational activation energy". The harmonic oscillator corresponds to the SV model where the specific interaction between molecule and lattice is strong and dominant. The corresponding activation energy is called "desorption activation energy". In reality, the ativation energy for the diffusion should be the combination of these two types of activation energy.

Combining Eqs. (2.7), (2.9), (2.15) and (2.16), and assuming $\alpha_b \approx \alpha_t \approx 0.5\alpha$, where α is the distance between the adjacent sites, we obtain the following expressions for the GT model and the SV model:

$$u_a = \sqrt{\frac{8kT}{\pi m}}\, e^{-E/kT} \qquad \textit{for the GT model} \tag{2.17}$$

where $E \equiv \Phi_{max} - \Phi_{min}$; and

$$u_a = \nu_e\, \alpha\, e^{-E/kT} \qquad \textit{for the SV model} \tag{2.18}$$

where $\nu_e (\equiv (1/\pi)(H/m)^{0.5})$ is the effective vibrational frequency of the molecule inside the zeolite.

Analogous to Eq. (2.2), the diffusivity formula for molecules in zeolites can be expressed as a product of z, u_a and α:

$$D = \frac{1}{z}\sqrt{\frac{8kT}{\pi m}}\, \alpha\, e^{-E/kT} \qquad \textit{for the GT model} \tag{2.19}$$

$$D = \frac{1}{z}\, \nu_e\, \alpha^2\, e^{-E/kT} \qquad \textit{for the SV model} \tag{2.20}$$

where z is the coordination number of the zeolite. It should be noted that the diffusivities given above are the diffusivities of molecules from a site to a particular adjacent site for the GT model and the SV model respectively. The average velocity in the lattice as in Eq. (2.17) or in Eq. (2.18) is the overall velocity of the molecule. A factor of 1/z is included in Eqs. (2.19) and (2.20) to indicate that the possibility of a molecule moving to other sites does not contribute to the diffusive flow in the direction under consideration.

In the section 2.3, we will re-derive Eqs. (2.19) and (2.20) more rigorously from Eqs. (2.17) and (2.18) using the stochastic theory.

Table 2.2 compares the diffusivity formulas derived above for the configurational regime with those for the four other well-known regimes. The range of the activation energy for diffusion in zeolites is from Ruthven (1984). As expected, the diffusion in zeolites is indeed bounded by Knudsen diffusion in one extreme and solid diffusion in the other end. For the GT model, if pore size becomes much larger than the molecule size, the activation energy approaches zero and the molecule-zeolite interaction might eventually diminish as in the case of Knudsen diffusion. The upper bound of the activation energy of zeolitic diffusion is close to the lower bound of the activation energy of solid diffusion, as shown in Table 2.2. The stronger molecule-lattice interaction might eventually make diffusion in zeolites approach solid diffusion.

Every term in Eqs. (2.19) and (2.20) is well-defined, and can be determined independently. The pre-exponential term of the GT model can be easily calculated once the coordination number, temperature, molecular weight, and distance between the intersections are specified. For example, z is equal to 4 for ZSM-5, and 6 for 5A. And α is about 10 Å for ZSM-5, and 12 Å for 5A. These values result in a pre-exponential term of about $4\times10^{-4}(T/M)^{1/2}$ (cm^2/s) for ZSM-5, and $3\times10^{-4}(T/M)^{1/2}$ (cm^2/s) for 5A, where M is the molecular weight. At room temperature, a molecule with molecular weight of about 80 would have a diffusivity of about 10^{-11} (cm^2/s) according to the GT model if the activation energy is 10 kcal/mol. The activation energy in the GT model is simply the potential difference between molecule residing in the channel and one residing at the intersection. It can be estimated, to be discussed in the next section, based upon the structure of the molecule and the lattice

$$J_x = - D \, \partial C/\partial x$$

$$D = g \; u \; L \; EXP(-E/RT)$$

		g	u	L	E
Gaseous		1/3	$(8kT/\pi m)^{1/2}$	$kT/\xi p \pi \sigma_m^2$	0
Liquid		1/3	$(8kT/\pi m)^{1/2}$	$3\alpha_T T \sigma_m$	0
Knudsen		1/3	$(8kT/\pi m)^{1/2}$	d_p	0
CF	GT	1/Z	$(8kT/\pi m)^{1/2}$	α	1–15
	SV	1/Z	$\nu_e \alpha$	α	
Solid		1/Z	$\nu \alpha$	α	10–90

* CF: Configurational Diffusion;
Z: coordination number;
E: kcal/mol.

** $\nu_e = (1/\pi)\sqrt{(H/m)}$

$E = \Phi_{max} - \Phi_{min}$ for GT & SV

Table 2.2 Summary of Diffusivity Formulas (2)

are known.

For the SV model, the "bonding" between the molecule and the site of adsorption, such as the site of a cation, needs to be specified and calculated before the pre-exponential term and the activation energy can be determined. The effective vibrational frequency is related to the curvature of the potential well and the molecular weight. If we assume that the effective vibrational frequency is about the order of 10^{12} s^{-1} (Barrer, 1978), the pre-exponential term of the diffusivity thus determined is about 10^{-3}.

In this thesis, we are interested in mainly non-polar molecules, such as branched paraffins and benzene, and temperatures above room temperature. As the results of the characterization of molecules in zeolites indicated, the behavior of these molecules is more likely in accord with the GT model. We will show later on that predictions of GT model on the orders of magnitude of the diffusivity are in good agreement with our experimental results. We will therefore use the GT model in our analysis. If one extends the study to polar molecules or to substantially low temperatures where molecules begin to attach to the surface of the lattice as discussed in the last section, the SV model might then become applicable.

2.2.2 Estimation of Activation Energy

In the last section, the dynamic problem of zeolitic diffusion was transformed to a simpler steric problem: the evaluation of the potential field of a molecule in a zeolite channel system. Once the activation energy of diffusion is estimated, the GT model can then be used to predict the diffusivity.

The following approximations are used in a quick estimation of the configurational activation energy attempted here:

(1). The potential energy is attributed to the interactions between the molecule and the oxygen atoms of the zeolite lattice only. Thus, the interactions due to silicon atoms and any cation are ignored in the calculation. No interaction between molecules is included.

(2). The geometry of zeolite frameworks is simplified. The intersection (or cage) is assumed to be spherical in shape with the oxygen atoms on the surface of the sphere. The channel is circular, and the oxygen atoms are equally spaced at the perimeter of the circle. The molecule at the intersection is modelled as "a sphere (molecule) in a concentric sphere (intersection)". The diameter of the molecule is determined from the spherical representation of the molecule; it is equivalent to the Lennard-Jones length constant, σ_m. A molecule at the channel is modelled as "a circlar disc (molecule) in a concentric circle (channel)". The diameter of the molecule is the minimum cross-sectional diameter of the molecule, d_m. The values of σ_m and d_m for different molecules are given in Table 1.1, together with the values of the potential-energy constant, ϵ_m. The molecule is either at the center of the intersection, or at the center of the channel.

Although the above assumptions are oversimplified, this model, as it will be shown later, can nevertheless reveal some very interesting features of the interaction between the molecule and the zeolite frameworks. In some cases, it can predict the activation energy for diffusion with good accuracy.

The above assumptions lead to the following sum of Lennard-Jones potentials:

$$\Phi_c \sim \sum_{O\ ions} 4\epsilon \left[\left(\frac{\sigma_c}{r_c}\right)^{12} - \left(\frac{\sigma_c}{r_c}\right)^{6}\right] \tag{2.21}$$

for the potential at the channel. The total number of oxygen ions is 8 for the eight membered ring of 5A, and 10 for the ten membered ring of ZSM-5. The distance, r_c, from the center of the channel to the nuclei of oxygens can be calculated as

$$r_c = \frac{1}{2}(d_c + d_o) \tag{2.22}$$

where d_c is the diameter of the channel and d_o is the diameter of the oxygen atom. In this study, d_c and d_o are given the values of 5.8 Å and 2.6 Å for ZSM-5 as used by Flanigen et al (1987), and 4.2 Å and 2.8 Å for 5A following Ruthven (1984). The potential length constant, σ_c, for each molecule-oxygen pair at the channel is taken as

$$\sigma_c = \frac{1}{2}(d_m + d_o) \tag{2.23}$$

The corresponding ϵ is

$$\frac{\epsilon}{R} = \sqrt{113\frac{\epsilon_m}{R}} \tag{2.24}$$

where R is gas constant and 113 is the value of ϵ_o/R for oxygen (Bird et al, 1960).

Similarly, the potential at the intersection can be estimated as:

$$\Phi_i \sim \sum_{O\ ions} 4\epsilon \left[\left(\frac{\sigma_i}{r_i}\right)^{12} - \left(\frac{\sigma_i}{r_i}\right)^{6}\right] \tag{2.25}$$

Since each unit cell of ZSM-5 contains 192 oxygen atoms and four intersections, we assume that each intersection contains 48 oxygen atoms. The average channel size of ZSM-5 is about 5.4 Å (=[5.1+5.8+5.4+5.4]/4). The effective diameter of the intersection, d_i, is therefore approximately 8.7 Å (=[$\sqrt{2}$ (5.4/2 +2.6/2)x2-2.6]), which is very close to the literature value of 9 Å (Nowak et al, 1987). According to assumption (2), all of the 48 oxygen atoms are assumed to be positioned on the surface of a sphere with 8.7 Å in diameter. For 5A, there are 72 oxygen atoms on a spherical cage of about 11.4 Å in diameter (Barrer, 1978; Breck, 1974).

Accordingly, we also have

$$r_i = \frac{1}{2}(d_i + d_o) \tag{2.26}$$

and

$$\sigma_i = \frac{1}{2}(\sigma_m + d_o) \tag{2.27}$$

The potentials at the channel and at the intersection can therefore be calculated respectively, by using Eqs. (2.21) to (2.27) once the values of d_m, σ_m, and ϵ_m are specified, together with the values of d_c, d_i, and d_o, and the numbers of oxygen atoms in the channel and in the intersection.

Figure 2.4 demonstrates the results of such calculations of Φ_i and Φ_c in ZSM-5 for molecules with different molecular diameters. A value of 210 was assumed for ϵ/R for illustrative purpose. The values of r_c and r_i were obtained from Eqs. (2.22) and (2.26) based on the values of d_c, d_i, and d_o specified above for ZSM-5. The x-axis is d_m and σm. As shown in the figure, molecules with Lennard-Jones length

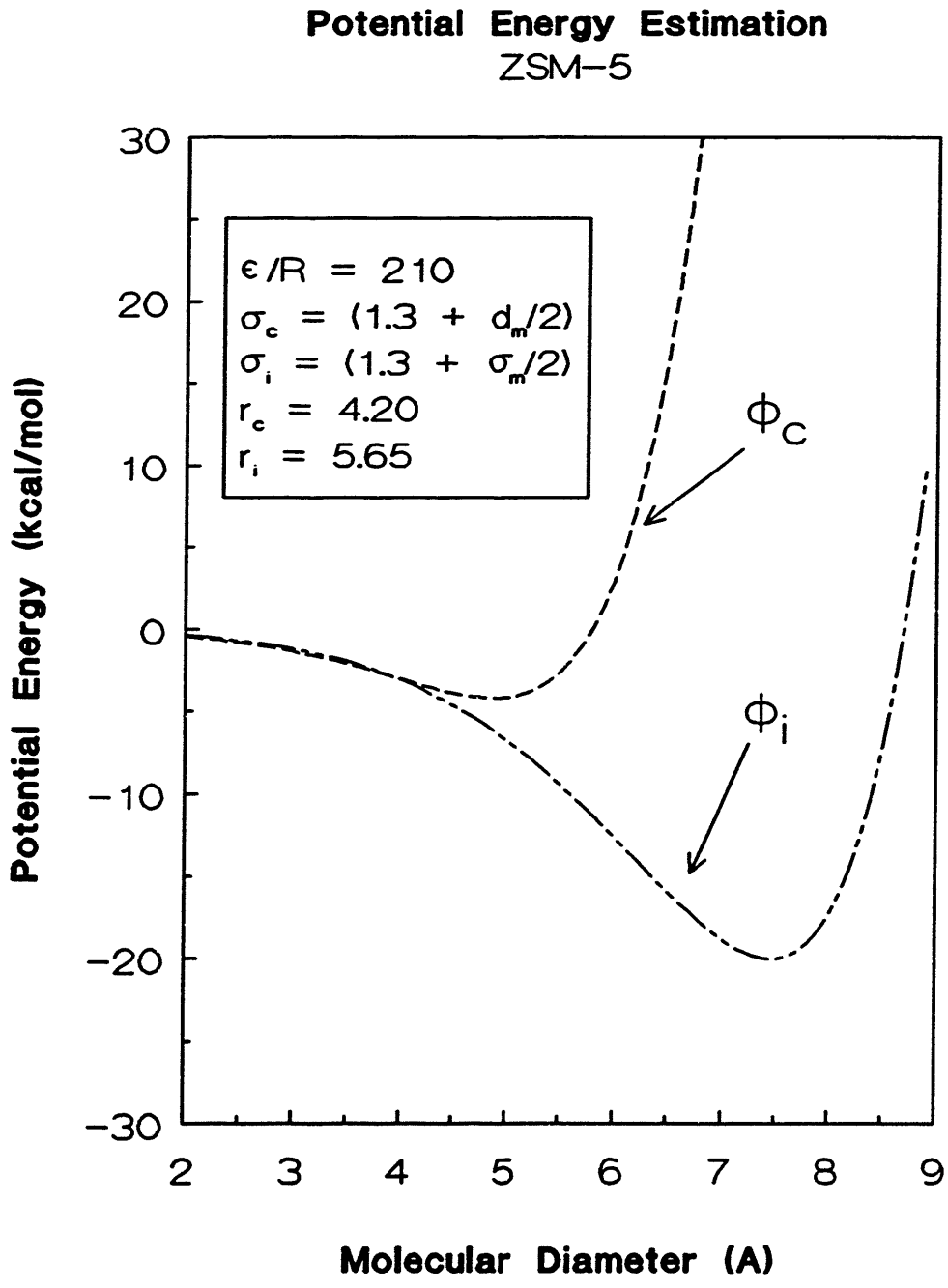

Figure 2.4 Potential Energy Estimations in ZSM-5

constants smaller than about 7.5 Å will experience stronger attractive forces from the zeolite framework at the intersection as the length constant increases. Once the potential length constant is larger than the intersection diameter (8.7 Å), the molecule will experience repulsive interactions from the intersection. It means that it will be difficult for a molecule with a length constant larger than about 8.7 Å to form at the intersection due to steric constraints. This corresponds to the case of the transition state selectivity as discussed in Chapter 1. The results of Φ_c show that even for a molecule with a diameter of about 3 Å, it will still experience moderate attraction from the wall while passing through the channel. The attractions become a little more pronounced for molecules with a diameter of about 5 Å. When the molecular diameter is larger the channel size, about 5.8 Å, the interaction between the molecule and the channel becomes repulsive. It will be very difficult for a molecule with a minimum diameter larger than 6.5 to 7 Å to enter the channel of ZSM-5 due to the strong repulsion from the channel (the repulsive potential is about 30 kcal/mol for a molecule with a minimum diameter of 6.5 Å).

From the calculations as demonstrated above, the activation energy can be estimated from the difference of Φ_c and Φ_i when d_m, σ_m and ϵ_m are given. For example, the values of d_m, σ_m, and ϵ_m/R for benzene are 5.85 Å, 5.4 Å and 214 ^oK from Table 1.1. The estimated E is about 9.62 kcal/mol. The experimental value of the activation energy is about 9.7 kcal/mol (see Chapter 3). The detailed atom-atom potential calculations (Nowak et al, 1987) predict an activation energy of about 5.25 kcal/mol to 10.75 kcal/mol for the diffusion of benzene in silicalite. These consistent results suggest that the Lennard-Jones potential method described above can be used at least for some systems to estimate the activation energy as a first-order approximation. More comparisons between the model predictions and the experimental data will be given in Chapter 4.

In the above calculations, a molecule is positioned at the center of the channel or the center of the intersection. Figure 2.5 shows that when the mass center of a benzene molecule ($d_m > d_c$) moves away from the center of the channel the interaction potential tends to increase. A similar result is presented in the same figure for 2-methylbutane ($d_m < d_c$) which experiences attractions from the channel while passing through. The molecule again is shown to preferably stay at the center of the channel. The center line approximation is therefore valid, at least for these systems we are interested in. The same conclusion was drawn by Nowak et al (1987).

All the parameters in this Lennard-Jones potential method can be determined independently, from structural information of the zeolite, and the molecular properties. No fitting parameter is therefore needed to predict the diffusivity of hydrocarbons in zeolites by using the GT model and this L-J method. Since it is oversimplified, this Lennard-Jones method has its limitations. Changing the molecular representation from spherical model to the more realistic shape by using more than one characteristic length constant, using the reported crystal structures to describe the geometry of the zeolite frameworks instead of assumption (2), and calculating the potential profiles at different positions in the channel system might improve the estimation and give us a more detailed understanding of the molecule-lattice interaction.

2.2.3 Intracrystalline Partitioning

When a rod shape molecule, such as a normal-paraffin, is inside a large-cage-small-channel zeolite, such as 5A, a concept of intracrytalline partitioning needs to be introduced. If the molecule is no longer than the cage size, it is plausible that the molecule can have head-over-tail rotation inside the cage. On the other hand, the

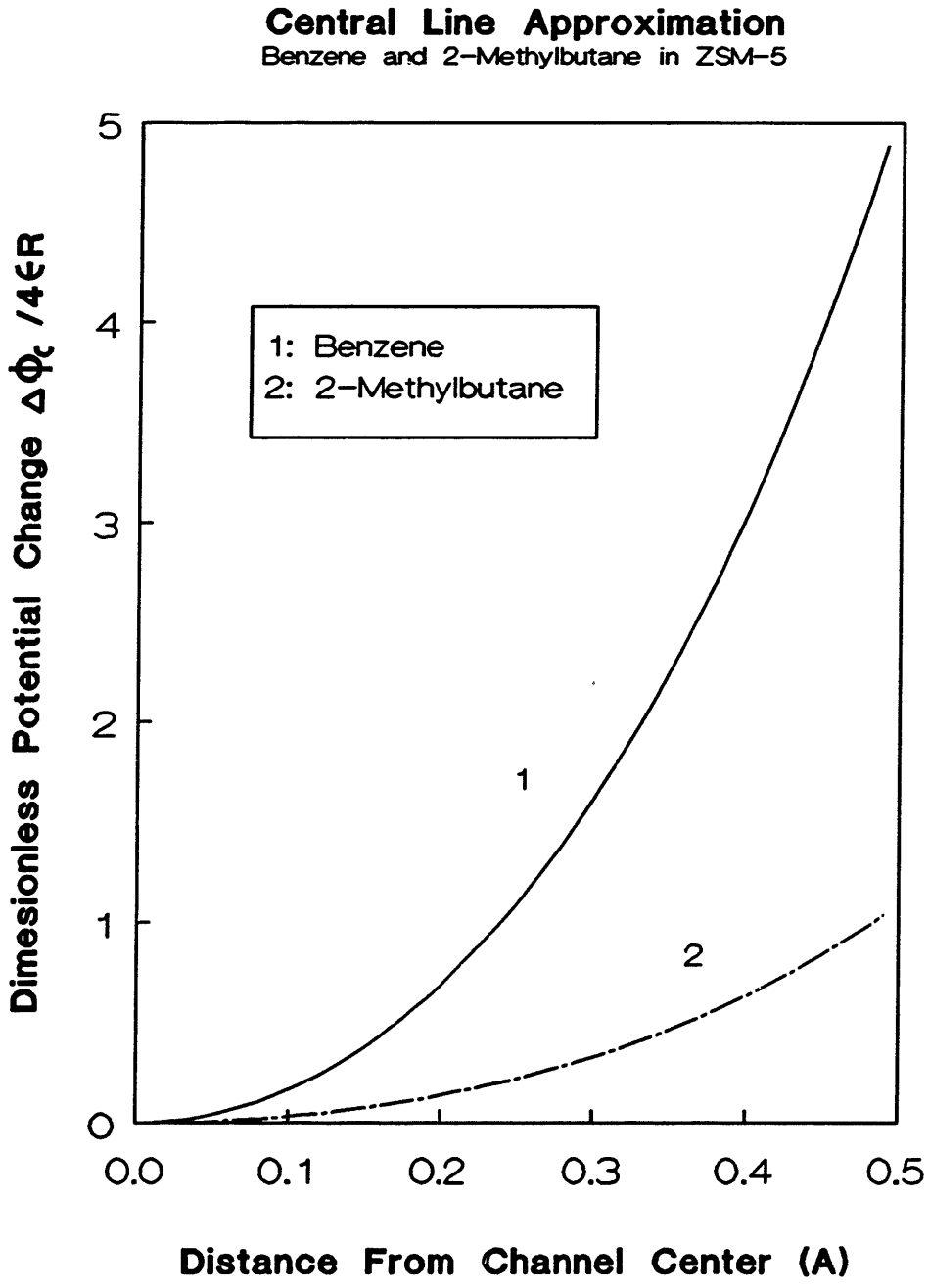

Figure 2.5 Central Line Approximation

molecule in the channel can not perform head-over-tail rotation. The molecule has to orient itself properly so that it can pass through the channel since the molecular length of a paraffin is larger than the channel diameter. The molecule, therefore, loses rotational degrees of freedom (head-over-tail) in the channel, as shown in Figure 2.6. In this case, the GT model should be modified to include the intracrystalline partitioning effect. For ZSM-5, however, this effect might be negligible since the channel size is close to the intersection size.

Assume that n-paraffins are rigid, one-dimensional, rod shape linear molecules. The rotational partition function is then

$$q_r = \frac{8\pi^2 IkT}{\zeta h^2} \tag{2.28}$$

where ζ is the external symmetry number, k is the Boltzmann constant, h is Planck's constant, and I is the moment of inertia (Barrow, 1973). The value of I can be estimated by

$$I = \sum_n m_n r_n^2 \tag{2.29}$$

where n numbers off the atoms of the molecule.

The corresponding GT model modified to include the intracrystalline partitioning effect, called the GT_{ip} model, can therefore be expressed as

$$\begin{aligned} D &= \frac{e}{q_r}\,\frac{1}{z}\sqrt{\frac{8kT}{\pi m}}\;\alpha\; e^{-\frac{E}{kT}} \\ &= \left[\frac{h^2\zeta e}{8\pi^2 IkT}\right]\frac{1}{z}\sqrt{\frac{8kT}{\pi m}}\;\alpha\; e^{-\frac{E}{kT}} \qquad \textit{for the } GT_{ip} \textit{ model} \end{aligned} \tag{2.30}$$

A factor of e is included in the pre-exponential term to account for the loss of

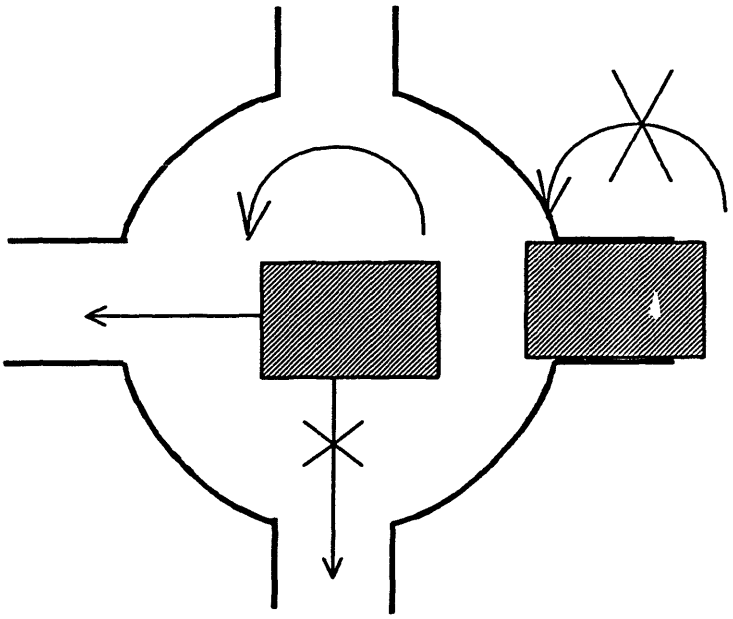

(e.g. n–Paraffin in 5A)

loss of rotational degree
of freedom in the channel

Figure 2.6 Intracrystalline Partitioning

rotational energy (kT) at the channel.

The diffusivity for this type of molecule/zeolite system decreases with increasing in the moment of inertia. The longer the n-paraffin, the larger the value of I, and the larger the effect of intracrystalline partitioning. For example, the intracrystalline partitioning factor, e/q_r, is of the order of 10^{-1} for ethane, and 10^{-3} for n-butane. The pre-exponential term of the diffusivity for n-butane/5A should be of the order of about 10^{-6} cm^2/s at room temperature, according to the GT_{ip} model. The intracrystalline partitioning can therefore reduce the pre-exponential term by as many as three orders of magnitude. More discussions will be given in Chapter 4.

In summary, we have proposed two mechanistic models capable of predicting the diffusivity in zeolites, the GT model (and its modified form, the GT_{ip} model), and the SV model, based on our understanding of the molecule-lattice interactions. For the diffusion of hydrocarbons in ZSM-5, the GT model should be used. The GT_{ip} model should be employed for n-paraffins in 5A. When dealing with the polar molecules, the SV model might be applicable. All the parameters in the models are well-defined, and can be estimated independently. A very simple Lennard-Jones method is introduced to estimate the activation energy as a first-order approximation. The orders of magnitude of zeolitic diffusivity can therefore be estimated.

2.3 Diffusivity In Zeolites: Concentration Dependence (I)

In section 2.2, the movement of an individual molecule is considered. In this section, the collective diffusional behavior of molecules inside the zeolite lattice will be studied by stochastic theory. The aim is to investigate how the interaction between molecules would affect their diffusion characteristics. We will first consider

the case where the soft-interactions, such as attraction or repulsion, between guest molecules are negligible. In the next section, the repulsive interaction between molecules will be included in the modeling.

Following Theodorou and Wei (1986), and Tsikoyiannis (1986), we make the following assumptions as the basic rules for diffusion in the lattice:

(1). The movement of molecules within the lattice is a series of activated jumps between sites.

(2). Each jump event is an independent Poisson Process.

(3). A molecule is activated, and one of its neighboring sites is randomly selected. If the site is not fully occupied, the activated molecule jumps to the new site. If the site is already occupied, then the molecule remains where it is. And a new choice of activated molecule and direction of jump is then made.

As we mentioned in Chapter 1, a different rule was used in the studies of Palekar and Rajadyakhsha (1984) and Aust et al (1989). They assumed that an activated molecule jumps to a new site unless all the adjacent sites are occupied.

There are at least three ways to solve the diffusion problem based on the assumptions described above: the Master Equation, Monte-Carlo simulations, and the correlation functions. The Master Equation gives the complete description of the correlation among all the molecules at all sites at a given time. It is, however, not realistic to solve such a large-dimensional system. The Monte Carlo simulations can provide a solution for the process given by three rules above. It is, however, not an

analytical solution so that it might be difficult to use, and the simulations are sometimes computation-intensive. Correlation functions can be used to achieve approximate analytic solutions to the problem. First-order correlation functions only consider the sites immediately adjacent to the target site, instead of all the sites in the lattice as in the Master Equation. In this study, first-order correlations will be used, following Tsikoyiannis (1986).

For the Non-Interacting Lattice Model, additional diffusion rules besides the three rules specified above are as follows:

(4). All molecules are non-interacting.

(5). Double occupancy is excluded.

The assumption (4) means that the soft-interactions between molecules are negligible, compared to the dominant interactions between the molecule and the lattice. The assumption (5) means that at a given time no more than one molecule can occupy a site.

The first-order occupancy correlation function, $\theta(S_i, X; t)$, is defined as the probability of finding a molecule, X, at site, S_i, at time, t, for a specified initial condition. Thus, knowledge of the first-order correlation functions is sufficient to give us the occupancy profiles of the species within the lattice. The second-order occupancy correlation functions give us a measure of how the state of two sites in the lattice are correlated for the particle motion. Although they can be defined for any pair of lattice sites, only the correlation functions corresponding to neighboring sites will concern us here. Therefore, $\theta(S_i, X; S_j, 0;t)$ is the joint probability of finding a

molecule at site, S_i, and no molecule at its neighboring site, S_j, at time,t, with the same initial condition for $\theta(S_i, X; t)$. According to the diffusion rules given above, we have

$$\frac{d\,\theta(S_i, X; t)}{d\,t} = q \sum_{S_j} \theta(S_j, X; S_i, 0; t) - \theta(S_i, X; S_j, 0; t) \qquad (2.31)$$

where the sum over S_j extends over all nearest neighboring sites of S_i.

Rigorously speaking, q in the above equation is the rate parameter of the Poisson distribution that describes the jump of a molecule from one site to a particular adjacent site. At the level of the first-order correlation functions, q can be simply viewed as the jump frequency from one site to a particular site.

In section 2.2, the average molecular velocity, u_a, is defined as the velocity of the molecule travelling in all directions. The value of q can then be related to u_a in accord with the definitions of q and u_a by

$$q = \frac{1}{z}\frac{u_a}{\alpha} \qquad (2.32)$$

where z is the coordination number of the lattice, and α is the distance between two neighboring sites.

Since the sum of the probability of mutually exclusive events is one, we have

$$\theta(S_i, X; S_j, 0; t) + \theta(S_i, X; S_j, X; t) = \theta(S_i, X; t) \qquad (2.33)$$

and

$$\theta(S_j, X; S_i, 0; t) + \theta(S_j, X; S_i, X; t) = \theta(S_j, X; t) \qquad (2.34)$$

If the correlations between neighboring sites are neglected, the joint probability can

then be written as

$$\theta(S_i, X; S_j, X; t) = \theta(S_i, X; t)\ \theta(S_j, X; t) \tag{2.35}$$

and

$$\theta(S_j, X; S_i, X; t) = \theta(S_j, X; t)\ \theta(S_i, X; t) \tag{2.36}$$

Eq. (2.31) can be rewritten as

$$\frac{d\ \theta(S_i, X; t)}{d\ t} = q \sum_{S_j} \theta(S_j, X; t)(1 - \theta(S_i, X; t)) - \theta(S_i, X; t)(1 - \theta(S_j, ,X; t)) \tag{2.37}$$

And Eq. (2.37) can be further simplified to

$$\frac{d\ \theta(S_i, X; t)}{d\ t} = q \sum_{S_j} [\ \theta(S_j, X; t) - \theta(S_i, X; t)\ ] \tag{2.38}$$

For a large lattice, Equation (2.38) can be approximated by a corresponding differential equation

$$\frac{\partial\ \theta}{\partial\ t} = q\ \alpha^2\ \nabla^2\ \theta \tag{2.39}$$

Thus, the Fick's law diffusivity is

$$D = q\ \alpha^2 \tag{2.40}$$

Combining Eqs. (2.40), (2.32), (2.17), and (2.18), we can then re-derive Eqs. (2.19) for the GT model, and (2.20) for the SV model.

The derivations of Eqs. (2.38) to (2.40) are virtually the same as those by

Riekert (1970), Kutner (1981) and Tsikoyiannis (1986). The same conclusion was reached by Barrer and Jost (1949) on the basis of quasithermodynamic approaches.

The resulting constant diffusivity is surprising and counter-intuitive. From Eq. (2.37), one can conclude that the "flux" of a molecule jumping from a site, S_i, to a site, S_j,, is the product of three factors: jump frequency, q; occupancy at the jump site, $\theta(S_i, X; t)$; and availability of vacancy at the site the molecule jumps to, $(1-\theta(S_j, X; t))$. In this case, q is a constant, independent of occupancy. The "driving factor", θ, happens to be just compensated by the "blocking factor", $1-\theta$. Qualitatively, molecules in a denser region have a higher probability to jump, or to be "pushed" by the others, toward a less dense region. At the same time, molecules in the denser region are more likely to be hindered by the others in their motion. In this case, these two effects counterbalance each other, resulting in a constant uptake diffusivity and dropping out of the joint probability in Eq. (2.38).

If Eq. (2.31) is applied to the boundary of the lattice, the equilibrium partitioning between the gas phase and the lattice can be obtained as

$$\theta = \frac{\frac{p}{q}}{1 + \frac{p}{q}} \tag{2.41}$$

where p is the bombardment rate from the gas phase into the lattice (Tsikoyiannis, 1986). The isotherm is of the Langmuir type.

Therefore, for the Non-Interacting Lattice Model where the interactions between molecules are negligible, the uptake diffusivity is a constant, and the equilibrium partitioning between the gas phase and the lattice is given by the

Langmuir isotherm.

2.4 Diffusivity In Zeolites: Concentration Dependence (II)

In this section, the stochastic approach used above will be extended to a more complicated case where the interaction between molecules inside the lattice is explicitly considered. We keep the basic rules for diffusion, assumptions (1) to (3), presented in the last section unchanged. Three more new rules are added as follows:

(6). One site can host two molecules at maximum.

(7). There is a repulsive interaction between two molecules at the same site. This interaction lowers the activation energy by ΔE.

(8). The interactions between molecules at different sites are negligible.

Figure 2.7 is a schematic for the above assumptions. The repulsive interaction between two molecules at the same site increases the potential at the intersection, Φ_c, which makes the potential well shallower and therefore decreases the activation energy for the jump from the doubly-occupied site. It should be noted that the molecule-lattice interaction is still the dominant factor under this condition. The molecule-molecule interaction considered here is important, yet it is a secondary factor in determining the diffusion behavior in the lattice. In the following discussions, we will first present the effect of the molecule-molecule interaction on the molecular distribution. The effect of molecular interaction on the diffusion and the equilibrium will then be investigated by the first-order correlation functions of stochastic theory.

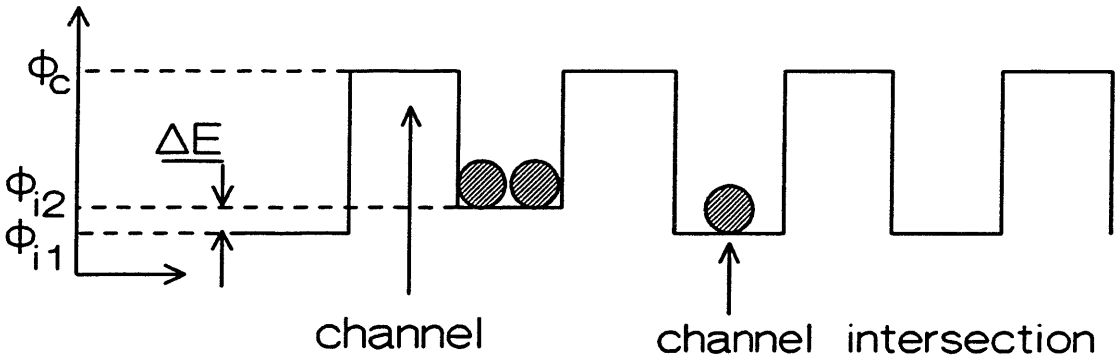

Figure 2.7 Particle in a Potential Field of Periodic Lattice: Effect of Repulsive Interaction between Molecules on the Activation Energy

2.4.1 Molecular Distribution

When one site can host two molecules, molecular distribution inside the lattice is no longer unique. Molecules can be distributed "statistically", i.e., molecules occupy unsaturated sites (less than two molecules at the sites) with equal probability. Molecules can also be distributed "uniformly", i.e., molecules occupy every empty site with one molecule first and then cover them with the second layer. Molecules can, of course, be distributed in a way somewhere in between these two limiting cases. In this section, a mathematical description will be given to different types of molecular distribution.

Define $\theta(S_i,0;t)$ as the probability of finding no molecule at the site considered, S_i, $\theta(S_i,1;t)$ as finding one and only one molecule, $\theta(S_i,2;t)$ as finding two and only two molecules. We have, following Fowler and Guggenhem (1960),

$$f = \frac{\theta(S_i, 0; t)\ \theta(S_i, 2; t)}{\theta^2(S_i, 1; t)} = \frac{e^{-w}}{4} \tag{2.42}$$

where f is the "equilibrium constant", and w ($\equiv \Delta E/RT$) is the nondimensionalized activation energy change due to the molecule-molecule interaction. And

$$\theta(S_i, X; t) = \theta(S_i, 2; t) + \frac{1}{2}\,\theta(S_i, 1; t) \tag{2.43}$$

$$\theta(S_i, 0; t) + \theta(S_i, 1; t) + \theta(S_i, 2; t) = 1 \tag{2.44}$$

For f=1/4 (w=0), the distribution is statistical (Hill, 1960) with

$$\theta(S_i, 0; t) = (1 - \theta)^2 \tag{2.45}$$

$$\theta(S_i, 1; t) = 2\,\theta\,(1 - \theta) \tag{2.46}$$

$$\theta(S_i, 2; t) = \theta^2 \tag{2.47}$$

where θ is the short-handed form of $\theta(S_i, X; t)$.

And for f=0 (w>>0), the distribution is uniform with

$$\theta(S_i, 0; t) = 1 - 2\,\theta \tag{2.48}$$

$$\theta(S_i, 1; t) = 2\,\theta \tag{2.49}$$

$$\theta(S_i, 2; t) = 0 \tag{2.50}$$

The above equations are valid for total occupancy $\theta \leq 0.5$. For $\theta \geq 0.5$, we have

$$\theta(S_i, 0; t) = 0 \tag{2.51}$$

$$\theta(S_i, 1; t) = 2\,(1 - \theta) \tag{2.52}$$

$$\theta(S_i, 2; t) = 2\,\theta - 1 \tag{2.53}$$

Figure 2.8 presents the molecular distributions in the lattice for those two limiting cases.

In reality, molecular distributions are probably neither statistical nor uniform. Figures 2.9, 2.10, 2.11 give $\theta(S_i, 2; t)$, $\theta(S_i, 1; t)$, $\theta(S_i, 0; t)$ for different values of parameter f ($w \neq 0$), according to the following formulas:

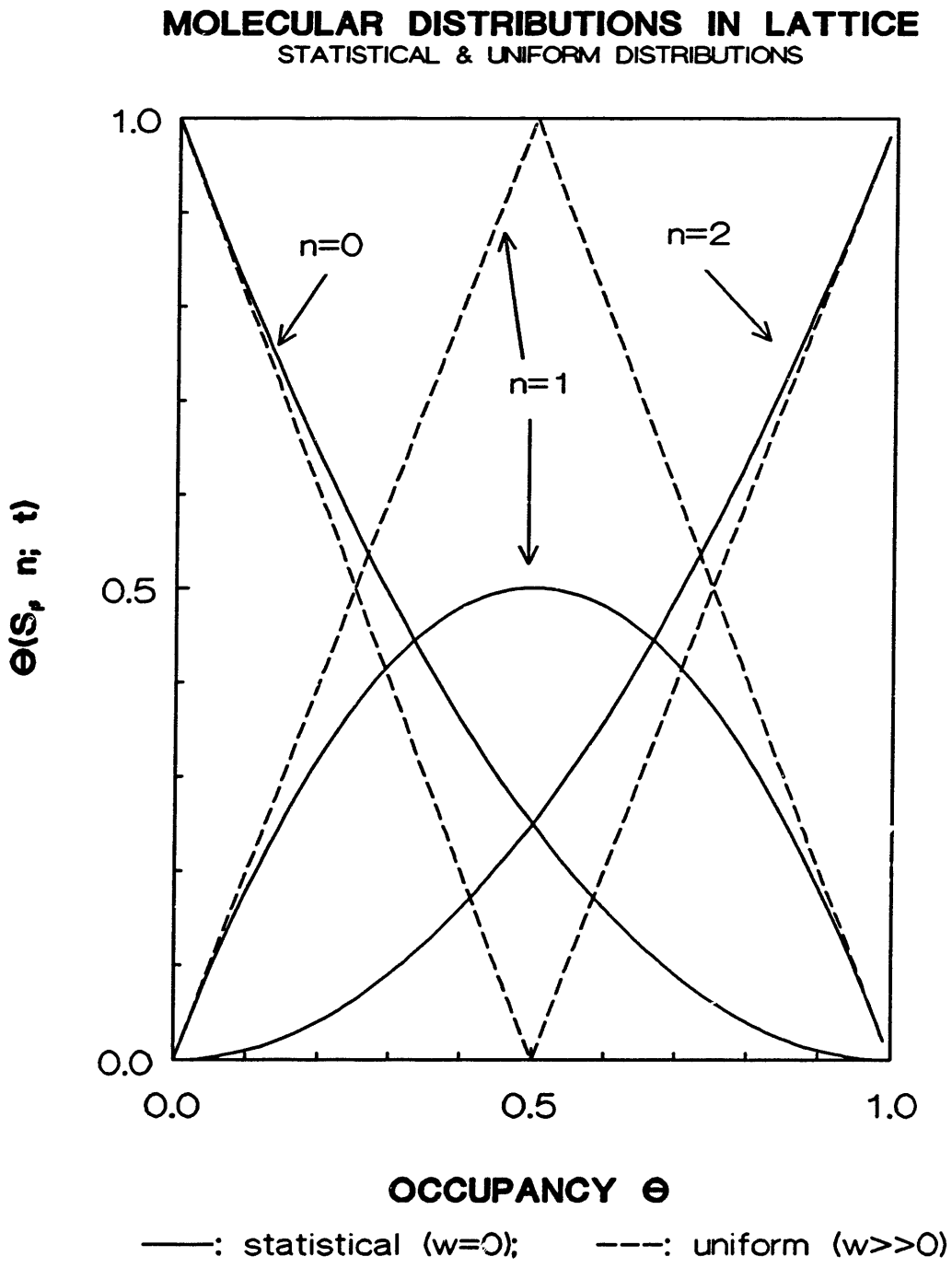

Figure 2.8 Statistical Distribution and Uniform Distribution in Lattice

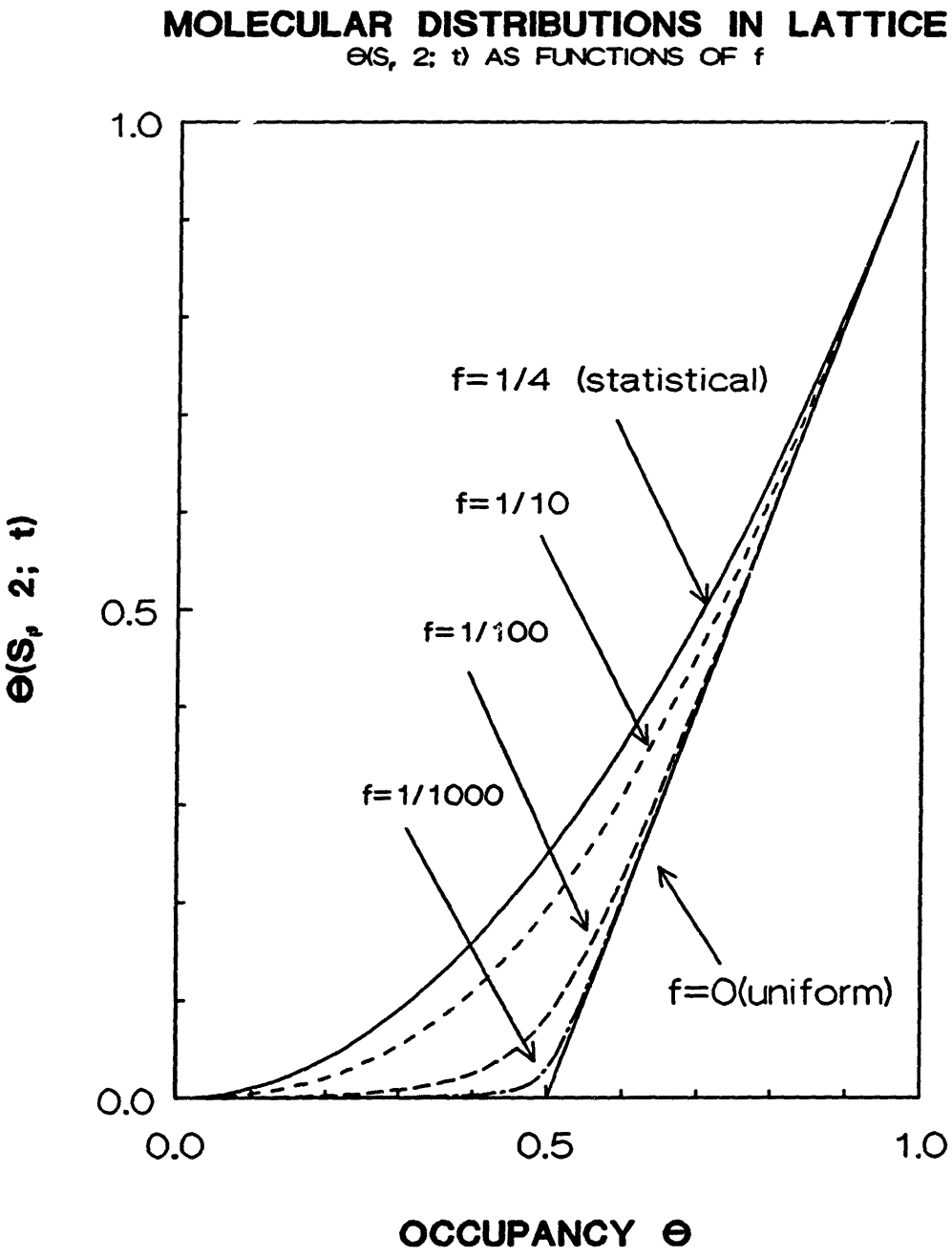

Figure 2.9 Effect of f on Double-Occupancy Probability

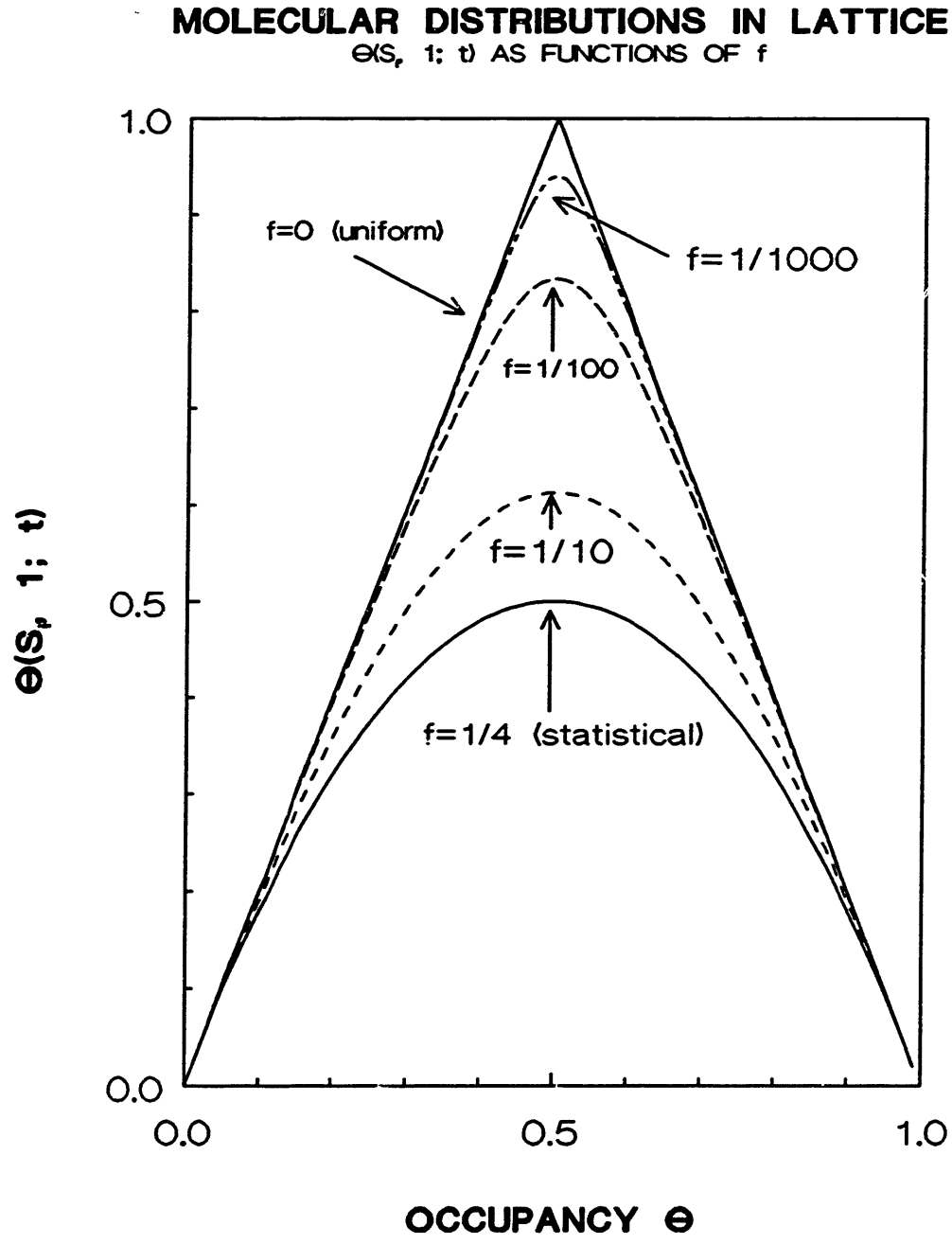

Figure 2.10 Effect of f on Single-Occupancy Probability

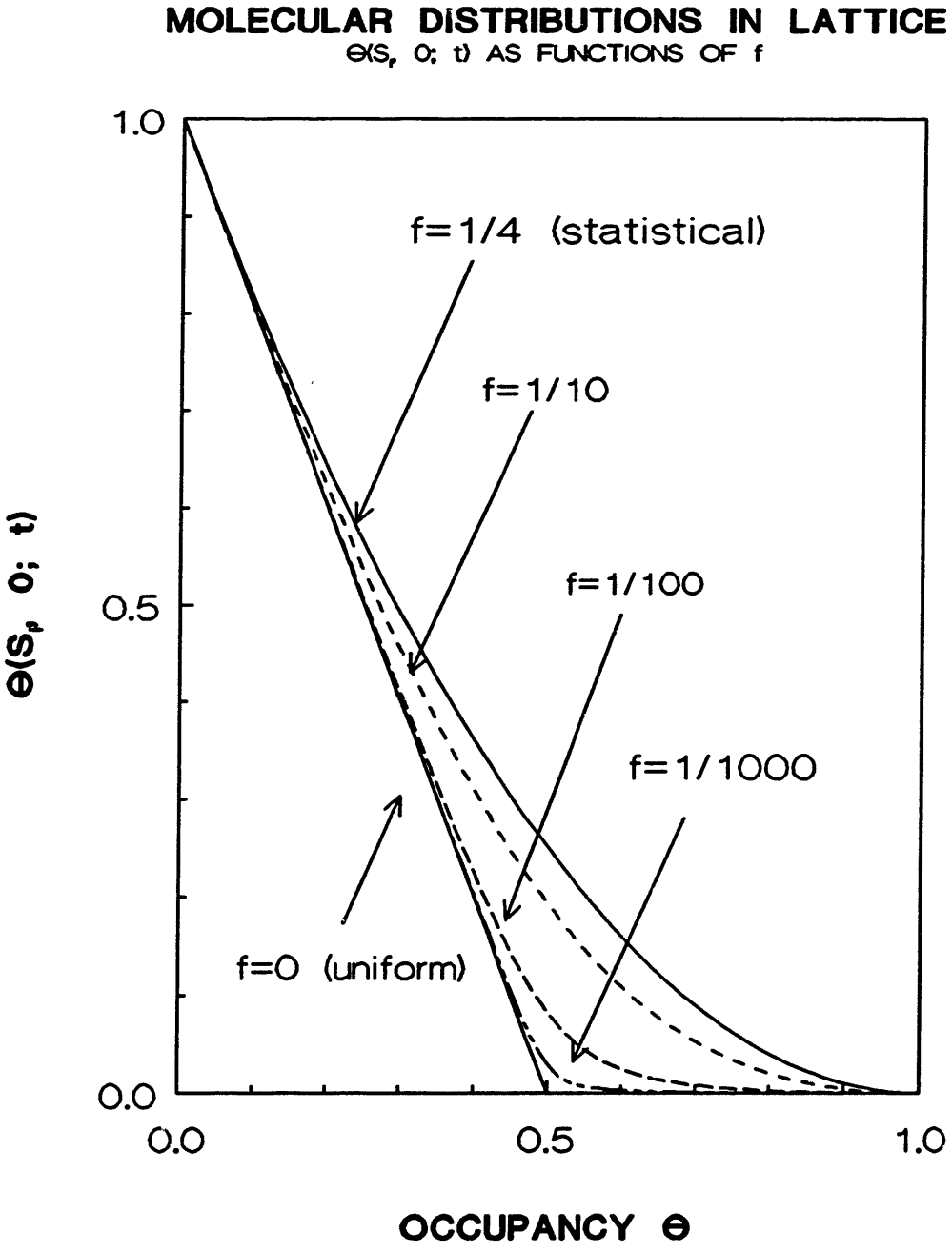

Figure 2.11 Effect of f on Empty-Site Probability

$$\theta(S_i, 2; t) = \frac{1}{2(1-4f)} \left[\sqrt{[1-2\theta(1-4f)]^2+16f(1-4f)\theta^2} - (1-2\theta(1-4f))\right] \quad (2.54)$$

$$\theta(S_i, 1; t) = 2\,[\theta - \theta(S_i, 2; t)] \quad (2.55)$$

$$\theta(S_i, 0; t) = 1 - 2\,\theta + \theta(S_i, 2; t) \quad (2.56)$$

From above equations, $\theta(S_i, n; t)$'s (n=0, 1, 2) can be determined once occupancy θ and the potential change due to the interaction between molecules are specified. From Figures 2.9 to 2.11, one can conclude that if the value of f is larger than 1/10, which corresponds to w smaller than about 0.9 and ΔE smaller than about 0.1 kcal/mol at room temperature, the distribution would be close to the statistical distribution. If the value of f is smaller than 1/100, which corresponds to w larger than about 3, and ΔE larger than about 2 kcal/mol, the stronger repulsion between molecules would therefore make the molecular distributions more close to the form of the uniform distributions.

2.4.2 Concentration-Dependent Diffusivity

If the potential energy of one molecule at a site is Φ_{i1} and the potential energy of two molecules at a site is Φ_{i2}, the potential energy at a site with occupancy probability $\theta(S_i, X; t)$, according to the mutually exclusive event principle, is

$$\begin{aligned} \Phi_i &= [1 - \theta(S_i, 2; t)]\,\Phi_{i1} + \theta(S_i, 2; t)\,\Phi_{i2} \\ &= \Phi_{i1} + \theta(S_i, 2; t)\,\Delta E \end{aligned} \quad (2.57)$$

where ΔE is defined as $\Phi_{i2}-\Phi_{i1}$, and $\Delta E > 0$, if the interaction between two molecules results in a repulsive force in between. The above equation is the mean-field approximation of the potential.

By definition,

$$q(S_i, X; t) = q\, e^{\theta(S_i, 2; t)\, w} \tag{2.58}$$

where q is the same as in Eq. (2.32), which is tne jump frequency in the absence of the molecule-molecule interaction. And w, as discussed in last section, is the nondimensionalized activation energy change due to the molecule-molecule interaction ($\Delta E/RT$). For the repulsive interaction between molecules, w is greater than zero. The apparent jump frequency, $q(S_i, X; t)$, increases with an increase in the probability of finding double-occupancy, $\theta(S_i, 2; t)$, since the repulsive force between molecules would push the molecules out of the site more easily.

The first-order correlation functions lead to

$$\frac{d\,\theta(S_i, X; t)}{d\,t} = \sum_{S_j} q(S_j, X; t)\, \theta(S_j, X; S_i, 2; t) - q(S_i, X; t)\, \theta(S_i, X; S_j, 2; t) \tag{2.59}$$

where $\theta(S_i, X; S_j, 2; t)$ is the joint probability of finding molecule(s) at site S_i and not two molecules at site S_j at time t.

We have

$$\theta(S_i, X; S_j, 2; t) + \theta(S_i, X; S_j, 2; t) = \theta(S_i, X; t) \tag{2.60}$$

$$\theta(S_j, X; S_i, 2; t) + \theta(S_j, X; S_i, 2; t) = \theta(S_j, X; t) \tag{2.61}$$

If the correlation between neighboring sites are neglected, the joint probability can be written as

$$\theta(S_i, X; S_j, 2; t) = \theta(S_i, X; t)\, \theta(S_j, 2; t) \tag{2.62}$$

and

$$\theta(S_j, X; S_i, 2; t) = \theta(S_j, X; t)\, \theta(S_i, 2; t) \tag{2.63}$$

Equation (2.59) can then be rewritten as

$$\begin{aligned} \frac{d\,\theta(S_i, X; t)}{d\,t} = q \sum_{S_j} & e^{\theta(S_j, 2; t)\, w}\, \theta(S_j, X; t)\, [1 - \theta(S_i, 2; t)] \\ & - e^{\theta(S_i, 2; t)\, w}\, \theta(S_i, X; t)\, [1 - \theta(S_j, 2; t)] \end{aligned} \tag{2.64}$$

The corresponding PDE approximation of Eq. (2.64) for the large lattice is

$$\frac{\partial\,\theta}{\partial\,t} = \nabla\,(D_{app}\,\nabla\,\theta) \tag{2.65}$$

where

$$D_{app} = D\, e^{\theta(2)\, w}\, [1 - \theta(2) + \theta\,(1 + (1 - \theta(2))\, w)\, \frac{\partial\theta(2)}{\partial\theta}] \tag{2.66}$$

D_{app} is the apparent diffusivity of Fick's law under the condition where the interaction between molecules is important. And D is the Fick's law diffusivity defined by Eq. (2.40) in the absence of intermolecular repulsion. In the above equation, $\theta(2)$ is the double-occupancy probability, the short-handed form of $\theta(S_i, 2; t)$. And $\theta(2)$ is related to total occupancy θ and parameter w by Eq. (2.54). Once w is specified, the dependence of $\theta(2)$ on θ can be uniquely determined for the molecular distributions. Eq. (2.66) can then be used to predict the concentration

dependence of the apparent diffusivity.

Figure 2.12 depicts how the repulsive interaction, characterized by a parameter, $w > 0$, between two molecules at the same site affects the observed apparent diffusivity of Fick's law, together with the predictions of the Non-Interacting Lattice model. The diffusion coefficients are normalized by the diffusivity defined by Eq. (2.40) in the absence of the molecule-molecule interaction, which can be estimated by the GT model or the SV model proposed in the section 2.2. For the Non-Interacting Lattice model, the diffusivity is a constant, independent of concentration (or occupancy). For the Interacting Lattice model, the repulsive interaction between molecules results in about a 10-fold increase in diffusivity near saturation, if w is approximately 1.5, which corresponds to a activation energy change of about 1 kcal/mol near room temperature. The stronger the repulsion, the more dramatic the concentration dependent trend. The repulsion is therefore mainly responsible for the increasing trend of the apparent diffusivity.

The model predictions of the macroscopic diffusional behavior are the results of the microscopic diffusion rules we specify for the model. In the above formulations, we assume that the molecules only interact with each other if they are at the same site. No interactions between molecules at different sites are considered. In reality, especially at high occupancy, it is possible for a molecule to interact with not only the molecule at the same site, but also the molecules at the neighboring sites. Qualitatively, these additional interactions, if they are repulsive, could make the increasing trend of the diffusivity even more dramatic at high occupancy. We also assume that the molecule-molecule interaction only changes the potential at the intersection, Φ_i. The potential at the channel, Φ_c, might, however, also be changed due to the interaction. Furthermore, a site might be able to host more than two

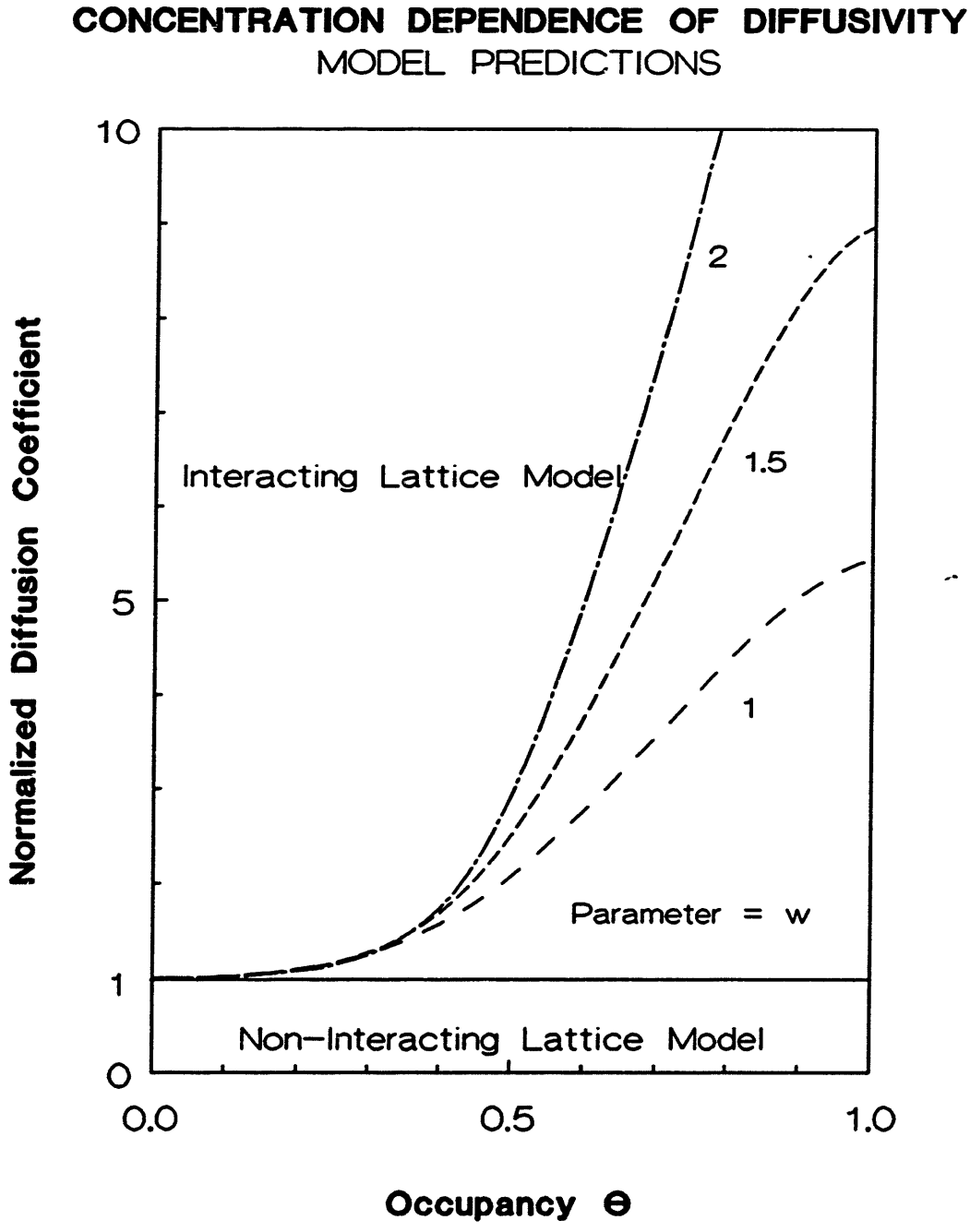

Figure 2.12 Effect of Repulsion between Molecules on the Apparent Diffusivity

molecules for some molecule/zeolite systems, which can further complicate the descriptions of molecule-molecule interactions and the effect of these interactions on the apparent diffusivity. The theoretical treatments for these systems become more difficult and more complicated. The same principles used above, however, still apply. In this thesis, we limit ourselves to the case stated by assumptions of (6) to (8).

Equation (2.66) can be simplified to

$$D_{app} = D\,(1 + \theta^2) \tag{2.67}$$

for the case where the value of w equals zero, and the molecular distributions are statistical as described by Eqs. (2.45) to (2.47). The model then predicts a factor of 2 increase in the apparent diffusivity when the lattice is close to be saturated, although there is no interaction between molecules since w equals zero. The small increase in the diffusivity is the result of the assumption (6), i.e., one site can host two molecules at maximum. When w = 0, the "blocking factor" in Eq. (2.64) is $(1 - \theta^2)$. A molecule can not jump into a site only if that site is occupied by two molecules at the same time. The "driving factor" is θ. A molecule can jump out of a site which is occupied by either one molecule or two molecules. Therefore, a molecule at a denser region is more likely to be "pushed" by the others toward a less denser region than to be "hindered" by the others due to the model assumption. The "blocking factor" no longer counterbalances the "driving factor". This effect on the diffusivity, however, is very minor (about a factor of 2 at most) in comparison with the effect of the repulsive interactions as discussed above. The repulsive force between molecules is therefore the dominant factor in causing the dramatic increase in the diffusivity.

Applying Eq. (2.64) to the boundary of the lattice, we obtain

$$\frac{p}{q} = \frac{e^{\theta(2)w}\,\theta}{1 - \theta(2)} \tag{2.68}$$

where p is the bombardment rate from the gas phase into the lattice, which is proportional to the gaseous pressure. The Langmuir parameter, K, in this case, can be related to the occupancy and the value of w as follow

$$K = \frac{\theta}{p\,(1 - \theta)} = q^{-1}\, e^{-\theta(2)w}\, \frac{1 - \theta(2)}{1 - \theta} \tag{2.69}$$

Figure 2.13 shows the concentration-dependent K for the different values of w. Decreasing trends are observed at high occupancy if the molecule-molecule interaction is repulsive. A slight increase at low concentraion is due to the model assumption (6).

Therefore, for the Interacting Lattice model where the interaction between two molecules at the same site is repulsive, the apparent uptake diffusivity increases with the concentration of guest molecules inside the lattice, and the equilibrium partitioning between the gas phase and the lattice is no longer of Langmuir type. The Langmiur parameter decreases at high concentration.

2.5 Conclusions

The diffusional characteristics of molecules in the zeolite lattice are probed by investigating the molecule-lattice interactions and the molecule-molecule interactions. The molecule-lattice interactions dominantly determine the diffusion mechanism and the orders of magnitude of the diffusivity, whereas the molecule-molecule interactions could alter the concentration dependence of the diffusivity:

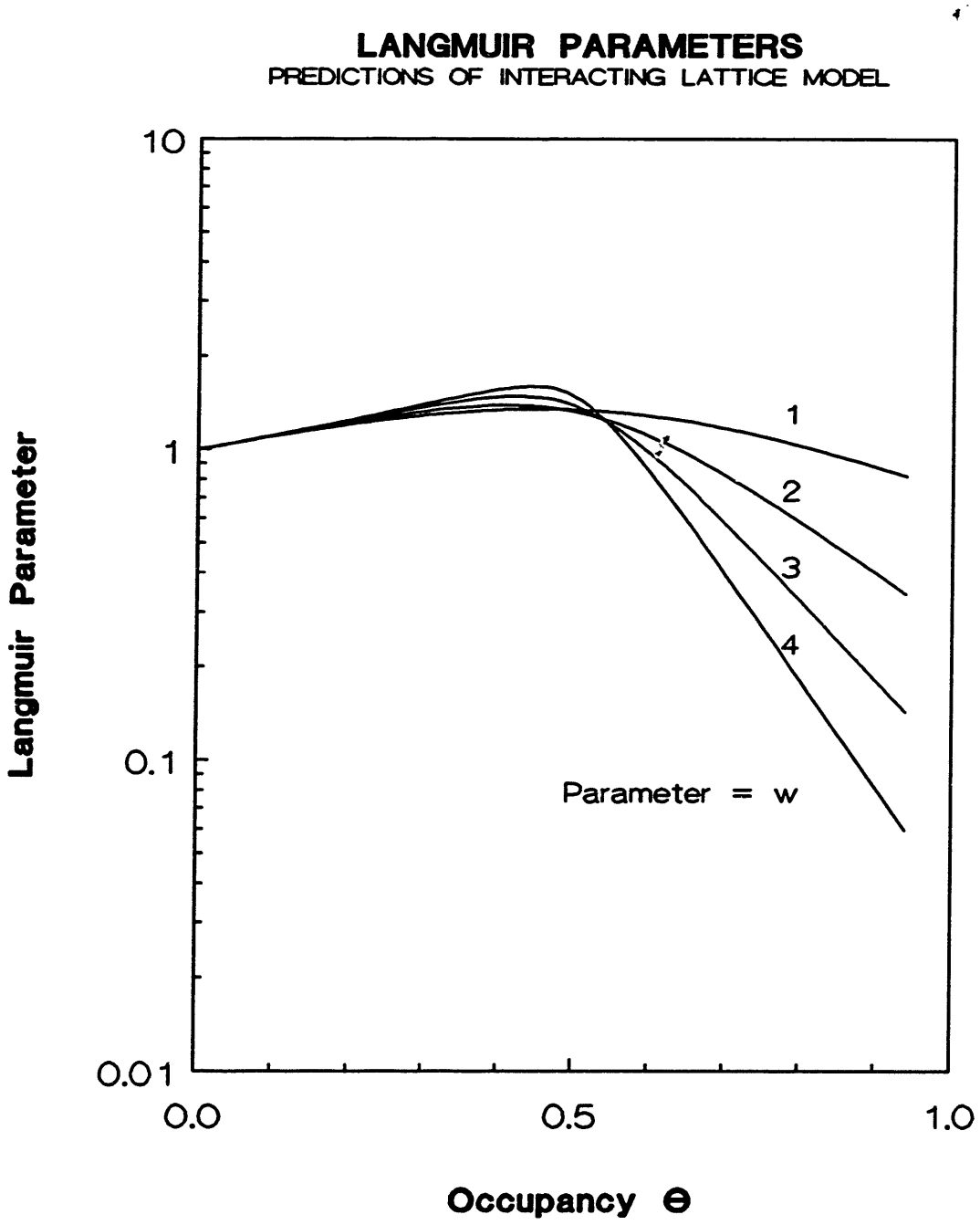

Figure 2.13 Effect of Repulsion between Molecules on Langmuir Parameter

On the orders of magnitude of diffusivity in zeolites:

(1). the GT model: the diffusion of the molecules inside zeolites are restricted by the potential field of the lattice whereas the molecules retain their gaseous entity. The pre-exponential term of the diffusivity of molecules for ZSM-5 is of the order of about $10^{-4}(T/M)^{1/2}$, the activation energy for the diffusion in the lattice can be estimated by the proposed Lennard-Jones potential method based on the information of zeolite structure and molecular properties. For 5A, the pre-exponential term of the diffusivity is of the same order of magnitude as that for ZSM-5 if a molecule is roughly spherical. The GT_{ip} should be used for the diffusion of rod shape molecules, such as n-paraffins, in 5A, in which the effect of intracrystalline partitioning is superimposed on the pre-exponential term. The intracrystalline partitioning could reduce the pre-exponential term by as many as three or more orders of magnitude. Literature results on the characterizations of molecules in zeolites suggest that the basic assumptions of the GT model might be valid for the molecules with no strong specific interactions with the lattice above room temperature.

(2). the SV model: the attachment of molecules to the lattice is so strong that molecules vibrate with the host lattice before accumulating enough energy to jump. The pre-exponential term of the diffusivity is related to the curvature of the potential well of molecule-lattice adsorption site. The SV model might resemble the diffusion of polar molecules, or the diffusion of molecules at very low temperature.

One the concentration dependence of diffusivity in zeolites:

(1). the Non-Interacting Lattice model: if the interaction between molecules inside the lattice is negligible and double-occupancy of a site is excluded, a constant Fick's

law diffusivity should be observed. The equilibrium isotherm is of Langmuir type.

(2). the Interacting Lattice model: if the interaction between molecules is significant at a doubly-occupied site, and the interaction is repulsive, a rising trend of apparent diffusivity and a decreasing trend of the Langmuir parameter should be observed at high concentration.

3. EXPERIMENTAL OBSERVATIONS

The aim of this chapter is to quantify experimentally the temperature and the concentration dependence of zeolite diffusion. The effects of the microscopic properties of molecule-zeolite systems, such as molecular size, molecular length, Si/Al ratio of ZSM-5, cages in zeolites, on the macroscopic diffusional behaviors are investigated. The objective is to generate reliable data to facilitate our understanding of zeolitic behaviors, and to serve as basis for comparison with the theoretical predictions. The model compounds are 19 different hydrocarbons, including paraffins, aromatics and naphthene. Zeolites include two types of ZSM-5, and 5A. Table 3.1 summarizes the tested molecules with different properties in three zeolites at various temperature ranges. The observed results are interpreted by the proposed mechanistic models in Chapter 2. More detailed discussions are given in Chapter 4.

3.1 Experimental

Most of the experiments were performed on a ZSM-5 sample supplied by Peter Jacobs of the Katholieke University, Leuven. This sample was labelled here as ZSM-5 (PJ), or sometimes simply as ZSM-5. It is in the hydrogen form, and has a Si/Al ratio of about 110. It is roughly spherical in shape with an average diameter of about 12 μm. Also used was a ZSM-5 sample synthesized in our laboratory by Waqar Qureshi, referred here as ZSM-5 (WQ). The Si/Al ratio of ZSM-5 (WQ) is about 6000$\pm$ 1000. ZSM-5 (WQ) has an elongated hexagonal shape with dimensions of approximately 12x20x30 μm. In the diffusion analysis, the smallest dimension of ZSM-5 (WQ) was taken as its characteristic diffusion length. More detailed characterizations of both ZSM-5 (PJ) and ZSM-5 (WQ) can be found in Qureshi

Table 3.1 Experimental Summary

ZSM-5 (PJ)

	Temperature	Molecular Diameter		Molecular Length	Concentration (<4 m/u.c)	Concentration (>4 m/u.c)
		E	D			
C_6 2-Methylbutane	+ (24°C-45°C)	+	+ (45°C)	+ (45°C)	+ (24, 45°C)	+ (24°C)
C_6 n-Hexane				+ (45°C)		
2-Methylpentane	+ (24°C-45°C)	+	+ (45°C)	+ (45°C)		
2,2-Dimethylbutane	+ (150°C-200°C)	+	+ (150°C)	+ (150°C)		
2,3-Dimethylbutane	+ (90°C-200°C)	+	+ (150°C)	+ (150°C)		
Cyclohexane	+ (150°C-200°C)	+	+ (150°C)			
Benzene	+ (23°C-200°C)	+	+ (45, 150°C)		+ (23°C-90°C)	+ (23°C-45°C)
C_7 n-Heptane			+ (45°C)	+ (45°C)		
2-Methylhexane				+ (45°C)		
2,2-Dimethylpentane				+ (150°C)		
2,3-Dimentylpentane				+ (150°C)		
2,4-Dimethylpentane				+ (150°C)		
Toluene						
C_8 n-Octane				+ (45°C)		
2-Methylheptane				+ (45°C)		
2,2-Dimethylhexane				+ (150°C)		
C_9 2-Methyloctane				+ (45°C)		
C_{10} n-Decane				+ (45°C)		
2-Methylnonane				+ (45°C)		
Figure number	3.3	3.4	3.5	3.6&3.7	3.8&3.9&3.10	3.15&3.16&3.17

+: exper. performed; E: activation energy; D: diffusivity.

Table 3.1 Experimental Summary (Conti. 1)

ZSM-5 (PJ)

	Adsorption & Desorption	Activation	Mg Modifier	Equilibrium Isotherm	Equilibrium Capacity
C_6 2-Methylbutane				+ (24°C,45°C)	+ (24°C)
C_6 n-Hexane				+ (45°C)	+ (45°C)
2-Methylpentane					
2,2-Dimethylbutane					
2,3-Dimethylbutane					
Cyclohexane					
Benzene	+ (65°C)	+ (65°C)	+ (65°C)	+ (23°C-90°C)	+ (23°C)
C_7 n-Heptane				+ (45°C)	+ (45°C)
2-Methylhexane					
2,2-Dimethylpentane					
2,3-Dimentylpentane					
2,4-Dimethylpentane					
Toluene					
C_8 n-Octane				+ (45°C)	+ (45°C)
2-Methylheptane					
2,2-Dimethylhexane					
C_9 2-Methyloctane					
C_{10} n-Decane				+ (45°C)	+ (45°C)
2-Methylnonane					
Figure number	3.10	3.13	3.26	3.11&3.12&3.14 &3.18&3.19&3.20 3.22	3.23

+: exper. performed

Table 3.1 Experimental Summary (Conti. 2)

	ZSM-5 (WQ)		5A
	Concentration (<4 m/u.c.) & Si/Al ratio	Equilibrium Isotherm	Concentration & Cage
C_6 2-Methylbutane			
C_6 n-Hexane			
2-Methylpentane			
2,2-Dimethylbutane			
2,3-Dimethylbutane			
Cyclohexane			
Benzene	+ (65°C)	+ (65°C)	
C_7 n-Heptane			+ (150°C)
2-Methylhexane			
2,2-Dimethylpentane			
2,3-Dimentylpentane			
2,4-Dimethylpentane			
Toluene	+ (65°C)	+ (65°C)	
C_8 n-Octane			
2-Methylheptane			
2,2-Dimethylhexane			
C_9 2-Methyloctane			
C_{10} n-Decane			
2-Methylnonane			
Figure number	3.10	3.12	3.21

+: exper. performed

(1989). Experiments were also carried out on a zeolite 5A of about 4 μm in size, purchased from Union Carbide.

Hydrocarbons were supplied by Aldrich, Mallinckrodt, Fluka, and Fisher. They were used without further purification.

A Cahn 2000 Vacuum Electrobalance, shown in Figure 3.1, was used to determine the transient uptake of diffusing molecules. The balance was located inside a cylindrical glass chamber. Powdered zeolite sample was placed on a circular platinum pan. The sample pan was suspended from the left arm of the balance through a vertical glass hangdown tube and placed in the middle of a furnace. During the experiment, the glass enclosure was isolated from the environment and connected to a pressure transducer. The temperature of zeolite was measured by a thermocouple located about 1 mm underneath the sample pan.

Zeolite samples were calcined at about 500 $^{\circ}$C in a furnace under air to burn off any adsorbed hydrocarbons. The calcination time, varied from 1 hour up to several days, showed no apparent effect on the diffusion or the equilibrium results. Approximately 1 to 5 mg of powdered zeolites was then loaded into the Cahn balance. The configuration and the amount of sample was varied to ensure that the experiments were free from possible heat transfer and external diffusional resistance. The apparatus was immediately evacuated by a vacuum pump, and the sample was then heated to the desired temperature by the furnace.

In the preliminary experiments, the sample was also "activated" by heating the system under vacuum up to 500 $^{\circ}$C for a period up to several hours before the run. It was found that the results were insensitive to whether this "activation process" was

DIFFUSION MEASUREMENT

UPTAKE EXPERIMENT SETUP FOR ONE COMPONENT

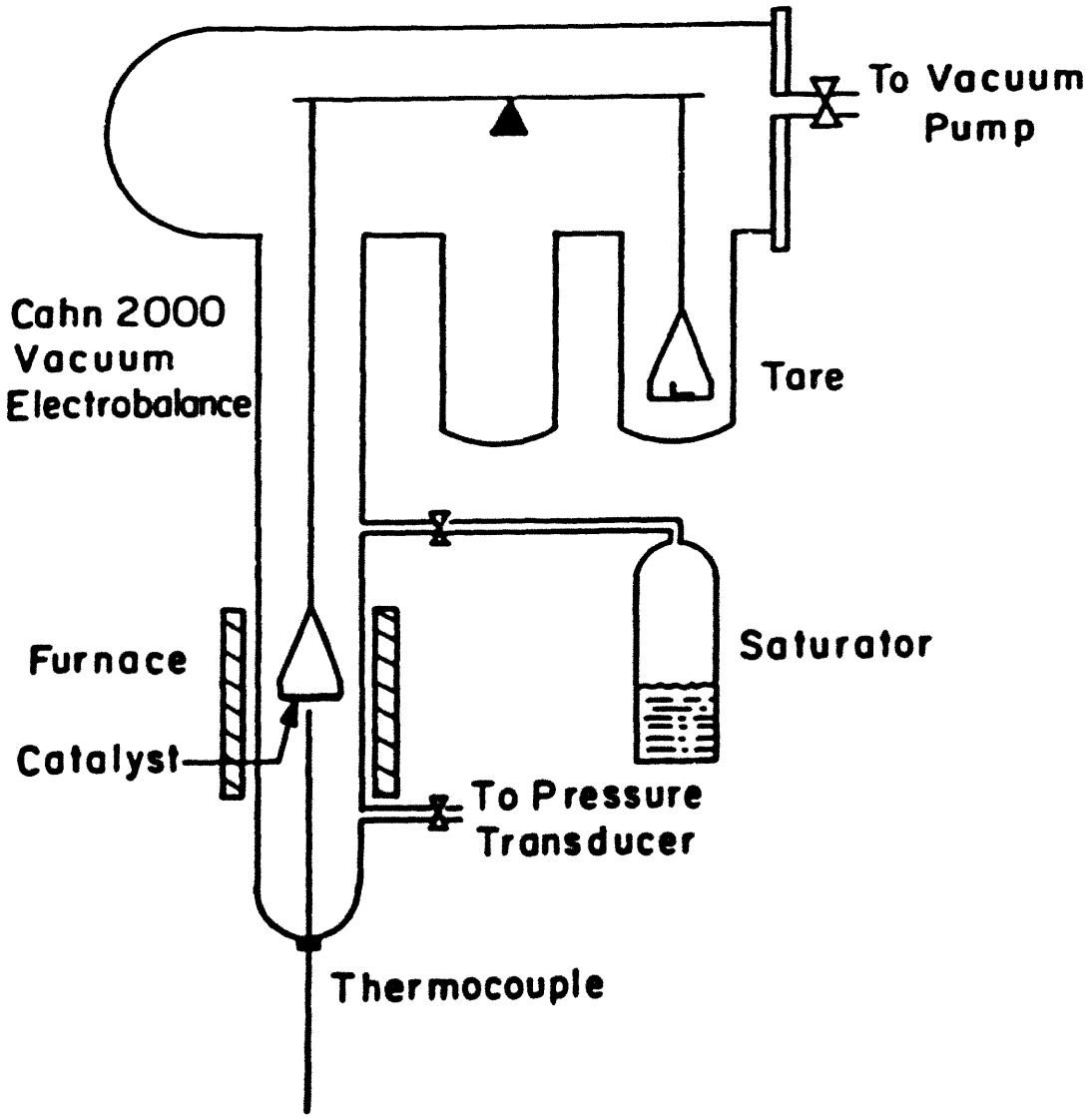

Figure 3.1 Experiment Setup for Diffusion Measurement

performed. The experiments were thereafter carried out without activating the sample. The preliminary experiments also showed that exposure of the sample to room air after calcination for a period of more than one day, or without thorough cleaning of the chamber before the run could sometimes lower the measured diffusivity and change its concentration dependent trend, probably due to the contamination of the samples. Care was taken to eliminate these effects.

To start an experiment, a stepwise increase of gas pressure within the balance chamber was made. The pressure was increased to a constant value by introducing a small quantity of testing gas through the saturator. The pressure could also be decreased by connecting the chamber to a vacuum line. With each pressure change, the weight of the zeolite sample was monitored until the system reached equilibrium, from which the diffusivity was determined and the equilibrium isotherm was generated. In measuring diffusivities at the concentration range where the diffusivity is concentration-dependent, the step size of the pressure change was varied and kept small so that it bore little effect on the measured diffusivities.

After an experiment was completed, the chamber was evacuated, and then the furnace temperature was raised to 500 $^{\circ}$C under a purge of dry air to clean the chamber before the next run. Care was also taken to eliminate possible condensation on the Cahn balance and the hangdown wires.

The transient uptake process can be described by Fick's second law of diffusion. The uptake curve was measured over a small differential change in adsorbed phase concentration, and the ambient gas concentration remained essentially constant during the course of uptake. The diffusion coefficient was then obtained by fitting the experimental uptake results to the solution of the diffusion

equation. Within each step change of sorbate concentration, a constant diffusivity was assumed. The diffusivity, D, was calculated from

$$\frac{M_t}{M_\infty} = 1 - \frac{6}{\pi^2}\sum_{n=1}^{\infty}\frac{1}{n^2}\, e^{-\frac{n^2\pi^2 Dt}{r_p^2}} \qquad (3.1)$$

where M_t/M_∞ is the fractional approach to equilibrium, r_p is the radius of the crystals, and D is the fitting parameter. Figure 3.2 shows a typical transient uptake curve with a fitted diffusivity of one experimental uptake.

3.2 Results and Discussions

3.2.1 Effects of Temperature, Molecular Diameter and Molecular Length

The diffusion measurements of one C_5 (2-methylbutane) and five C_6 hydrocarbons(2-methylpentane,2,2-dimethylbutane,2,3-dimethylbutane,cyclohexane and benzene) were performed over different temperature ranges, as indicated in Table 3.1. An Arrhenius plot is given in Figure 3.3 where the y-axis is the product of the diffusivity and the square root of molecular weight over temperature, according to the Gas Translation (GT) model. For the six tested molecules, the lower the diffusivity, the higher the activation energy. The pre-exponential terms determined experimentally here for these six different molecules are, however, independent of molecular shapes, and all are of the order of 10^{-4}.

Table 3.2 compares the diffusion characteristics of benzene, cyclohexane and 2,2-dimethylbutane observed in the present study with those reported in the literature. The differences between the diffusivities found in this study and those by various groups are all within about one order of magnitude. Three of the diffusivity

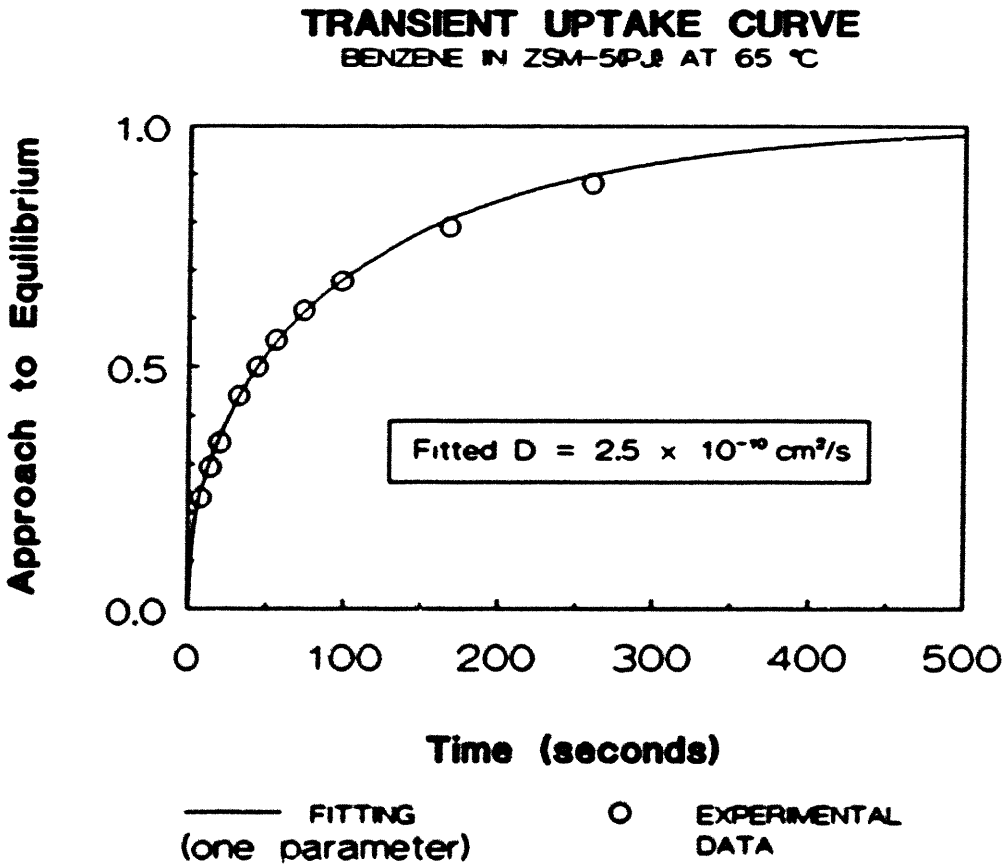

Figure 3.2 Transient Uptake Curve for Benzene/ZSM-5(PJ)

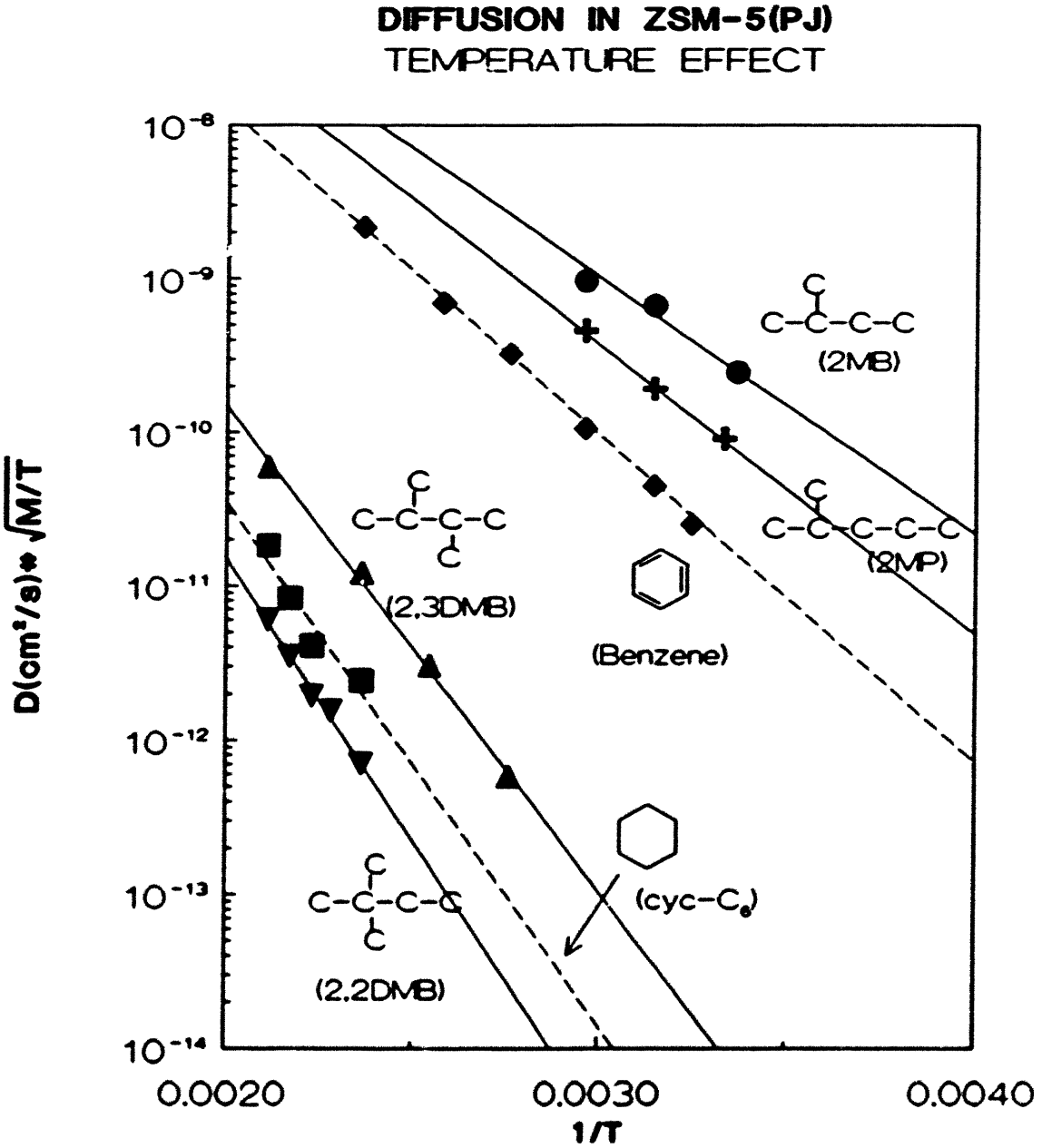

	2MB	2MP	BENZ	2.3DMB	Cyc-C_6	2.2DMB
pre-exp.term (x 10^4)	1.0	1.6	2.2	2.9	2.1	2.9
E (kcal/mol)	7.62	8.60	9.70	14.40	15.51	16.67

Figure 3.3 Diffusion in ZSM-5(PJ): Temperature Effect

Table 3.2 Comparison of Experimental Data

Literature Data				Present Study		
T (K)	Reference	D (cm^2/s)	E (kcal/mol)	T (K)	D (cm^2/s)	E (kcal/mol)
Benzene:						
293	Doelle et al (1981)	2.3×10^{-10}				
298	Shah et al (1988)	4×10^{-11}	6.9	296	2.7×10^{-11}	9.7
303	Nayak et al (1985)	6×10^{-12}		308	5.3×10^{-11}	
	Prinz et al (1986)	7×10^{-12}		318	1.0×10^{-10}	
	Wu et al (1983,84)	10^{-11}	5	338	2.6×10^{-10}	
	Zikanova et al (1987)	4×10^{-10}	5–6.2	363	6.9×10^{-10}	
308	Qureshi et al (1988)	3×10^{-11}	5.7	386	1.6×10^{-9}	
363	Tsikoyiannis (1986)	3×10^{-10}		423	5×10^{-9}	
386	Bulow et al (1986)	10^{-9}	6.7	588	1.5×10^{-7} (extrapolated)	
588	Olson et al (1981)	10^{-7}				
Cyclohexane:						
388	Chon et al (1988)	7×10^{-10}	12.1	388	8.3×10^{-10} (extrapolated)	
				423	5.5×10^{-10}	15.51
				448	9.4×10^{-10}	
				460	1.9×10^{-11}	
				473	4.4×10^{-11}	
2,2-Dimethylbutane:						
423	Post et al (1984)	10^{-10}	15.8	423	1.6×10^{-10}	16.67
	(uptake/chromatographic)			438	3.5×10^{-10}	
811	Haag et al (1981)	2×10^{-8}		448	4.4×10^{-10}	
	(effectiveness factor)			460	8.0×10^{-10}	
				473	1.4×10^{-11}	
				811	3×10^{-8} (extrapolated)	

* uptake methods were used, unless otherwise indicated.

** only limited data were listed from each reference for the comparison.

values were extrapolated from our results to compare with the literature data at different temperatures. The diffusivity of benzene at 588 K was extrapolated from the values below 423 K, the diffusivity of cyclohexane at 388 K from the values above 423 K, and the diffusivity of 2,2-dimethylbutane at 811 K from the values below 473 K. Our extrapolated values are in good agreements with the reported data, even for the case of 2,2-dimenthylbutane where the extrapolation was over 300 K and a different method was used in the literature.

The activation energy values were plotted against the molecular diameters of six molecules in Figure 3.4. A rising trend of activation energy with increasing molecular diameter were observed. The molecular diameters used here were the minimum cross-sectional diameters of molecules, as suggested by Breck (1974) (see Table 1.1). Normal-paraffins, mono-methyl-paraffins, benzene, cyclohexane, dimethyl-paraffins were characterized by diameters of 4.3 Å, 5.0 Å, 5.85 Å, 6.0 Å and 6.2 Å respectively. Diffusion measurements were performed on a normal paraffin (nC_7), 2-methylbutane, 2-methylpentane, and benzene at 45 °C, and on benzene, cyclohexane, 2,3-dimethylbutane and 2,2-dimethylbutane at 150 °C respectively in ZSM-5 (PJ). It was found that the magnitudes of observed diffusivities, as shown in Figure 3.5, were strongly affected by the molecular diameter, especially when molecular diameter approaches the characteristic size of ZSM-5 channels, about 5.7-5.8 Å by assuming that oxygen ions have a radius of 1.3 Å (Flanigen et al, 1978).

The effect of molecular length on the diffusion coefficient is much less pronounced than that of molecular diameter. The results of the diffusion of monomethyl-paraffins and dimethyl-paraffins in ZSM-5 were presented in Figure 3.6, where the values of molecular length were from Gorring (1973). When the molecular length is longer than about 8-9 Å, its effect on the diffusivity is diminishing.

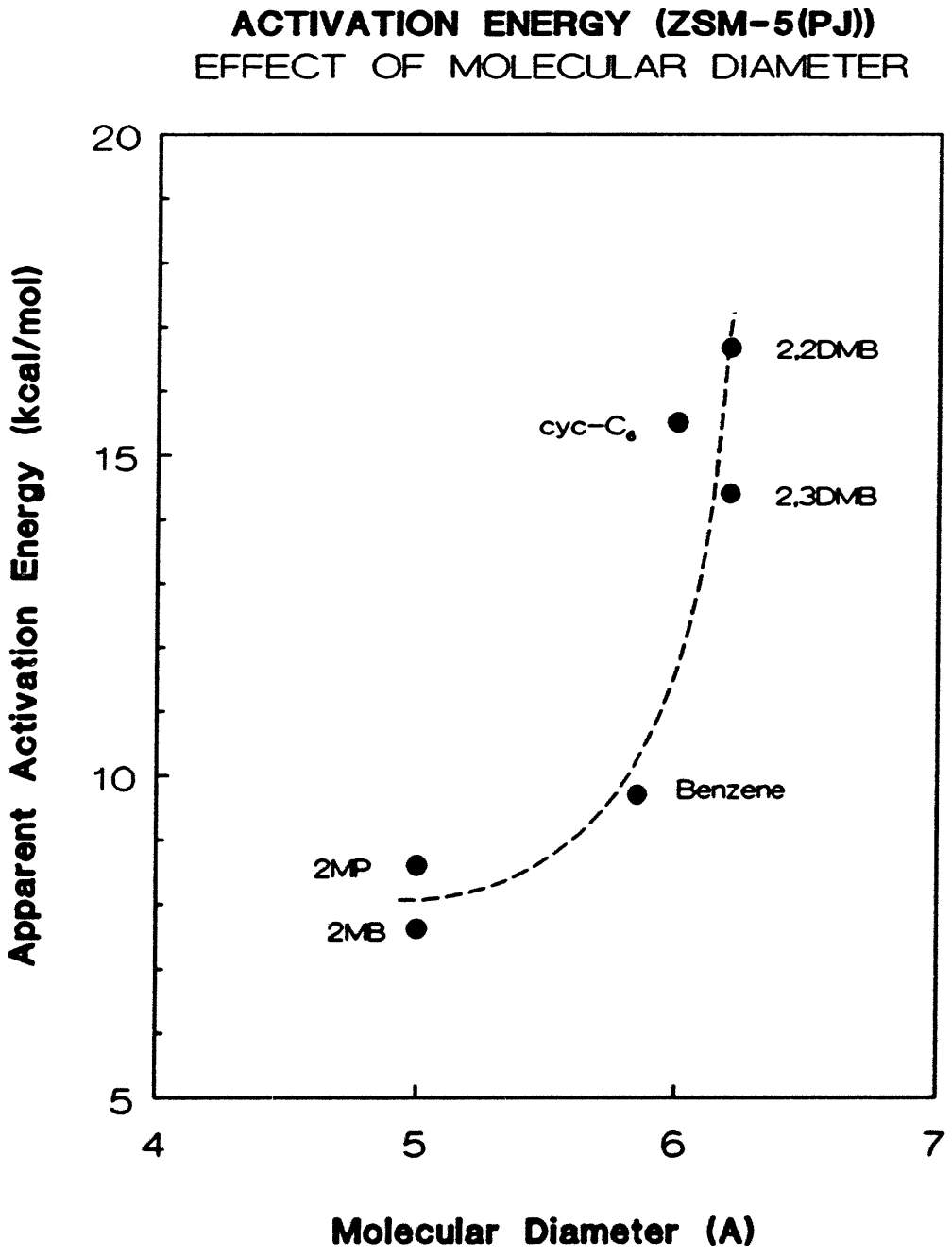

Figure 3.4 Activation Energy in ZSM-5(PJ): Effect of Molecular Diameter

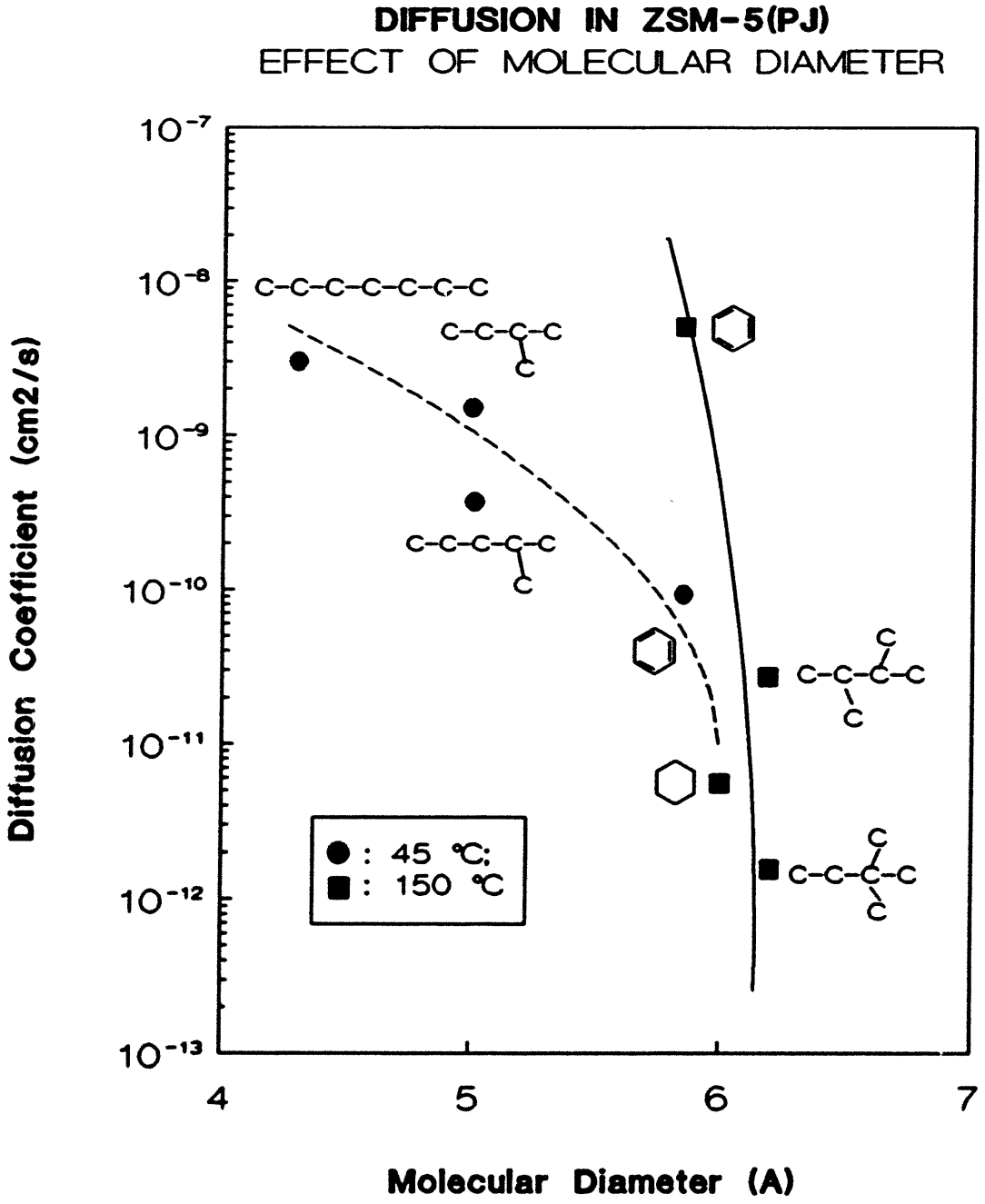

Figure 3.5 Diffusion in ZSM-5(PJ): Effect of Molecular Diameter

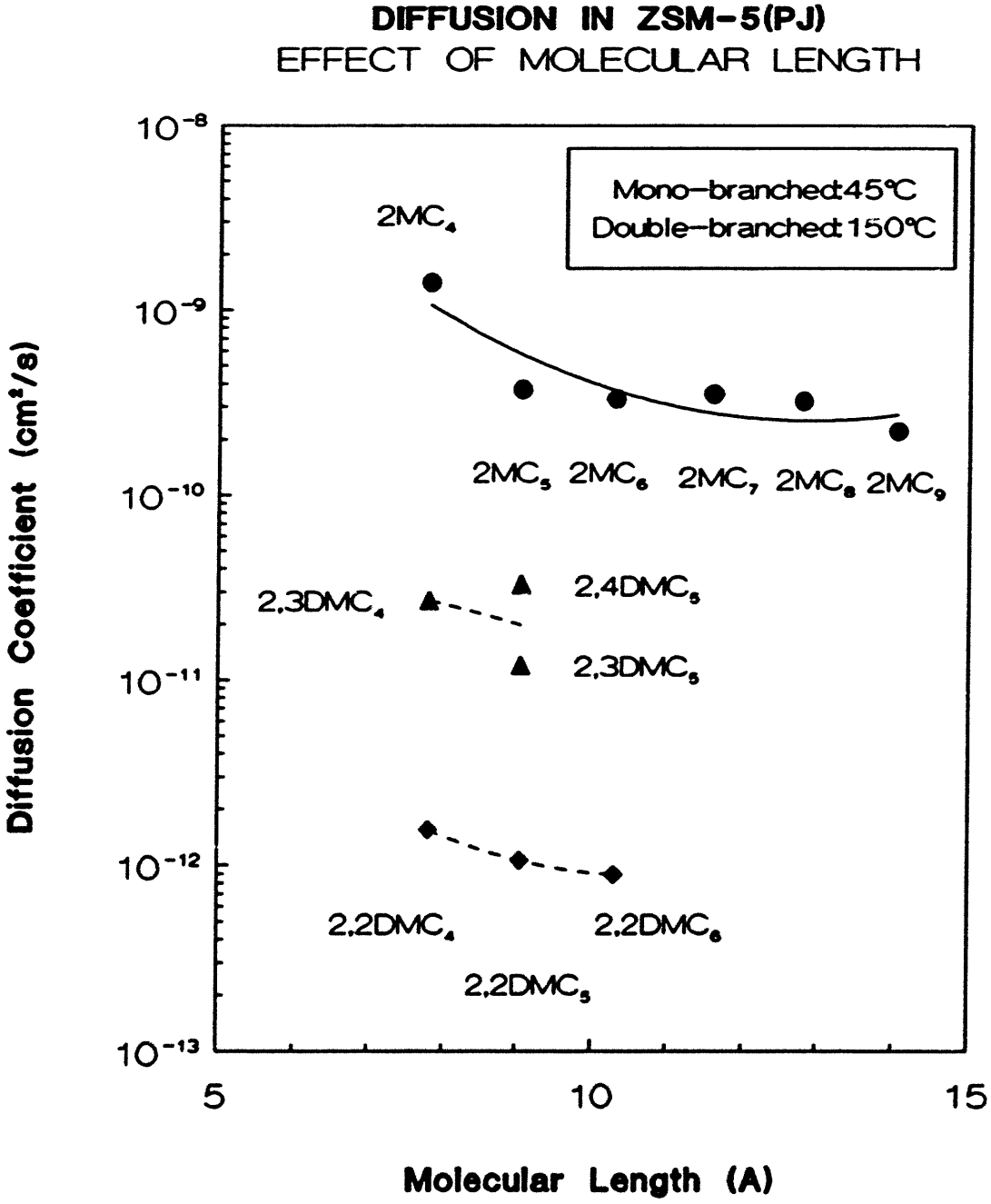

Figure 3.6 Diffusion in ZSM-5(PJ): Effect of Molecular Length (1)

The diffusivity values for double-branched pentanes are in the order of 2,4-dimethylpentane > 2,3-dimethylpentane > 2,2-dimethylpentane. A paraffin molecule with two methyl groups branched at the different carbons might have a smaller effective minimum diameter and, therefore, experience less difficulties when passing through a channel than on with two methyl groups branched at the same carbon. Figure 3.7 presents the results of the diffusion of n-paraffins, from nC_6 to nC_{10}, in ZSM-5 at 45 °C. Since the diffusions are very fast for these systems, the external heat and mass transfer might affect the results. This set of data can be, therefore, viewed as the roughly estimated orders of magnitude of the diffusivities for these system. The approximate differences between their diffusivities are at most within about a factor of 3 to 4. Hayhurst and Paravar (1988) observed an approximate 30-fold decrease in diffusivities from methane to butane in Silicalite. The diffusivities of butane, pentane and hexane are, however, all of the same order of magnitude (Hayhurst and Paravar, 1988; Kärger and Ruthven, 1989).

In the GT model, it is assumed that molecules within zeolite lattice retain their entity and their gaseous velocity, although the movement of molecules becomes more restrictive due to the energy barrier imposed by the channel system. The diffusivity for ZSM-5 is related to the molecular velocity, zeolite structural parameters, and the energy barrier the molecule has to overcome during the hopping. It is of the form as follows:

$$D = 3.6 \times 10^{-4} \sqrt{\frac{T}{M}}\, e^{-\frac{E}{RT}} \qquad (3.2)$$

where M is the molecular weight of the diffusant. The experimentally determined pre-exponential terms are in good agreement with the predicted value of the GT model, considering the compensation effect between the activation energy and the

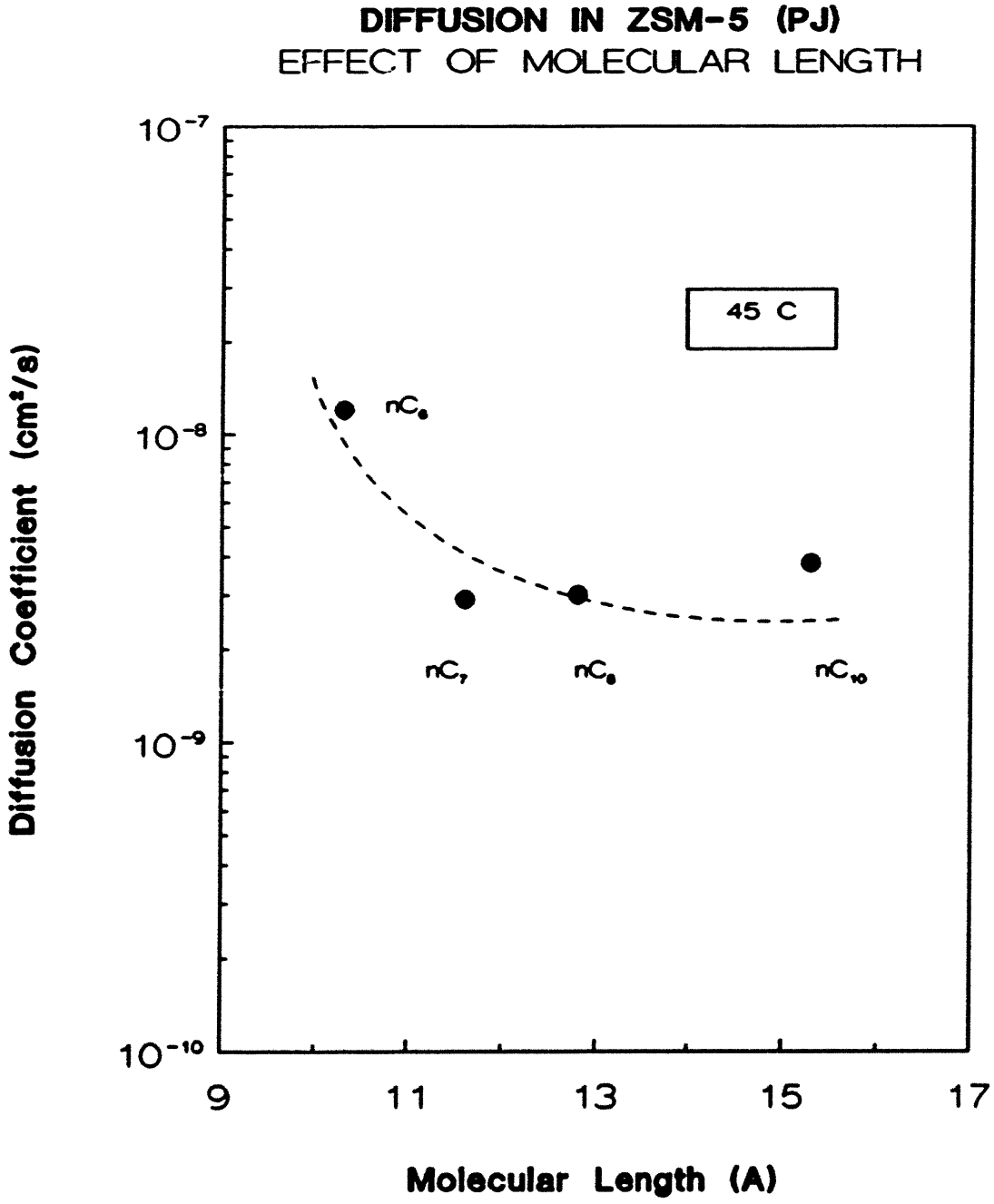

Figure 3.7 Diffusion in ZSM-5(PJ): Effect of Molecular Length (2)

pre-exponential term in the experimental data fitting. The difference in the diffusivity values for the different molecules in ZSM-5 is, therefore, mainly due to the difference in their activation energies.

A molecules, such as benzene, would reside at the energetically preferable sites, the channel intersections, since the intersections are larger in size (about 9 Å, Nowak et al, 1987) than the channels. Diffusion takes place by molecular jumps between these sites when a molecule has acquired sufficient energy to overcome the barrier at the channels. For the case where the molecular diameter is close, but still smaller than the channel size, molecules might experience a net attraction when passing through the channels. When the molecular diameter is slightly larger than the channel size, molecules might experience a moderate repulsive force instead. A further increase in molecular diameter would dramatically increase the potential barrier and eventually exclude the molecule from entering the zeolite due to the strong repulsive force. A molecule with a larger diameter would be of higher potential at the channels. On the other hand, the molecular shape and the configurations of channel intersections would determine how strongly a molecule is attracted by zeolite framework at the intersections. The activation energy for a jump, E, arises from the difference of the potential of a molecule at the transition sites (i.e. the channels), Φ_c, and the potential at the adsorption sites (i.e. the channel intersections), Φ_i:

$$E = \Phi_c - \Phi_i \qquad (3.3)$$

The activation energy is, therefore, a complicated interplay among the molecular shape (e.g. its diameter and length), the channel size, and the size of the channel intersection.

The following calculations can further elaborate above argument. Table 3.3 lists the diameters of molecules in interest, d_m; the potential energy constants, ϵ_m. The potential energy of a molecule with a diameter d_m at the center of a 10-membered oxygen ring, Φ_c, was approximated by a Lennard-Jones equation

$$\Phi_c = 10 \times 4\epsilon \left[\left(\frac{\sigma_c}{r_c}\right)^{12} - \left(\frac{\sigma_c}{r_c}\right)^{6}\right] \qquad (3.4)$$

as discussed in Chapter 2. It was assumed that all oxygens were positioned at a 10-membered ring with a diameter of 5.8 Å. The distance between the center of the ring to the nuclei of oxygens, r_c, was equal to 4.2 (= ½ (5.8 + 2.6)), where the diameter of oxygen ions was taken as 2.6 Å following Flanigen et al (1978). The potential length constant, σ_c, for each pair of molecule-oxygen was taken as ½ (d_m + 2.6). And the corresponding ϵ/R was the square root of (ϵ_m/R)*113, where R is gas constant and 113 is the value of ϵ_m/R for oxygen (Bird et al, 1960). Although oversimplified, above descriptions retain some critical features of ZSM-5 channels.

Table 3.3 shows that the resulting values of Φ_c for the interested molecules ranges from -3.90 kcal/mol of soft attractions from the channel for 2-methylbutane, to 0.64 kcal/mole of moderate repulsions for benzene, and to 7.00 kcal/mol of strong repulsions for 2,2-dimenthylbutane. When we subtracted the values of Φ_c from the respective activation energies, E, observed in the experiments, the values of Φ_i are about 9 to 12.5 kcal/mol for those molecules. These values are no longer strongly dependent on the molecular diameters. The increase in the activation energy from mono-branched paraffin, to benzene, cyclohexane , and double-branched paraffin is, therefore, mainly due to the increase in the molecular diameter.

Table 3.3 Potential Energy Estimations

	d_m (A)	ϵ_m/R (K)	Φ_e (kcal/mol) (estimated)	E (kcal/mol) (experi.)	$\Phi_i = E - \Phi_e$
2-Methylbutane	5.0	346	-3.90	7.62	11.5
Benzene	5.85	404	0.64	9.70	9.1
Cyclohexane	6.0	407	2.97	15.51	12.5
2,2-Dimethylbutane	6.2	371	7.00	16.67	9.8

Although the molecular diameter is the dominant factor in determining the activation energy and thus the value of diffusivity, other factors, such as the molecular length, can also affect the diffusion characteristics. The small decrease in diffusivity and the increase in the activation energy from 2-methylbutane to 2-methylpentane is probably resulted from the stronger molecule-lattice interaction of 2-methylpentane at the intersection due to the longer length of 2-methylpentane.

3.2.2 Concentration Dependence

For both 2-methylbutane, which might experience soft attractions when passing through the channels as indicated in the above calculations, and benzene, which might experience soft repulsions at the channels, diffusivities were found to be almost independent of concentration up to about 4 molecules/unit cell, as shown in Figures 3.8 and 3.9. The same kind of concentration dependent trend was observed for both benzene and toluene in ZSM-5(WQ) at 65 °C over the same concentration range (Figure 3.10). In the same figure, it is shown that the adsorption and the desorption bear no effect on the diffusional results. And there is no hysteresis effect on the isotherms, as shown in Figure 3.11. Furthermore, the equilibrium data on Figures 3.11 were fitted by a Langmuir isotherm model. In Figure 3.12, the Langmuir isotherm parameters, defined as

$$K = \frac{c}{P(c_s - c)} \tag{3.5}$$

where c_s is the saturation concentration, were plot against the concentration for several different systems at the different temperatures. The constant values of Langmuir parameters were observed. It shows that the Langmuir isotherm gives a reasonably good description of the equilibrium behavior for the concentration range

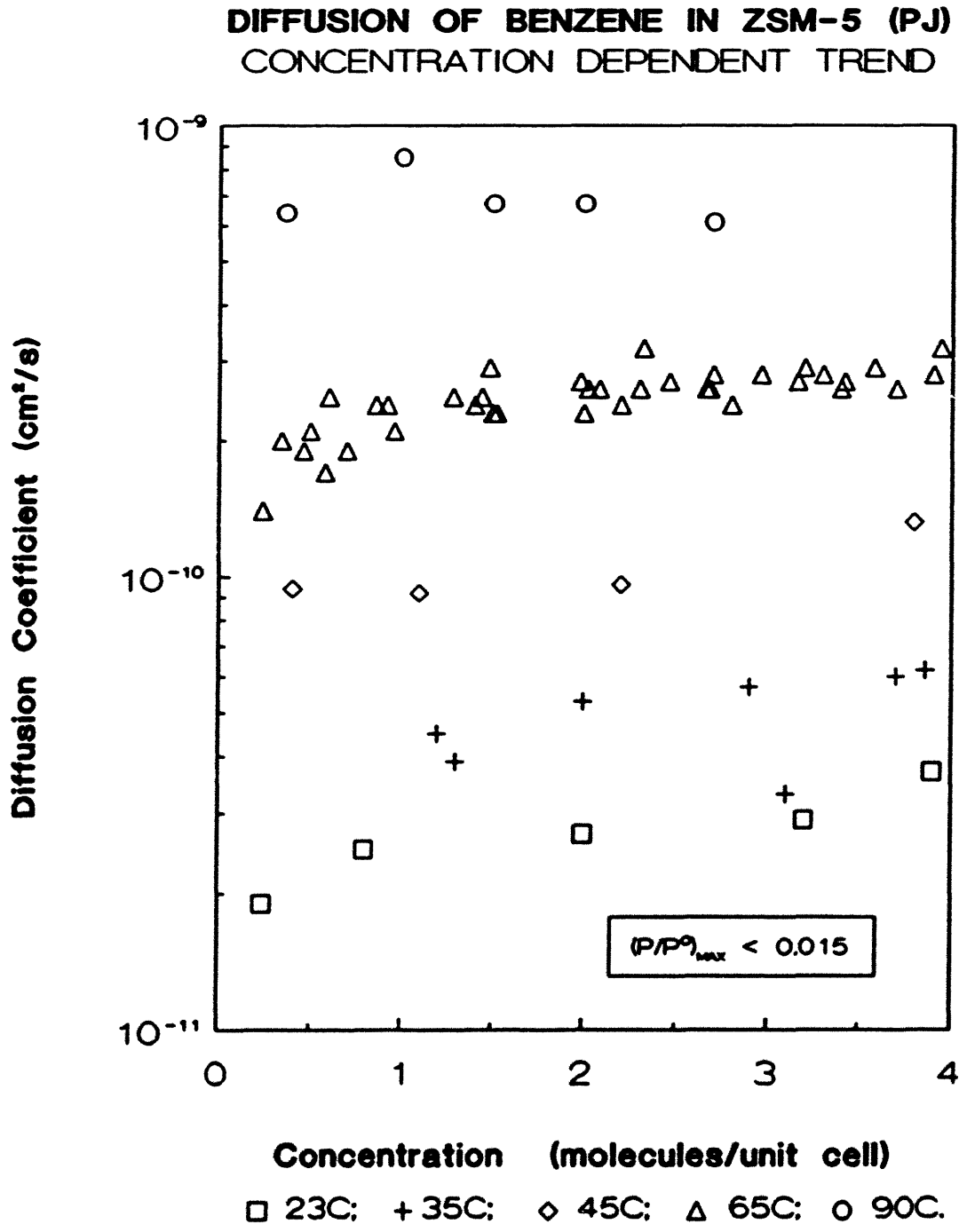

Figure 3.8 Diffusion of Benzene in ZSM-5(PJ): Concentration Effect (1)

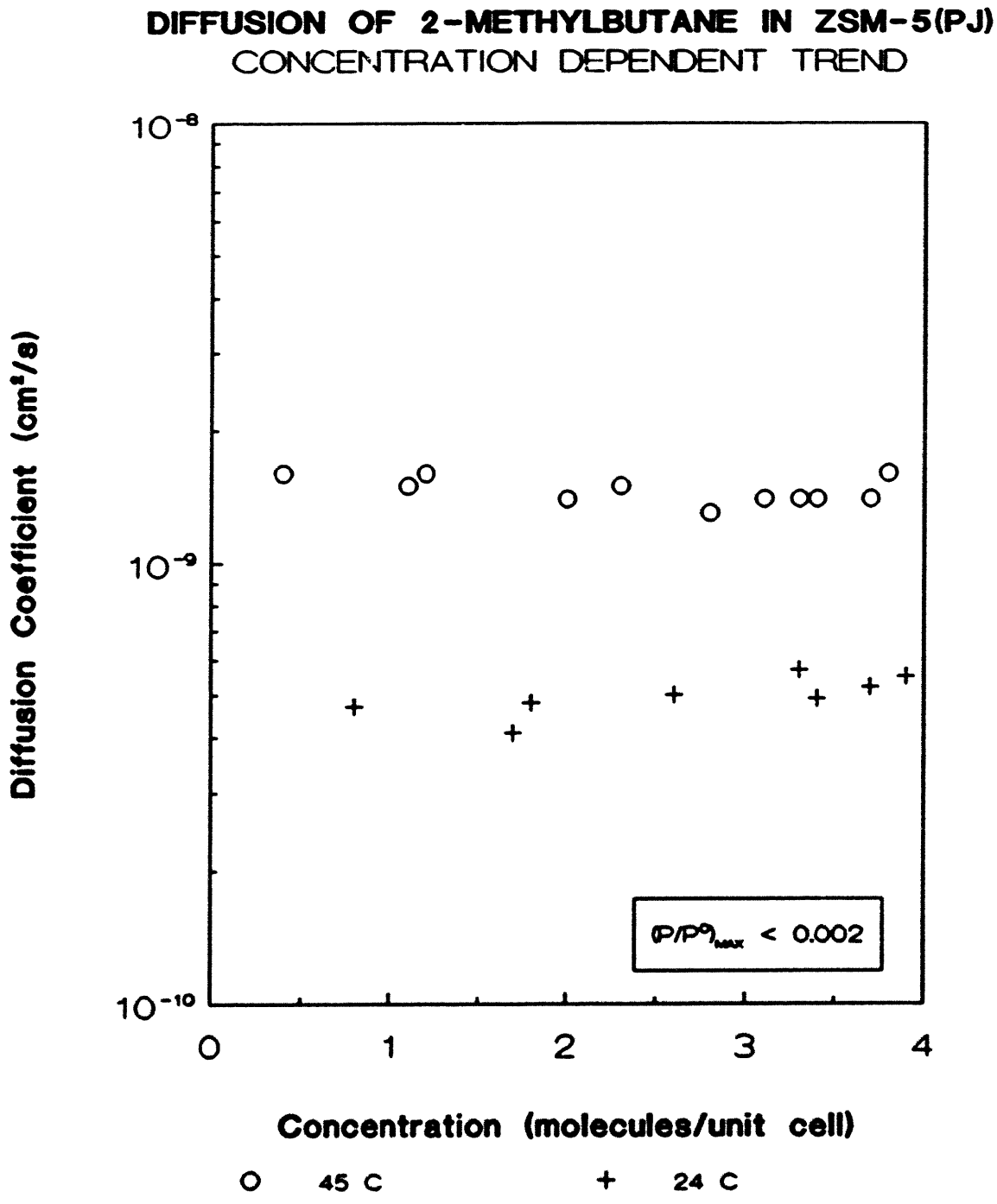

Figure 3.9 Diffusion of 2-Methylbutane in ZSM-5(PJ): Concentration Effect (1)

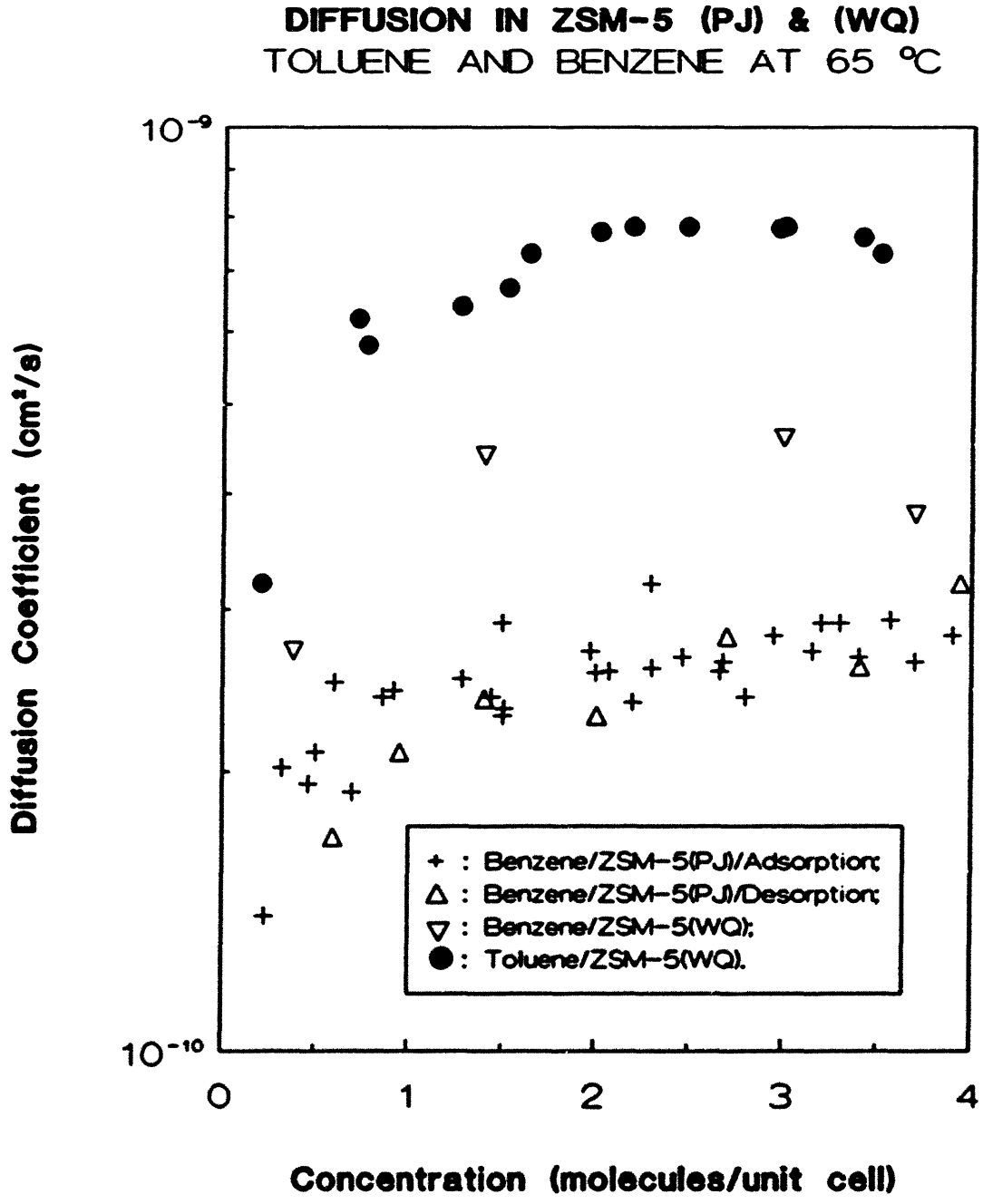

Figure 3.10 Diffusion of Toluene & Benzene in ZSM-5 (PJ) & (WQ)

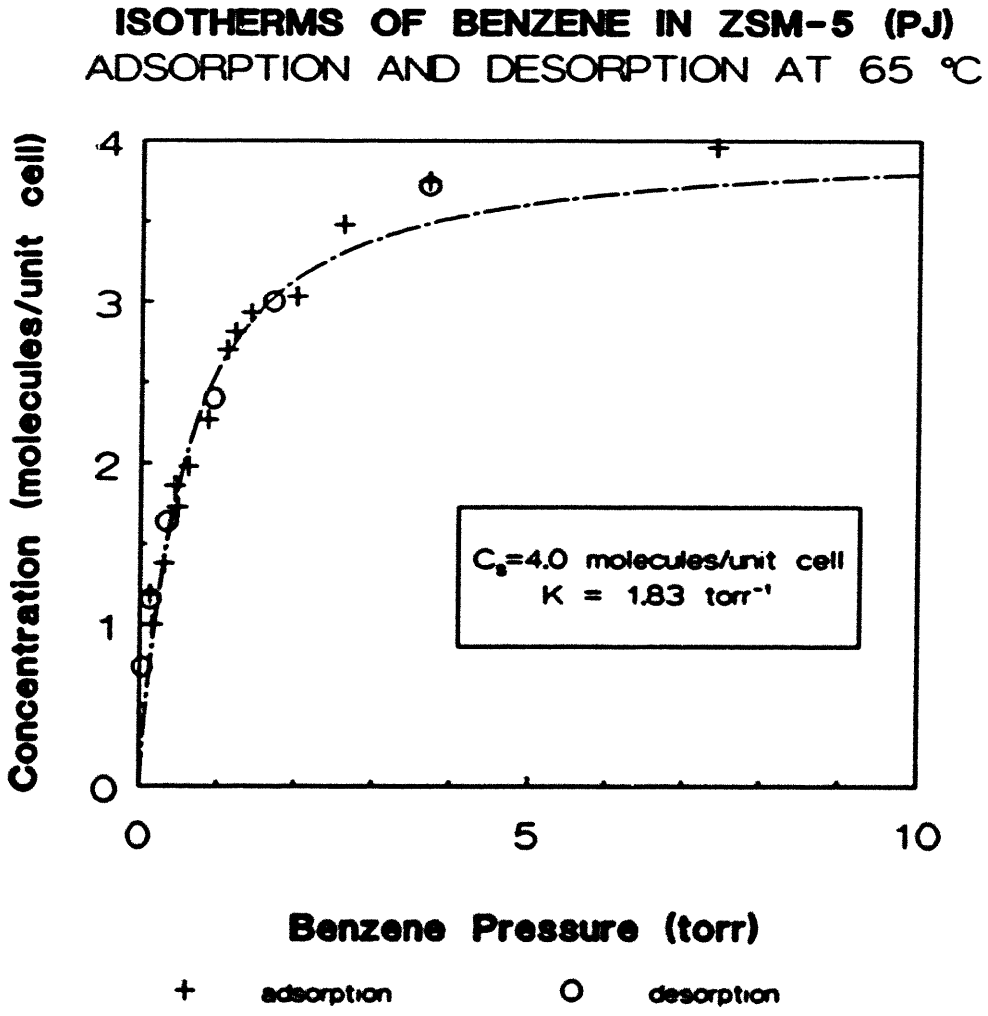

Figure 3.11 Equilibrium Isotherms of Benzene in ZSM-5(PJ) at 65 °C

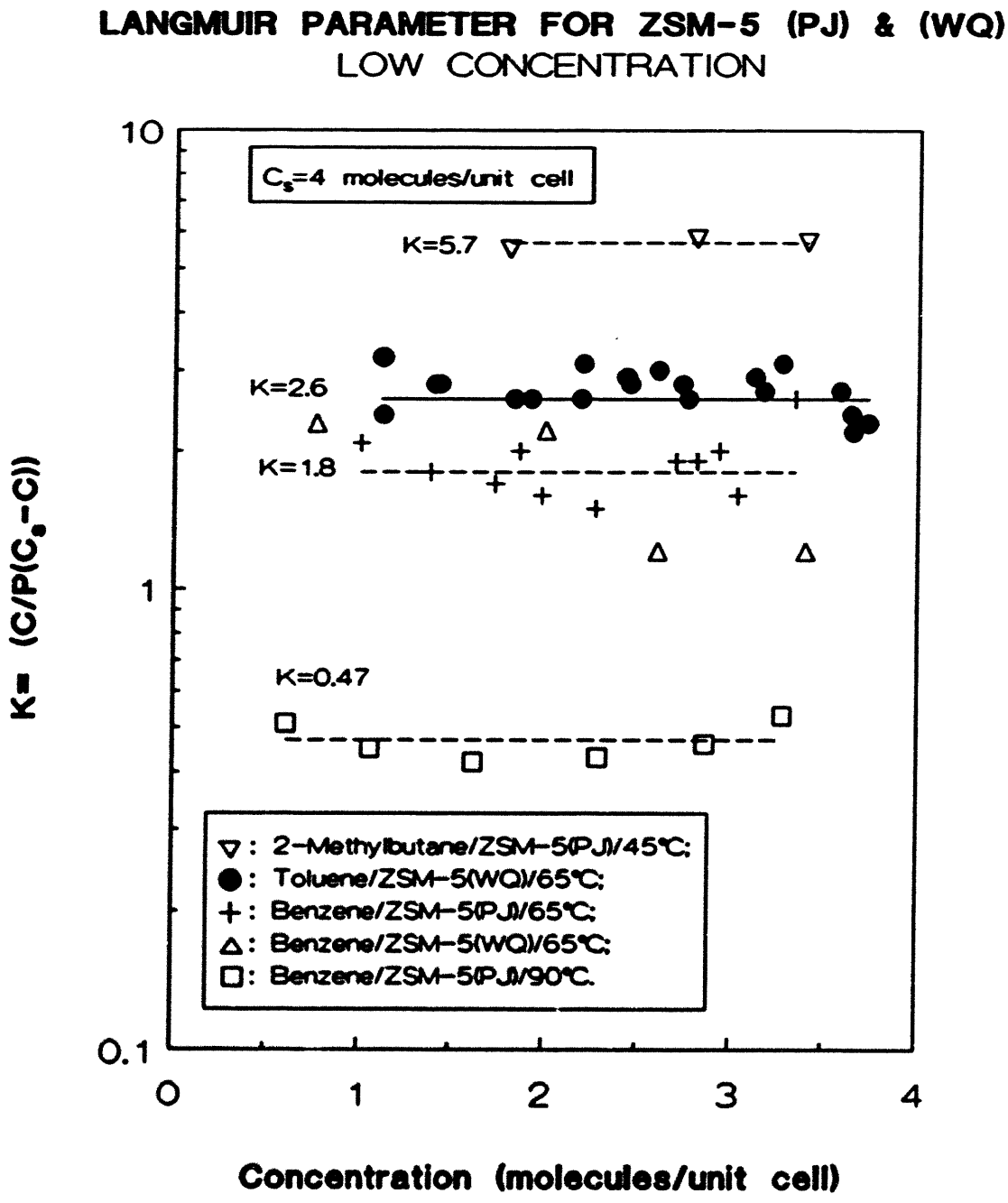

Figure 3.12 Langmuir Parameters: Concentration Effect (1)

of less than 4 molecules/unit cell. Figures 3.13 and 3.14 show that the "activating process" described in section 3.1 bears little effect on the diffusion and the equilibrium.

The concentration-independent trend of the diffusivity for benzene within this concentration range is consistent with the results of Qureshi and Wei (1988), and of Zikanova et al (1987) when their results were converted back to the uptake diffusivities from the corrected diffusivities given in the paper, based upon the isotherms. They also observed Langmuir type for the equilibrium isotherms. Tsikoyiannis (1986), Choudhary and Scrinivasan (1986) reported dramatic rising trends of benzene diffusivity for the concentration less than 4 molecules/unit cell.

Since one unit cell of ZSM-5 contains four intersections, four molecules per unit cell thus correspond to one molecule per intersection. Bulky molecules such as benzene were experimentally shown to be present at the channel intersections up to about 4 molecules/unit cell (Mentzen, 1987). The average distance between molecules for the concentration of 4 molecules/unit cell is then approximately the distance between the channel intersections, about 10 to 12 Å (Richards and Rees, 1987). The Lennard-Jones potential for the interaction between benzene molecules separated by such a distance is of the order of less than -0.05 kcal/mol (see next chapter). The effect of such interaction on the diffusion is negligible since the activation energy for the diffusion is of the order of 10 kcal/mol. The molecule-zeolite interactions are, therefore, far more important than the molecule-molecule interactions in this case. The molecules within the zeolite lattice, therefore, execute a more or less random walk. The dominant molecule-lattice interaction gives a constant diffusivity and an isotherm of Langmuir type, according to the Non-Interacting Lattice model in Chapter 2.

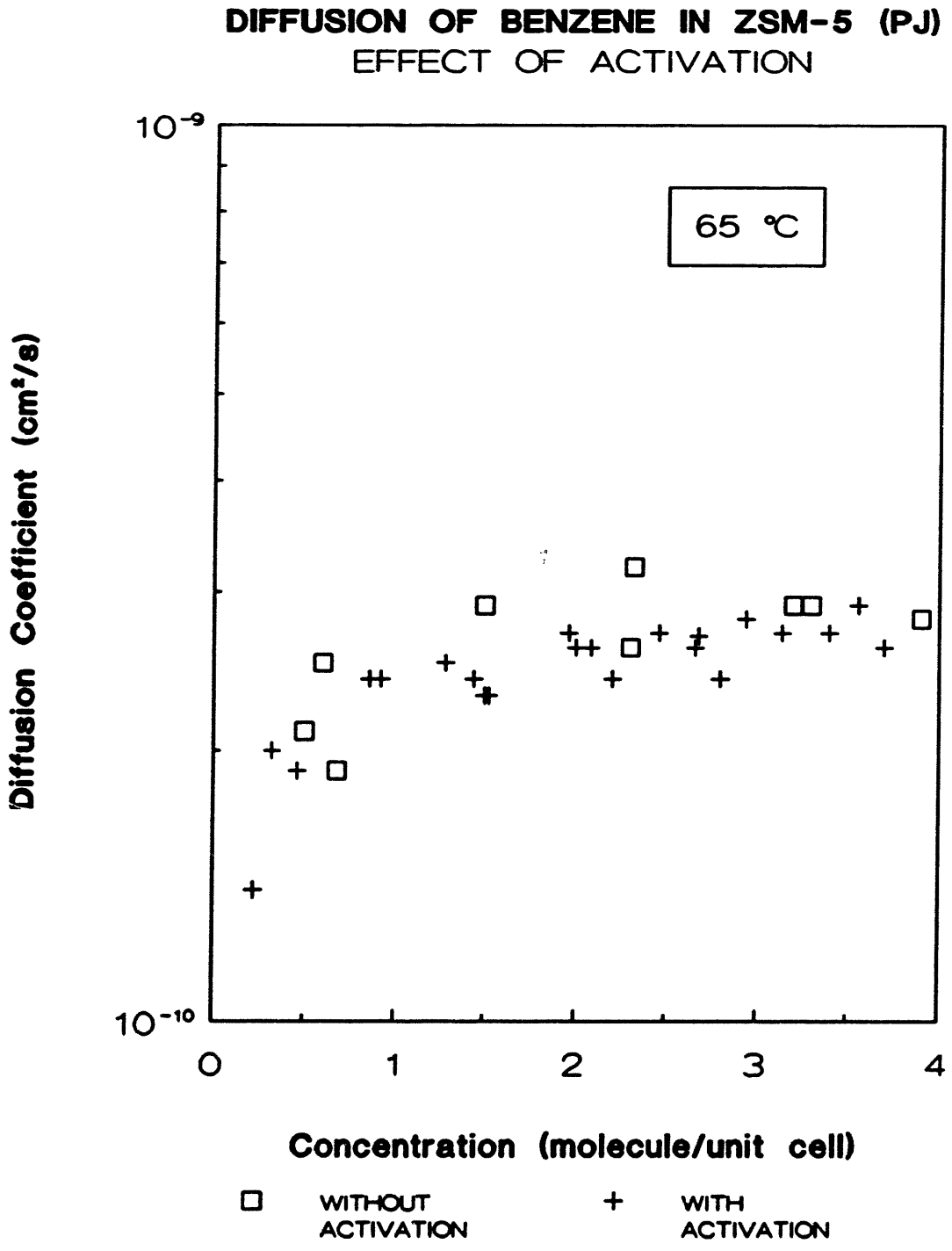

Figure 3.13 Diffusion of Benzene in ZSM-5(PJ): Effect of Activation Process

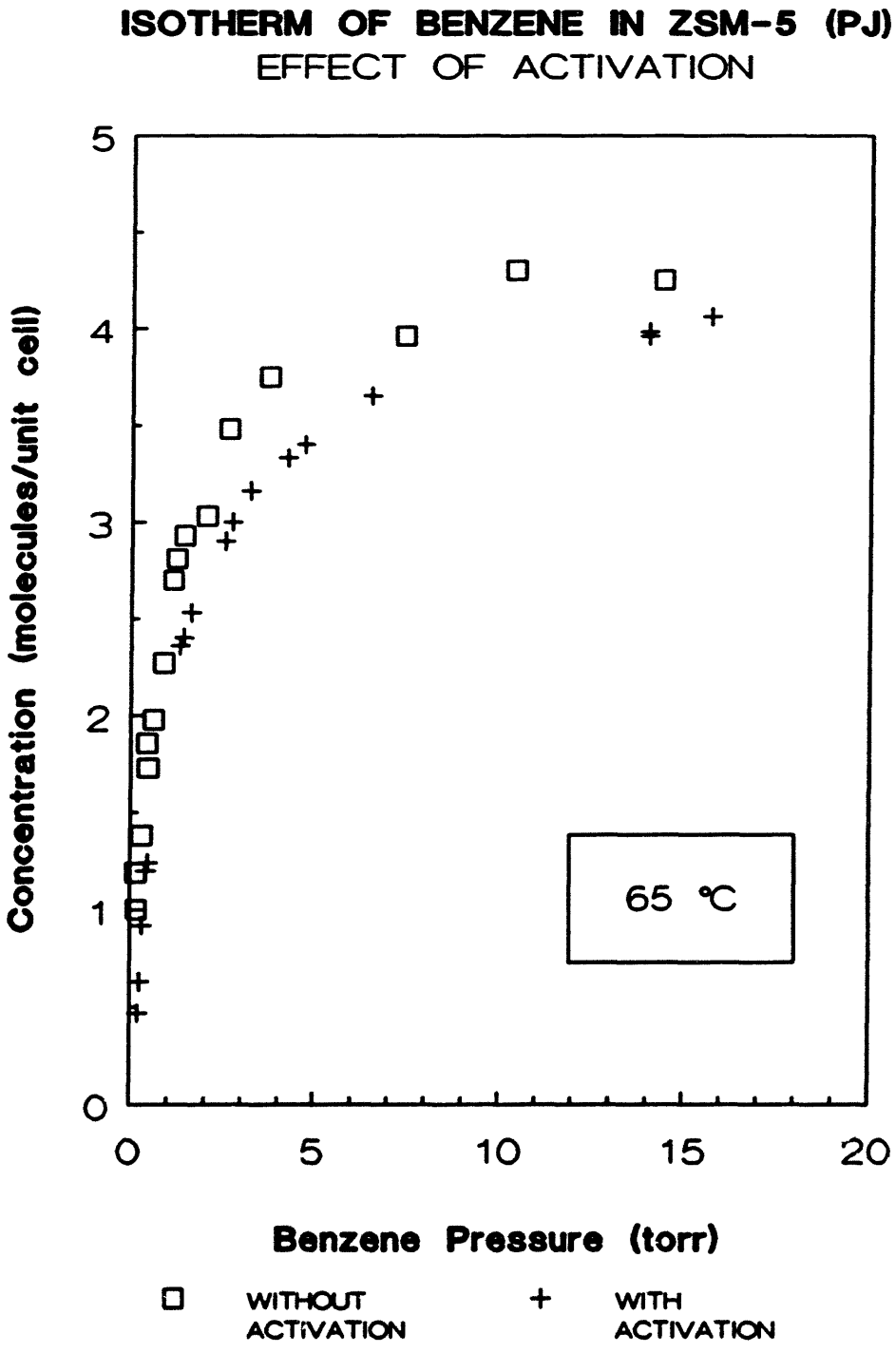

Figure 3.14 Equilibrium Isotherms of Benzene in ZSM-5(PJ): Effect of Activation

Another interesting conclusion drawn from Figures 3.10 and 3.12 is that toluene diffuses about twice as fast as benzene, although toluene is adsorbed more strongly. The stronger adsorption of toluene is also supported by the observation made by Stach et al (1983) and Pope (1984) that the adsorption heat of toluene is higher than that of benzene. The methyl group on the aromatic ring of toluene might increase the attractive interaction at the channel intersections between the molecule and the lattice, which makes toluene adsorb more strongly. The methyl group, on the other hand, might make the passing of the molecule through the narrow channels easier due to the attractive interaction between the methyl group and the lattice. A larger diffusivity for toluene might be resulted from the compensation between the lower potential at the adsorption site (stronger adsorption at the intersection) and the lower potential at the transition state (easier passing through the channel).

In Figure 3.10, a comparison between benzene diffusion in ZSM-5 (PJ) (Si/Al = 110) and ZSM-5 (WQ) (Si/Al = 6000) was made at 65 °C. A Si/Al ratio of 110 corresponds to about 0.22 Al atom per intersection, and that of 6000 to less than 0.004 Al atom per intersection. The difference in the diffusivities between these samples is less than factor of two with the diffusion in ZSM-5(WQ) being faster. The uncertainty in choosing the sample's diffusion length makes this difference even less significant.

A further increase of concentration changes the concentration dependent trend of diffusivity dramatically. Figures 3.15 and 3.16 show a sharp increasing trend in the diffusivities of both benzene/ZSM-5 and 2-methylbutane/ZSM-5 for the concentration higher than 4 molecules/unit cell. The corresponding relative pressures were indicated in the figures. Those diffusivity values are also plotted

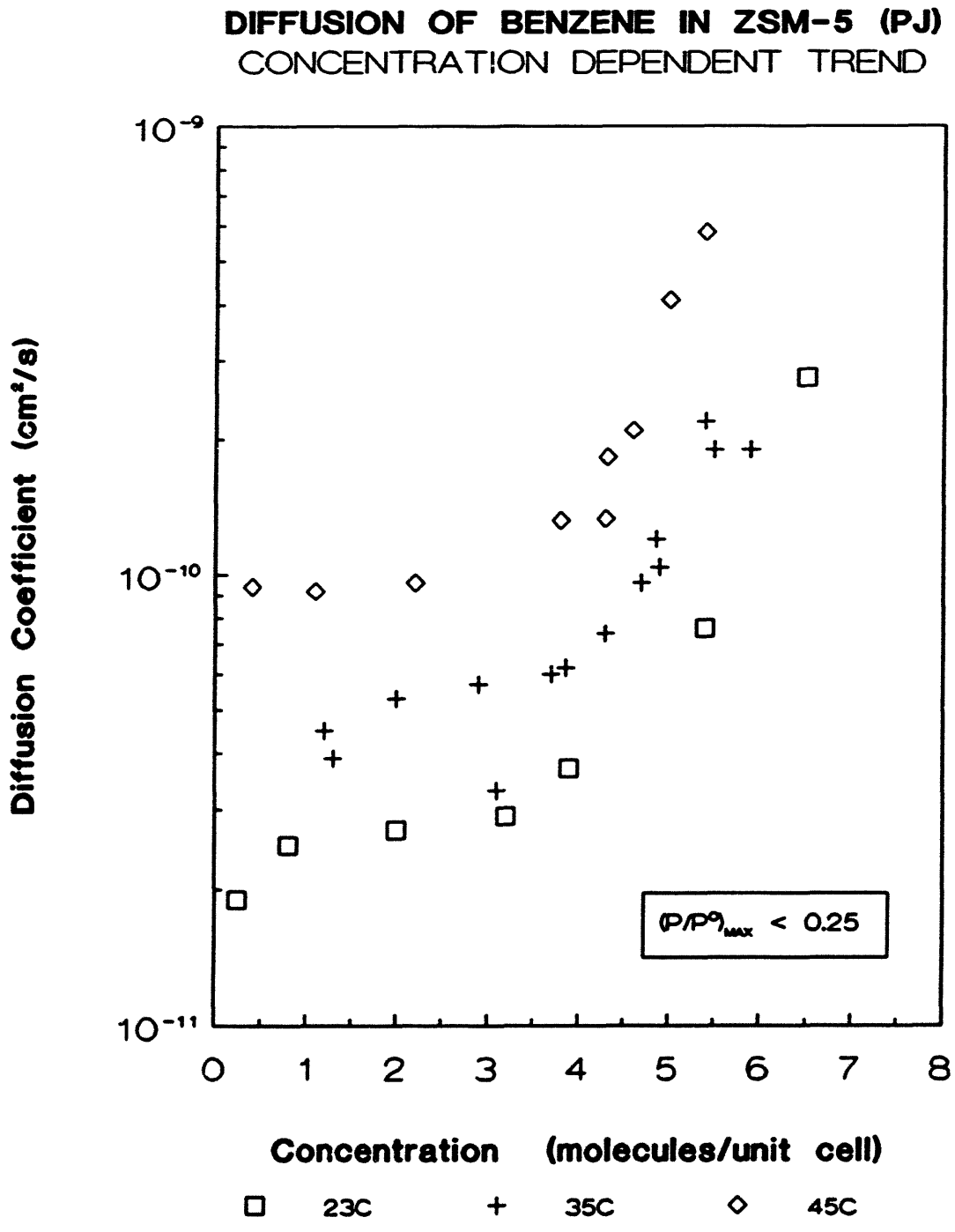

Figure 3.15 Diffusion of Benzene in ZSM-5(PJ): Concentration Effect (2)

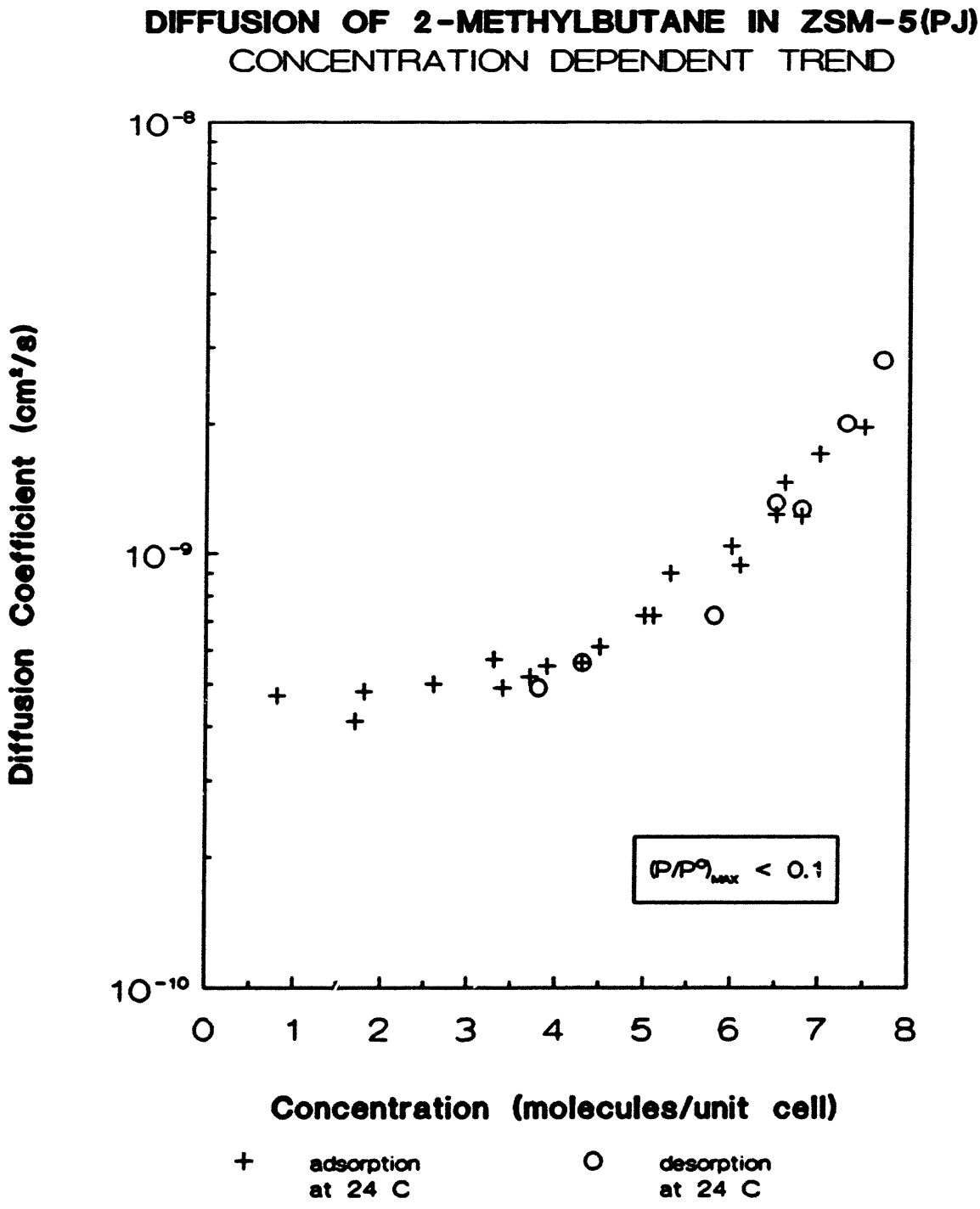

Figure 3.16 Diffusion of 2-Methylbutane in ZSM-5(PJ): Concentration Effect (2)

against the relative pressures in Figure 3.17. The equilibrium isotherms for benzene and 2-methyl-butane are given in Figures 3.18 and 3.19. And Figures 3.20 displays the concentration dependence of the Langmuir parameters for these two systems. The Langmuir isotherm is apparently no longer applicable at concentration higher than about 3.5 to 4 molecules/unit cell. The measurements of the isotherms of benzene at 23 °C and 35 °C, and that of 2-methylbutane at 24 °C were not performed for the concentration lower than 4 molecules/unit cell where the vapor pressures were too low to be accurately recorded. Desorption was also performed for 2-methylbutane as shown in Figure 3.19. No hysteresis was detected. Guo et al (1989) observed that the isotherms of benzene and toluene on ZSM-5 were not of Langmuir type at concentration higher than about 3.6 molecules/unit cell at temperature lower than 30 °C.

For the concentration higher than 4 molecules within one unit cell, the molecules begin to reside at the channels in addition to the more preferable site of the intersections (Mentzen et al, 1988). The distance between the molecules at the channel and at the channel intersection, about 5 to 6 Å, makes repulsive interactions between them possible. The repulsive force between molecules would lower the activation energy of the diffusion, in this case by the order of 1 kcal/mol, resulting in an increasing trend in the observed diffusivity, as discussed in chapter 2. The molecules within the region of higher concentration would be "pushed" by the surrounding molecules out of the region more quickly than those at a region of lower concentration where the molecules are non-interacting and perform simple random walks. The repulsive forces between molecules might also make it more difficult for molecules to enter zeolite lattice at a given pressure, which would result in a decrease in the Langmuir parameters.

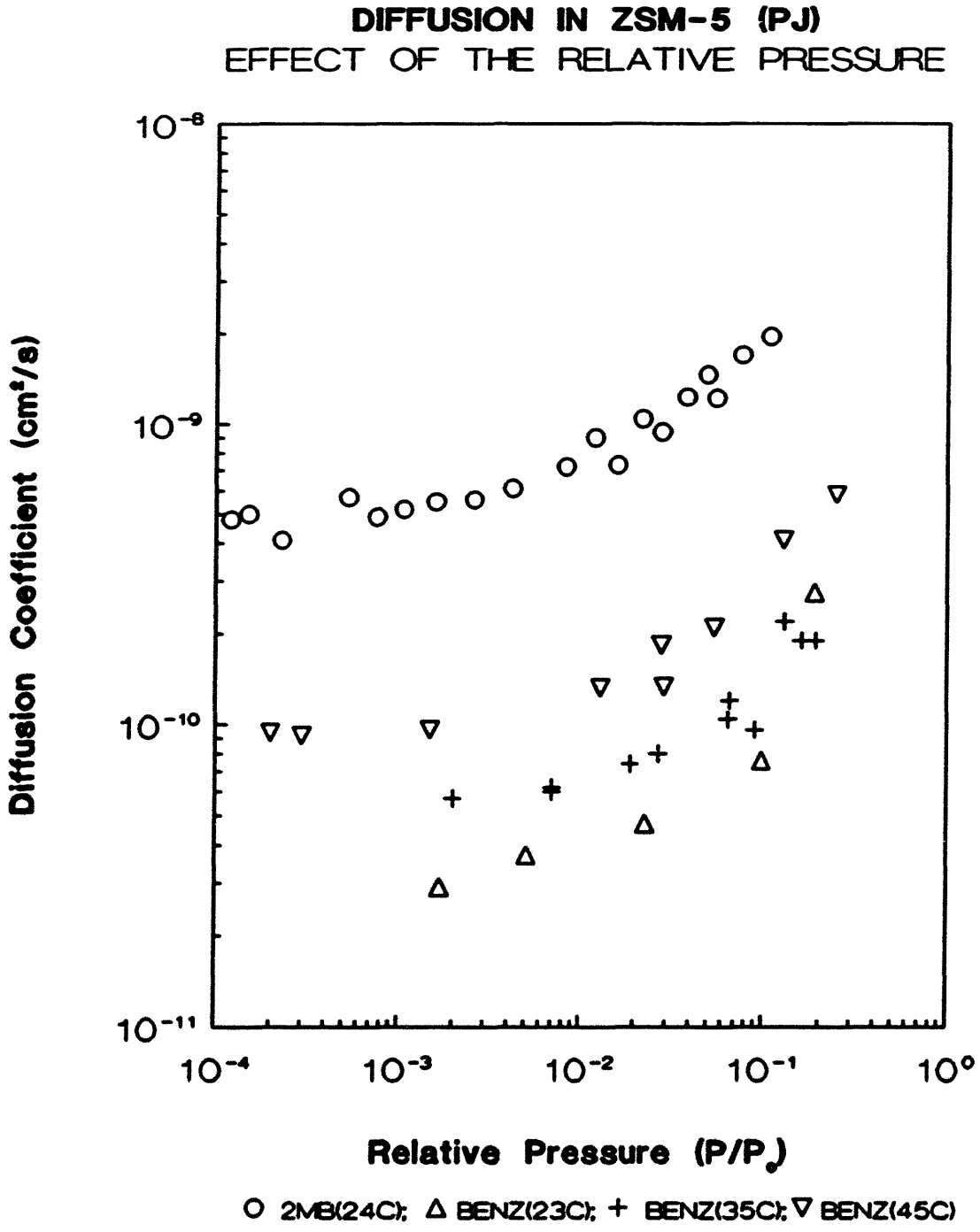

Figure 3.17 Diffusion in ZSM-5(PJ): Effect of Relative Pressure

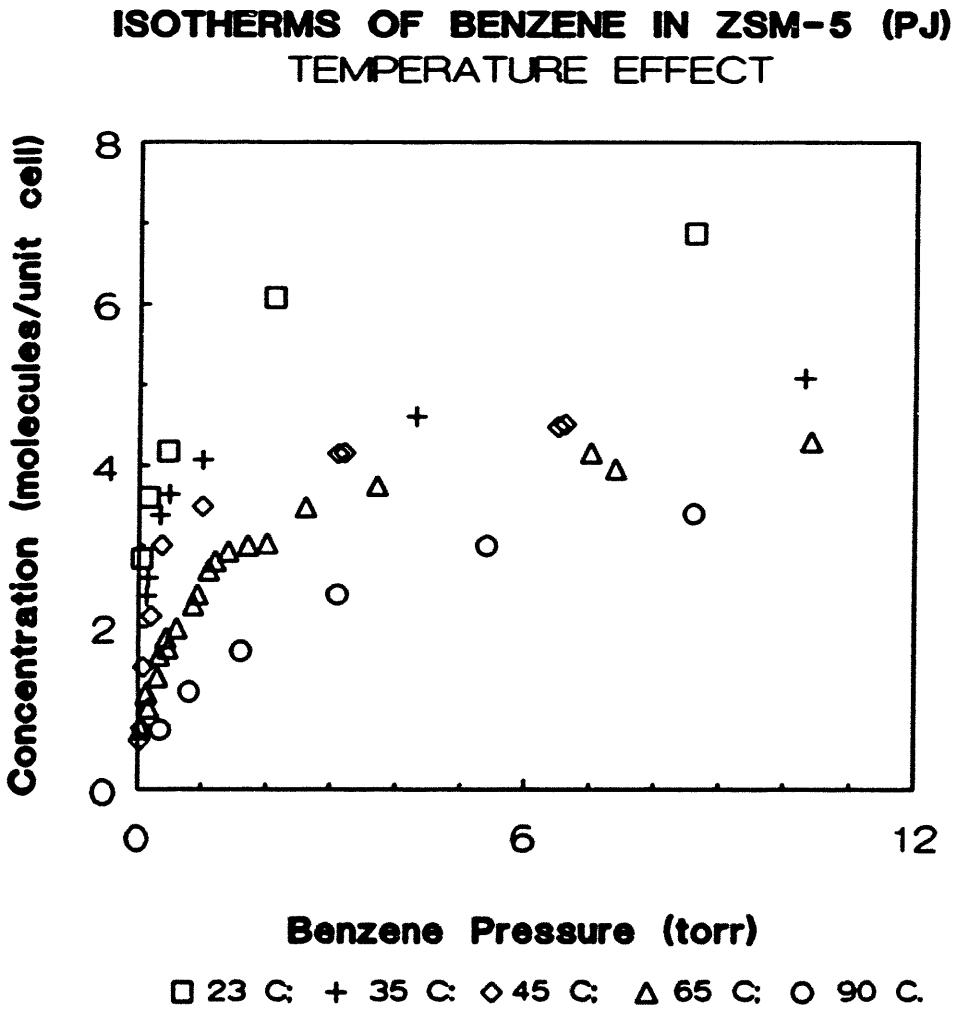

Figure 3.18 Equilibrium Isotherms of Benzene in ZSM-5(PJ): Temperature Effect

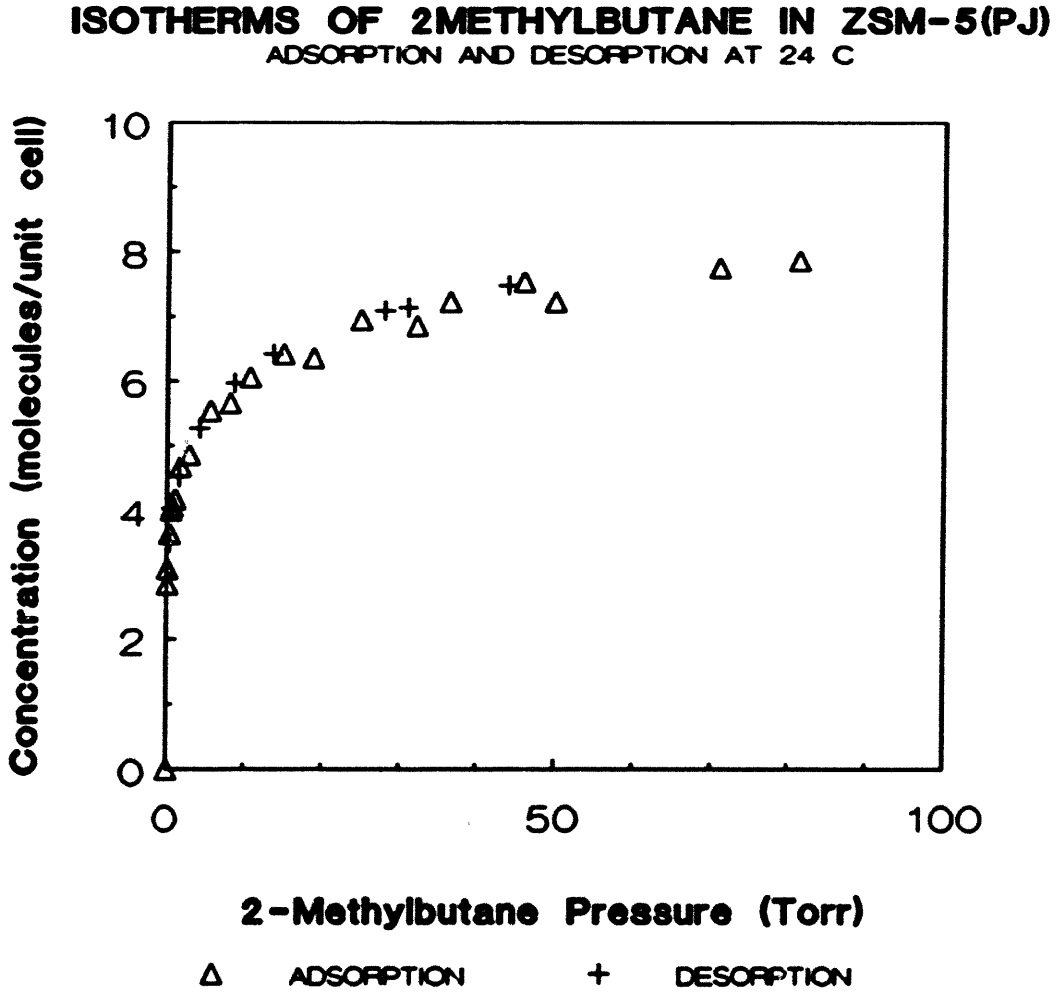

Figure 3.19 Equilibrium Isotherms of 2-Methylbutane in ZSM-5(PJ): Adsorption and Desorption

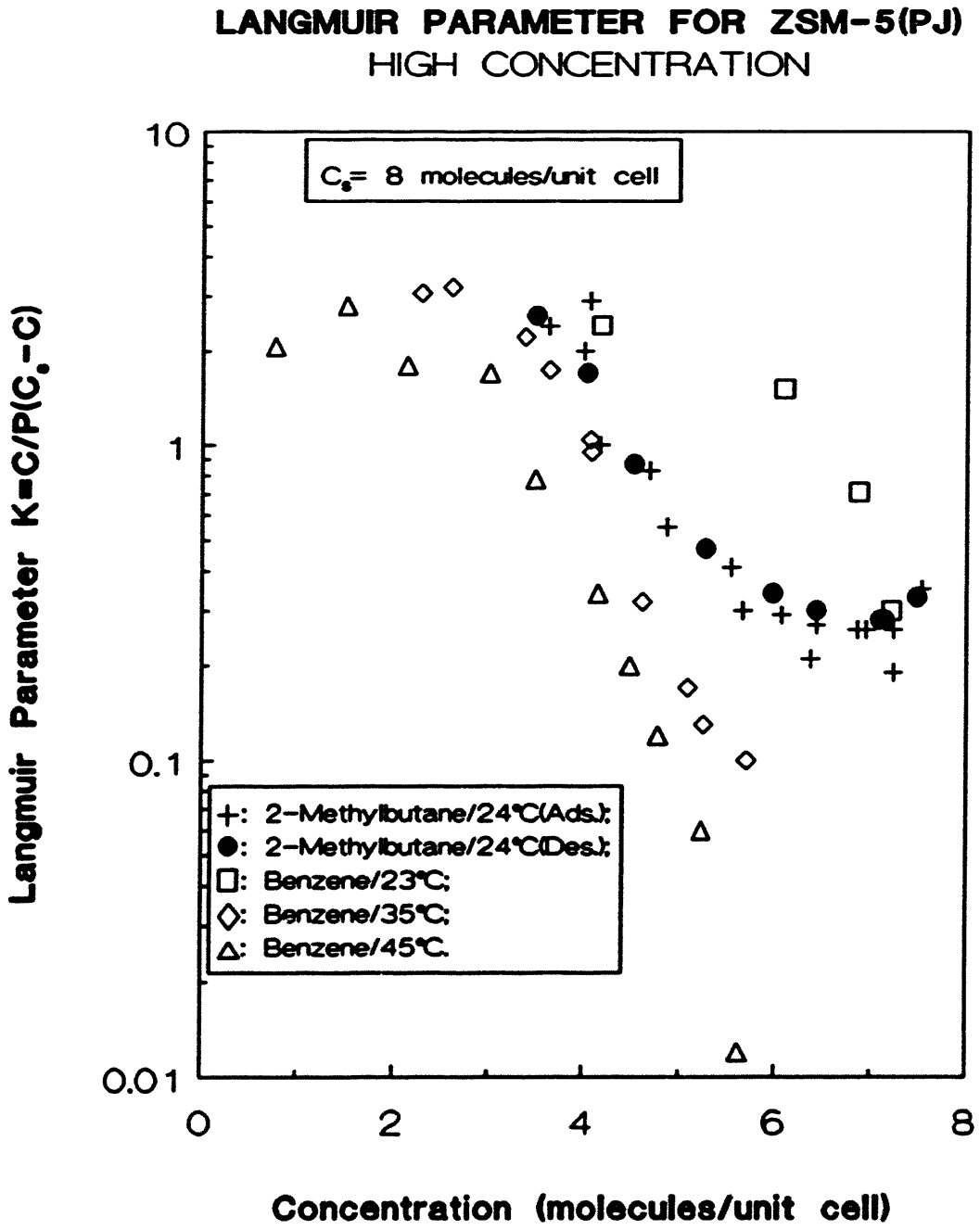

Figure 3.20 Langmuir Parameters: Concentration Effect (2)

3.2.3 Cage Effect

The existence of cages of much larger diameter (about 12 Å) within zeolites, such as 5A, may also remarkably change the concentration dependence of the observed diffusivity. In the case of the diffusion of heptane in 5A, as shown in Figure 3.21, as much as a twenty-fold increase in diffusivity was observed as heptane concentration increases from about 0.3 molecule/cage to about 1.7 molecules/cage. These results are consistent with the literature data (Ruthven, 1984). Since it is possible for one cage to host two molecules due to the large cage size, the confined molecules may interact with each other instead of sole interaction between the molecule and the lattice. A resulting repulsive interaction between the molecules reduces the activation energy of the jumping, and consequently increases the apparent diffusivity. Hosting more than one molecule at the same cage, however, is not a sufficient condition for the increasing trend in diffusivity to be observed. For smaller molecules, such as ethane, only a very moderate increase of diffusivity, about a factor of 2, was reported even when the concentration was changed from about 2.5 molecules/unit cell to about 4 molecules/unit cell (Ruthven et al, 1975b). This is probably because the molecules are so small that even packing more than two molecules within one cage is not enough for any interaction between molecules to become significant. For the larger molecules, such as normal decane, the increasing trend was observed even below 1 molecule/unit cell (Vavlitis et al, 1981).

Table 3.4 lists the Lennard-Jones potential length constants for normal paraffins, determined by Wilke-Lee method (Reid et al, 1977). We assume that each molecule has a van der Waals interacting-volume of the spherical shape with a diameter of about 1.8 times of its potential length constant, σ_m. Beyond this volume, the interactions between this molecule and other molecules are negligible, since the

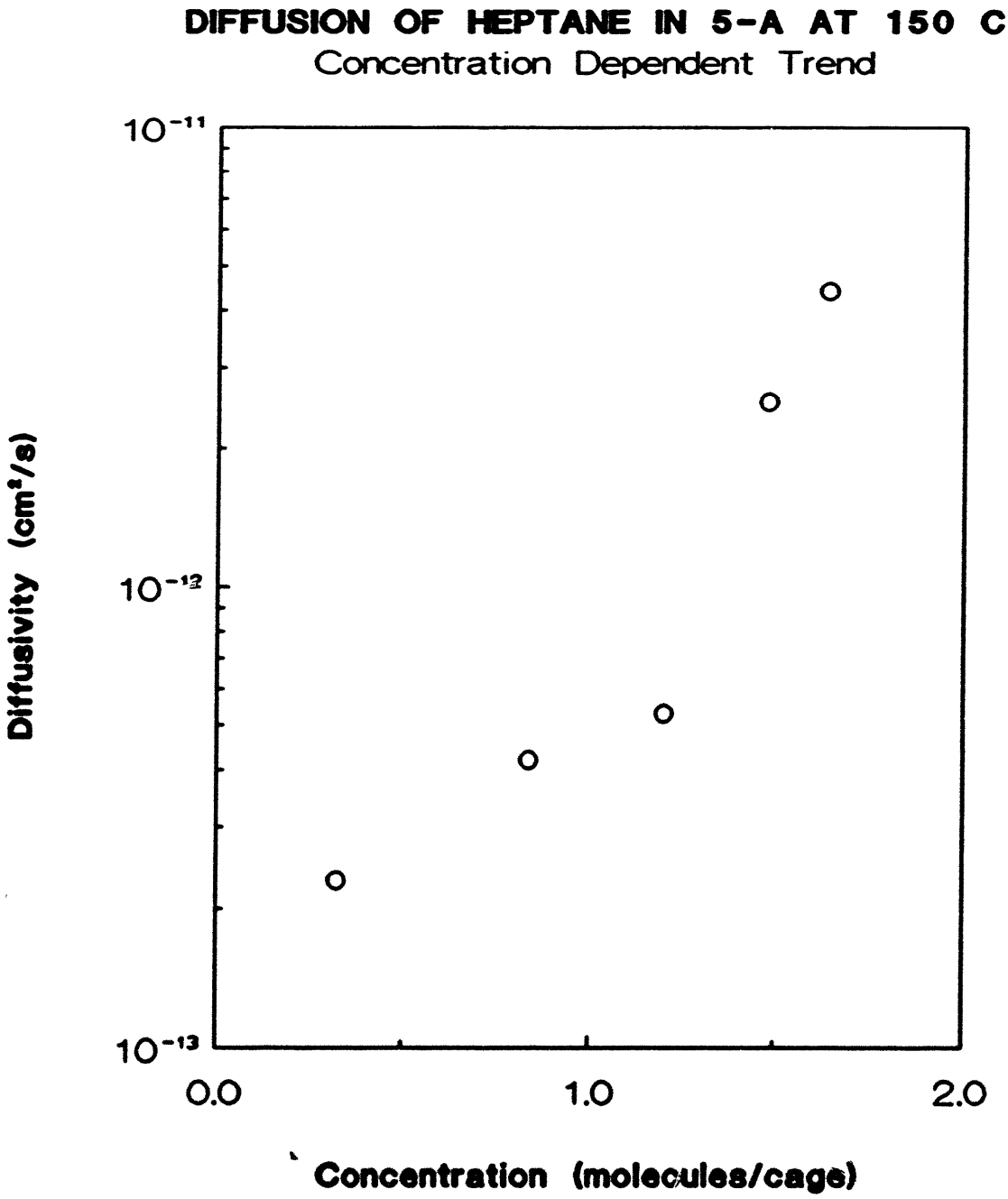

Figure 3.21 Diffusion of Heptane in 5A: Concentration Effect

Table 3.4 V_w for Normal Paraffins

	σ_m (A)	V_w (A^3)	V_{mol}/V_w
CH_4	3.65	148	5.2
C_2H_6	4.40	260	3.0
C_3H_8	4.95	370	2.1
nC_4	5.41	483	1.6
nC_5	5.79	593	1.3
nC_6	6.14	707	1.1
nC_7	6.40	800	0.97
nC_8	6.72	927	0.84
nC_9	6.98	1038	0.75
nC_{10}	7.22	1149	0.68

interacting potential between two molecules separated by such a distance is no longer significant (at the order of -0.1 kcal/mol) compared to the activation energy for the diffusion (at the order of 10 kcal/mol). Within this volume, the soft attractions and, more importantly, the repulsive interactions between molecules become possible. The ratio of the cage volume, V_{cage} (=776 $Å^3$ for 5-A, from Ruthven, 1984) and the van der Waals interacting-volume, V_w, thus gives us at least a semi-quantitative estimation of the importance of molecule-molecule interactions. According to these calculations, no interactions between molecules, thus no concentration dependence of the diffusivity, would be significant for ethane if the concentration is less than about 3 molecules/cage. For heptane, the concentration is about 1 molecule/cage. And the concentration for decane is about 0.7 molecule/cage. Above these concentration values, the interaction between molecules might begin to affect the activation energy of diffusion and result in a increase in the diffusivity. These agree closely with the experimental observations from this and the past studied cited above. In the above analysis, the spherical representations of molecules were used. For long chain molecules, such as normal-paraffins, these presentations are not very accurate. These values are, however, at least give us some semi-quantitative understanding of molecule/zeolite systems.

3.2.4 Sorption Capacity

Experiments were carried out for benzene, 2-methylbutane, and normal paraffins (nC_6, nC_7, nC_8, nC_{10}) around room temperature up to relative pressures above 0.1. Figure 3.22 shows the isotherms of normal-paraffins (nC_6, nC_7, nC_9, n_{10}). These isotherms are roughly rectangular in shape. Figure 3.23 relates the approximate molecular lengths with the sorption capacities, showing a decrease from about 8 molecules/unit cell for the relatively short molecules to about 4

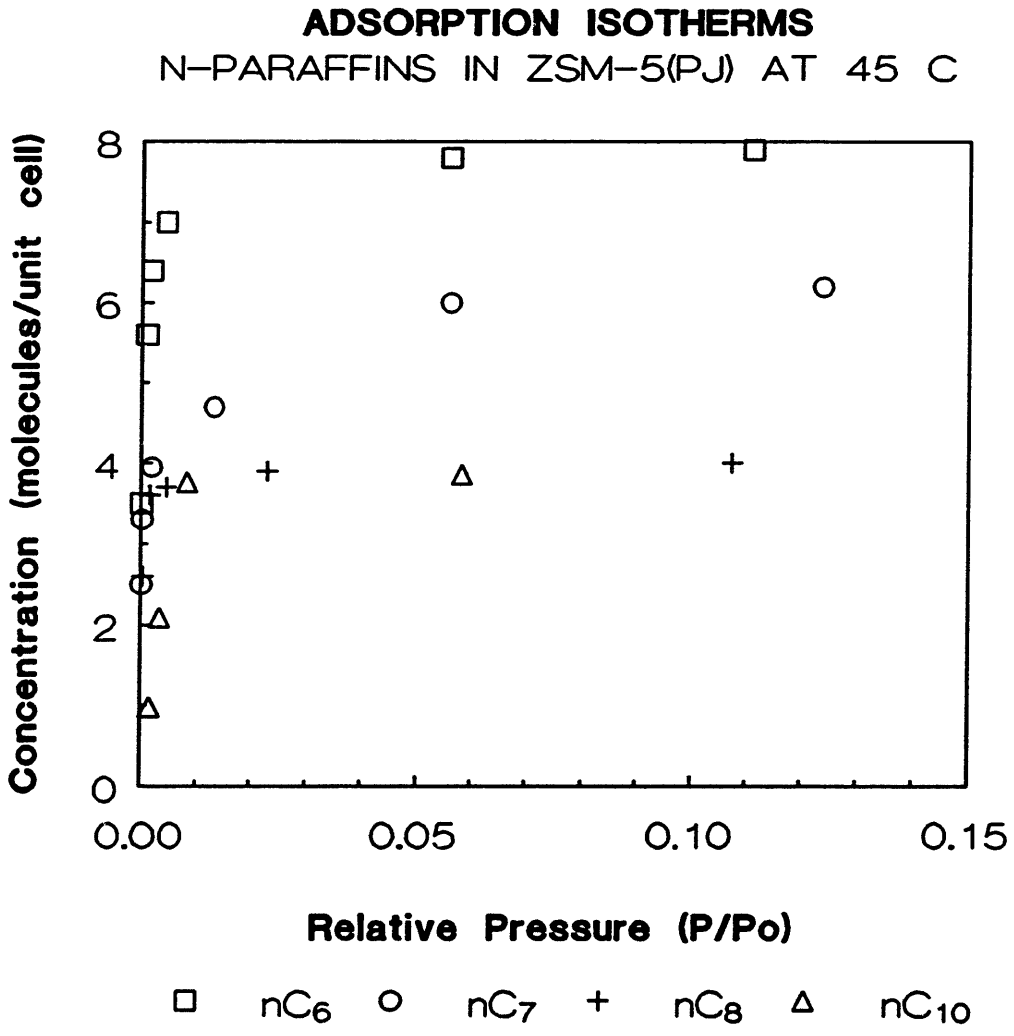

Figure 3.22 Equilibrium Isotherms of N-Paraffins in ZSM-5(PJ)

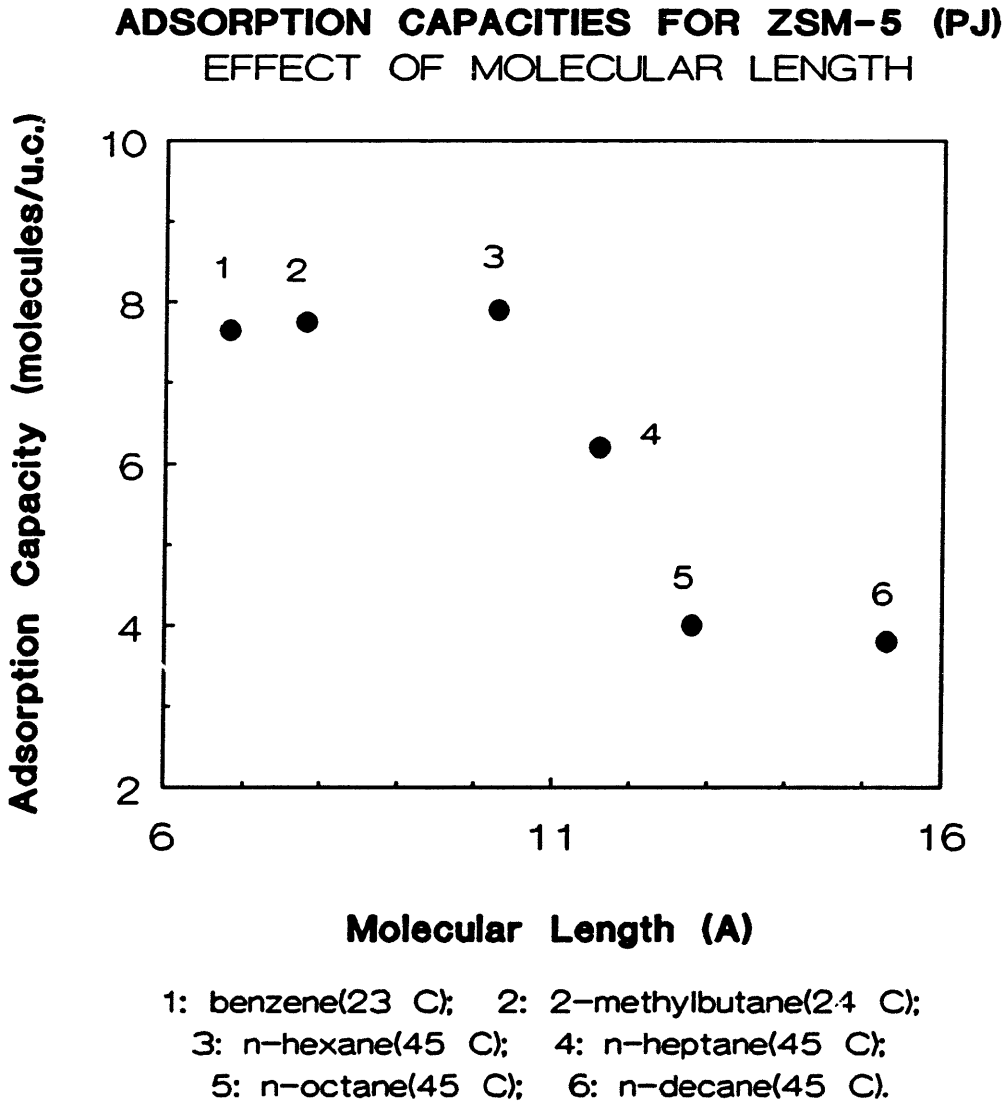

Figure 3.23 Adsorption Capacities for ZSM-5(PJ): Effect of Molecular Length

molecules/unit cell for the long chain molecules. The smaller molecules, such as ethane and propane, could have capacities higher than 8 molecules/unit cell. Richards and Rees (1987) reported capacities for ethane and propane of about 10.6 molecules/unit cell.

Since the diameters of paraffins and aromatics are close to the channel size of ZSM-5, the possibility of double occupancy for molecules at a given site within the channel system is excluded. Based upon the total length of channels in a unit cell, we estimated the sorption capacities according to the values of molecular length. Table 3.5 compares the theoretical estimations of capacities of several hydrocarbons with their experimental values from this and past studies, following Richards and Rees (1987). And Figure 3.24 verifies that for the molecules presented here we can approximately estimate the sorption capacities based on their molecular lengths.

3.2.5 Sample Contamination and Sample Modifications

We observed in our preliminary experiments that exposure of the sample to room air after calcination for a period of more than one day, or without thorough cleaning of the chamber before the run, could sometimes lower the measured diffusivity and change its concentration dependence trend, as shown in Figure 3.25. The variation in the diffusional results may be due to "contaminants" such as hydrocarbons adsorbed on the surface of crystals results in a "surface barrier". These samples usually turned brown after the run instead of the normal white color of the powder.

A systematic study of the magnesium modifications of ZSM-5 (PJ) was carried out by Mo (1988). The zeolites were modified under controllable conditions to

Table 3.5 Sorption Capacities for ZSM-5

		Sorption Capacity (m/u.c)	
	Molecular Length (A)	Theoretical	Experimental
Ethane	5.25	12.6	10.58[1]
Propane	6.52	10.2	10.66[1]
n-Butane	7.78	8.5	9.27[1]
			10.9[2]
2-Methylbutane	7.78	8.5	7.75[3]
n-Hexane	10.30	6.4	7.9[3]
			7.85[1]
			8.8[2]
n-Heptane	11.56	5.7	6.2[3]
n-Octane	12.82	5.2	4.0[3]
n-Decane	15.34	4.3	3.8[3]
Benzene	6.8	9.7	7.65[3]
			8.0[3]
			8.32[4]
			8.4[5]
			8.7[2]

* all of the molecular length are from Gorring (1973), except benzene (Vedrine, 1985)

** data sources: (0): present study;
(1): Richards and Rees (1987);
(2): Flanigen et al (1978);
(3): Wu et al (1983);
(4): Guo et al (1989);
(5): Thamm et al (1987).

*** total length of channels in a unit cell: 66.4 (A) (Richards and Rees, 1987)

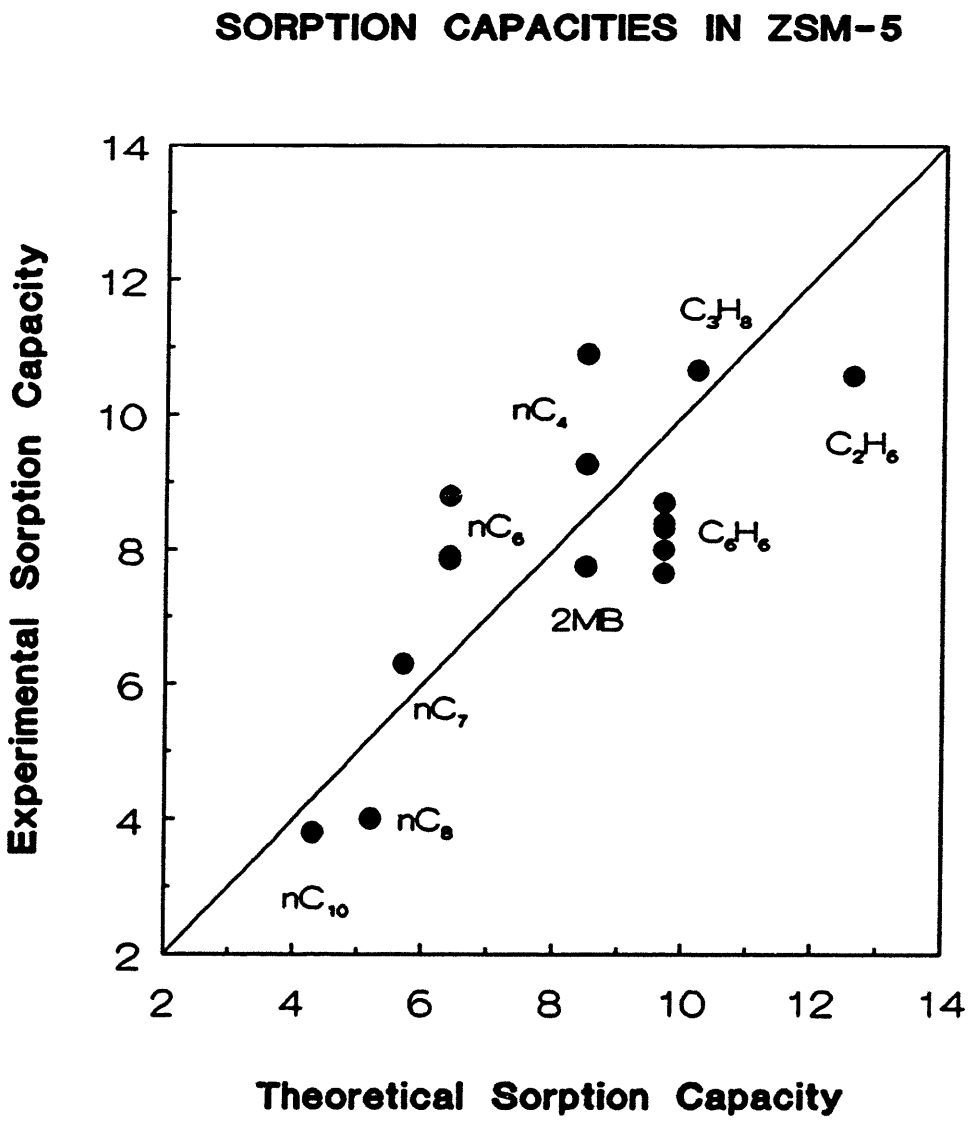

Figure 3.24 Sorption Capacities in ZSM-5: Comparison

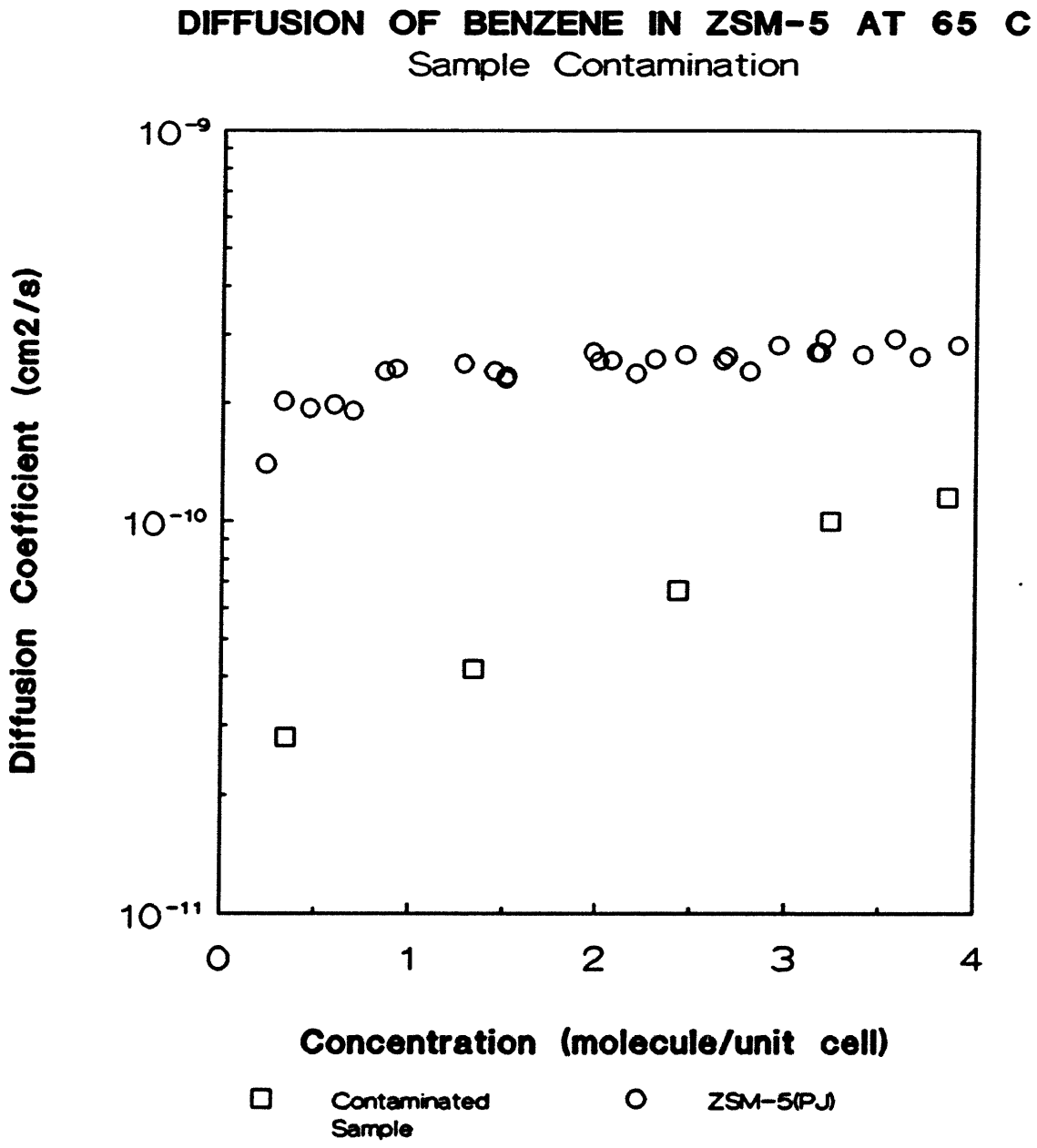

Figure 3.25 Diffusion of Benzene in ZSM-5: Effect of Sample Contamination

achieve either a surface-coated or an ion-exchanged modification. The surface-coated sample was obtained by concentrating the mixture of a magnesium acetate-water solution with powdered ZSM-5 crystals in an oven at 100°C to reduce the water content, but not to remove any excess magnesium, followed by calcination at 500 °C overnight before the diffusion experiments. The ion-exchanged sample was obtained by first filtering out the remaining solution with a membrane filter. The wet cake was then rinsed with distilled water and filtered before the final calcination so that all the excess magnesium solution adhered to the crystal surfaced was removed.

For the surface-coated samples, all the excess amount of Mg introduced into the system is segregated on the surface, while the interior of the zeolites still has very low concentration of uniformly distributed Mg. For the ion-exchanged zeolites, the state of magnesium is limited to a very low degree of uniform intrazeolitic incorporation. Figure 3.26 are the results of benzene for two surface-coated samples and one ion-exchanged sample, along with the diffusion results for the fresh, unmodified ZSM-5 (PJ).

The ion-exchange process could alter the zeolitic diffusion in two ways. Replacing H^+ with Mg^{2+} in the lattice and introducing excess Mg in the channel system after the ion-exchange could reduce the effective diffusivity because of the larger size of Mg. On the other hand, the reduction of acidity due to the ion-exchange could weaken the interaction between the molecules and ZSM-5 to cause an increase in diffusivity. Here, probably the latter effect prevails so that the observed diffusivity for the ion-exchanged sample is slightly larger than that for the fresh ZSM-5.

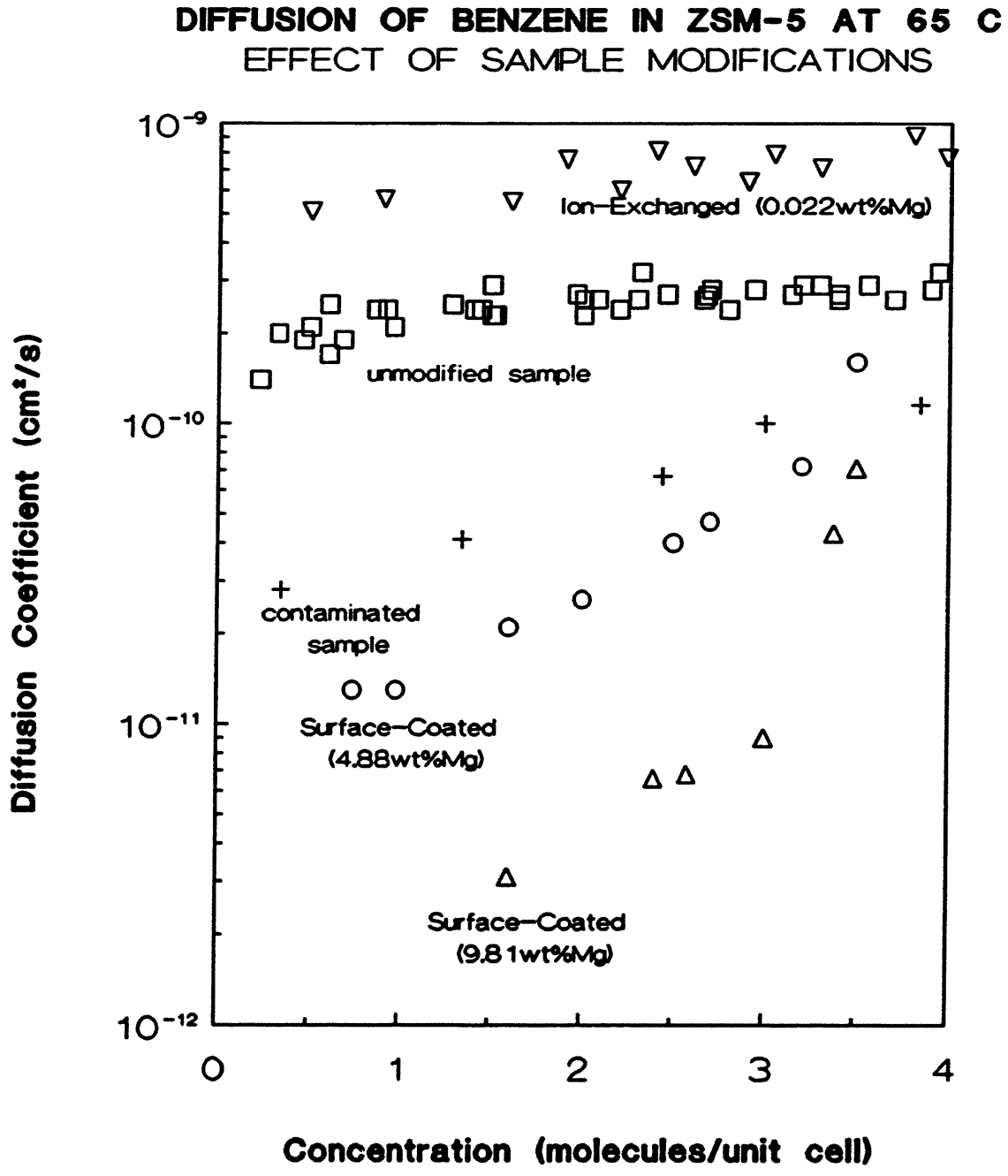

Figure 3.26 Diffusion of Benzene in ZSM-5: Effect of Mg Modifier

The concentration dependent trends of the diffusivity for the surface-coated samples are very similar to that for the contaminated sample. It is expected since the surface-coated sample could be viewed as the "heavily contaminated sample". The lower diffusivities for those samples are due to probably the blocking effect of the diffusion path entrance, while the reason for the rising trend of diffusivities for those samples remains unclear. The isotherms are not dramatically affected by the modification of the samples, as shown in Figure 3.27.

3.3 Conclusions

The temperature dependence of the diffusivity can be determined by an Arrhenius relationship, the GT model, where the pre-exponential term is the product of a constant (about 10^{-4}), which is almost independent of the tested molecules, and the square root of the testing temperature over the molecular weight. The activation energy reflects the complicated interaction between the guest molecule and the host zeolite lattice, and is mainly responsible for the different diffusivity values of various compounds.

The orders of magnitude of the diffusivity of hydrocarbons are strongly affected by molecule shapes. The larger the molecular diameter is, the more pronounced the decrease in the diffusivity. The effect of the molecular length diminishes once the molecular length exceeds about 8-9 Å.

The diffusion coefficients of benzene, toluene and 2-methylbutane in ZSM-5 are not dramatically influenced by the concentration up to about 4 molecules/unit cell, within which the interaction between molecules is insignificant due to the relatively long distance between them. The isotherms are of the Langmuir type.

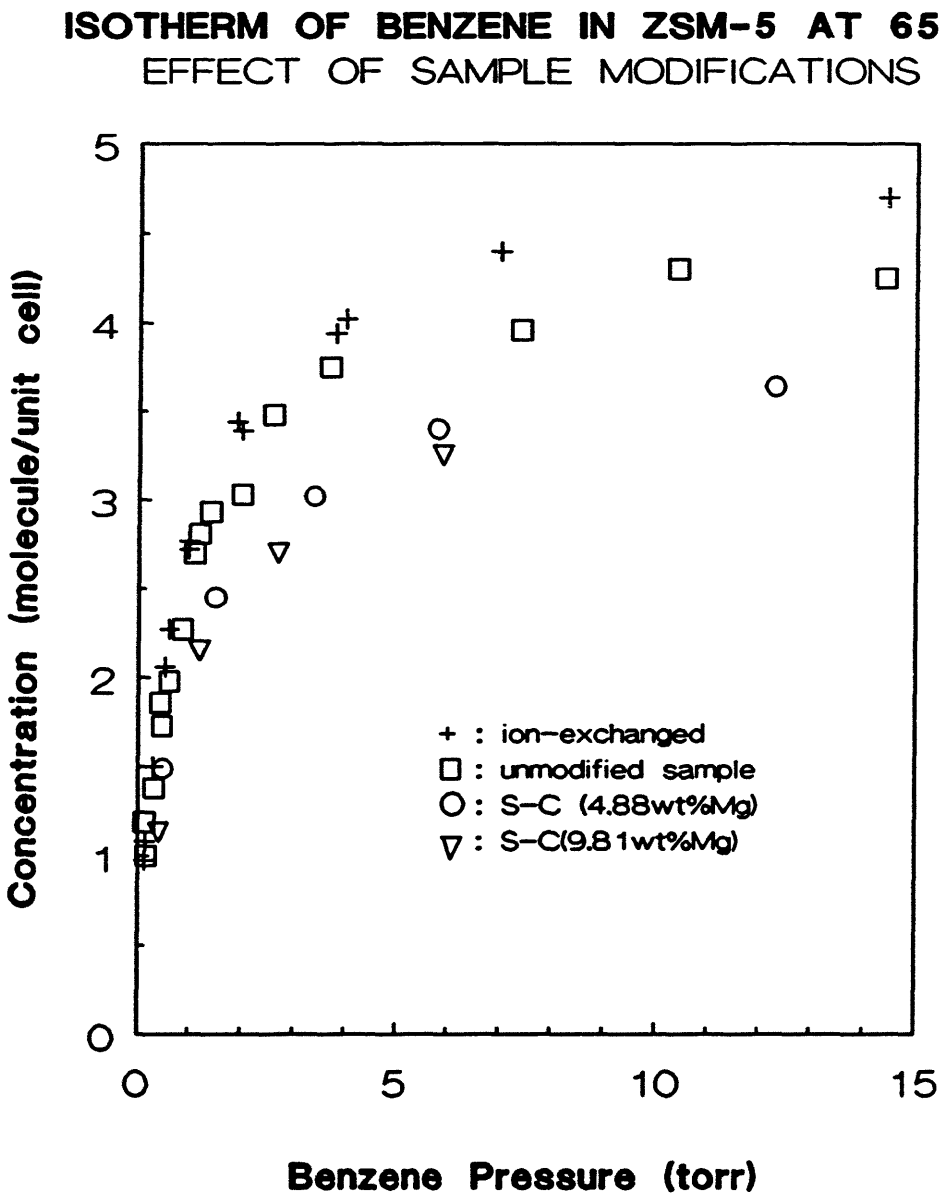

Figure 3.27 Equilibrium Isotherms: Effect of Mg Modifier

At higher concentrations, the diffusivities of benzene and 2-methylbutane show strong concentration dependent trends. The Langmuir adsorption isotherm can no longer describe the equilibrium data. The rising trend of diffusivity is also observed for the diffusion of heptane in 5A, where one cage can host two molecules. The repulsive interaction between molecules is proposed to be responsible for these observations.

The equilibrium capacities for ZSM-5 depends mainly on the molecular length, changing from about 8 molecules/unit cell for the relatively short molecules such as benzene to about 4 molecules/unit cell for the long chain molecules such as n-decane.

The diffusivity results are not sensitive to the Si/Al ratio, and to whether adsorption or desorption is performed. The results are, however, very sensitive to the contaminant on the crystals. Surface-coated Mg not only decreases the diffusivity but also changes the concentration dependent trend.

4. DISCUSSIONS

In this chapter, the theory proposed in Chapter 2 are compared quantitatively with the experimental observations in Chapter 3. Some of the experimental data in the literature, which are consistent among different research groups, are also included in the discussions. Two key issues in these comparisons are : the orders of magnitude of the diffusivity for a given molecule/zeolite system; and the concentration dependence of diffusivity. Two zeolites are of interest: ZSM-5 and zeolite 5A. The objective is to capture the fundamentals of the diffusion in zeolites.

4.1 On the Orders of Magnitude

The GT model predicts that the pre-exponential term of the diffusivity of molecules in ZSM-5 is of the orders of about $3.6x10^{-4}(T/M)^{1/2}$. The activation energy for the diffusion in the lattice can be estimated by the Lennard-Jones potential method proposed in Chapter 2. And for 5A, the pre-exponential term is of the same orders of magnitude as that for ZSM-5 if a molecule is roughly a spherical. For the diffusion of rod shape molecules, such as n-paraffins, in 5A, the effect of intracrystalline partitioning is included in formulations.

Table 4.1 lists the experimental results, reported in Chapter 3, of the pre-exponential terms and the values of activation energy for the diffusion of 2-methylbutane, 2-methylpentane, benzene, cyclohexane, and 2,2-dimethylbutane in ZSM-5. These values are compared with the predictions of the GT model in the same table. The pre-exponential terms of these five molecules, from about $1x10^{-4}$ to $3x10^{-4}$, are in good agreement with the theoretical prediction, $3.6x10^{-4}$. The values

Table 4.1. Comparison Between the GT Model & Experimental Results

(ZSM-5)

the GT MODEL:

$$\frac{D}{\sqrt{\frac{T}{M}}} = 3.6x10^{-4}\, e^{-\frac{E}{RT}}$$

	Experimental		the Lennard-Jones potential		
	pre-expo. term	E (kcal/mol)	Φ_c	Φ_i	$E=\Phi_c-\Phi_i$
2MB	$1.0x10^{-4}$	7.62	-3.9	-10.6	6.7
2MP	$1.6x10^{-4}$	8.60	-3.9	-13.4	9.5
Benzene	$2.2x10^{-4}$	9.70	0.6	-9.0	9.6
Cyc-C_6	$2.1x10^{-4}$	15.51	3.0	-11.5	14.5
2,2DMB	$2.9x10^{-4}$	16.67	7.0	-13.3	20.3

of Φ_c, the potential of the molecule at the channel, and Φ_i, the potential of the molecule at the intersection, are also listed in the table. These values were calculated by the following formulas based on a Lennard-Jones potential method:

$$\Phi_c = 10 \times 4\epsilon \times [(\frac{\sigma_c}{r_c})^{12} - (\frac{\sigma_c}{r_c})^{6}] \qquad (4.1)$$

for the 10-membered ring, where $\epsilon=[113(\epsilon_m/R)]^{1/2}R$, $\sigma_c=\frac{1}{2}(d_m+2.6)$, and $r_c=4.2(=\frac{1}{2}(2.6+5.8))$. The values of ϵ_m and d_m are given in Table 1.1. And

$$\Phi_i = 48 \times 4\epsilon \times [(\frac{\sigma_i}{r_i})^{12} - (\frac{\sigma_i}{r_i})^{6}] \qquad (4.2)$$

for the intersection, where $\sigma_i=\frac{1}{2}(\sigma_m+2.6)$ and $r_i=5.65(=\frac{1}{2}(2.6+8.7))$. The values of σ_m can be found in Table 1.1. In these calculations, no-fitting parameter was used. The values of the estimated activation energy were the difference between these two potentials. The values of the estimated activation energies, E, are close to the experimental values, as shown in Table 4.1

It is interesting to note that, in Table 4.1, all five molecules experience very strong attractions from the intersection of ZSM-5, as shown by the calculated values of Φ_i for these molecules. The major difference among these five molecules are the potentials at the channels. The relatively small molecules, 2-methylbutane and 2-methylpentane (d_m = 5.0 Å), experience a moderate attraction when passing through the channel, and benzene (d_m = 5.85 Å) experiences a little repulsion. For cyclohexane (d_m = 6.0), passing the channel becomes difficult due to the strong repulsion force from the 10-membered oxygen ring. The repulsive potential for bulky 2,2-dimethylbutane at the channel might be as high as 7 kcal/mol.

Figure 4.1 plots the values of the activation energy determined experimentally against the values of the potential at the channel, Φ_c, estimated theoretically for these five molecules in ZSM-5. As shown in the figure, the activation energies for the diffusion increase as the potentials at the channel increase. In Figure 4.2, the x-axis is changed to the values of the potential at the intersection, Φ_i. The data are scattered. There is no simple correlation between the activation energy and the potential at the intersection for these system.

Figure 4.3 presents the diffusivities values of benzene in ZSM-5 obtained both by this study and by 9 different studies. The sources for these literature data are: (1). Tsikoyiannis (1986); (2). Nayak et al (1985); (3). Doelle et al (1981); (4) Wu et al (1983,84); (5). Choudhary et al (1986); (6). Olson et al (1981); (7). Shah et al (1988); (8 & 8'): Zikanova et al (1987); (9). Qureshi et al (1988). In the same figure, the solid line represents the predictions of the GT model. The model predicts the experimental results with good accuracy, although no fitting parameter is used in the model. Most of the experimental data at the same temperature are within one (at most two) order(s) of magnitude. Considering the experiments were performed in different lab on different crystals, and sometimes with different techniques, the scattering of these data is not unexpected. The result of Chaudhary et al, however, is at least four to five orders of magnitude smaller than the model prediction. Their experiments were performed by a gas chromatographic method. Their results on other systems are also orders of magnitude smaller than the results reported by other groups.

The diffusion in 5A has been studied for more than two decades. Several orders of magnitude difference between the results obtained by the NMR method and those obtained from classic sorption rate measurements led to a critical

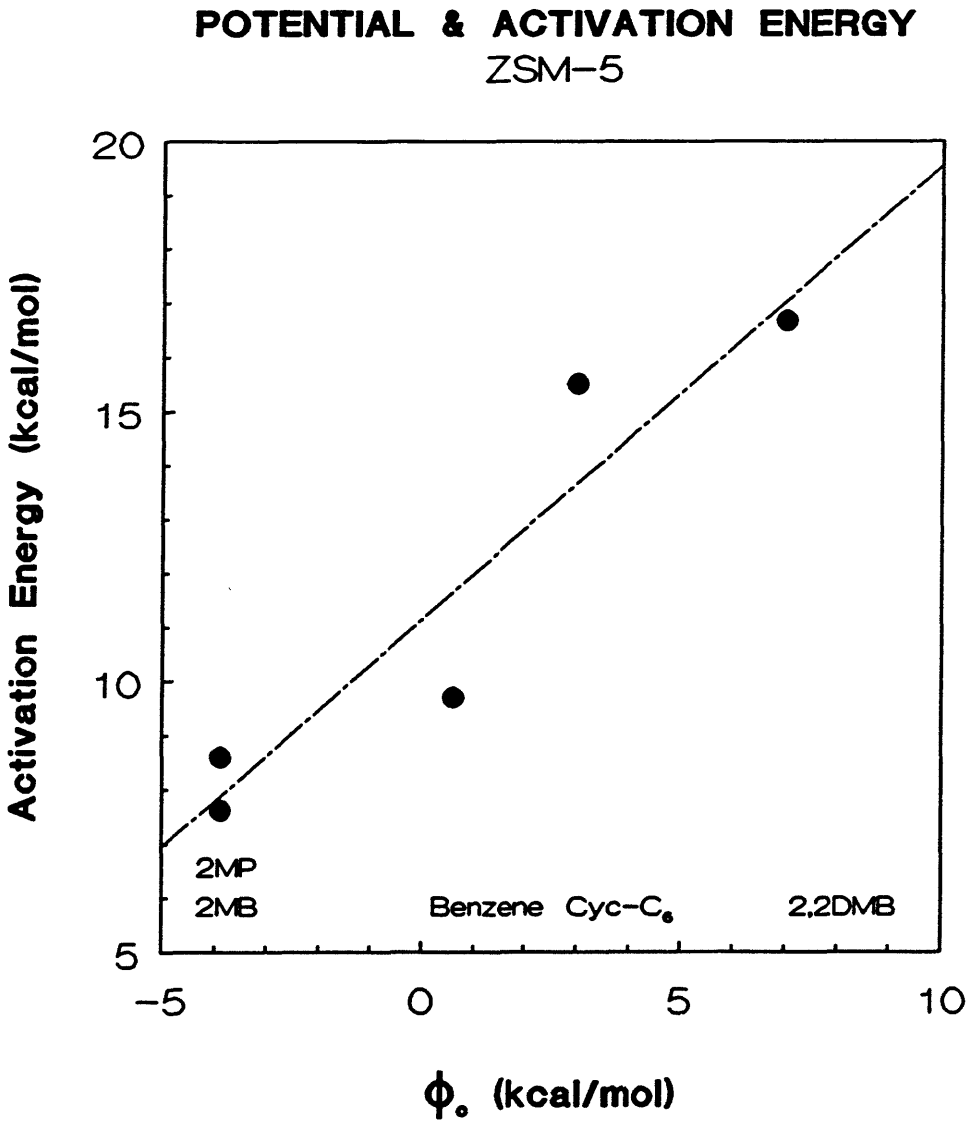

Figure 4.1 Potential & Activation Energy (ZSM-5): Effect of Channel

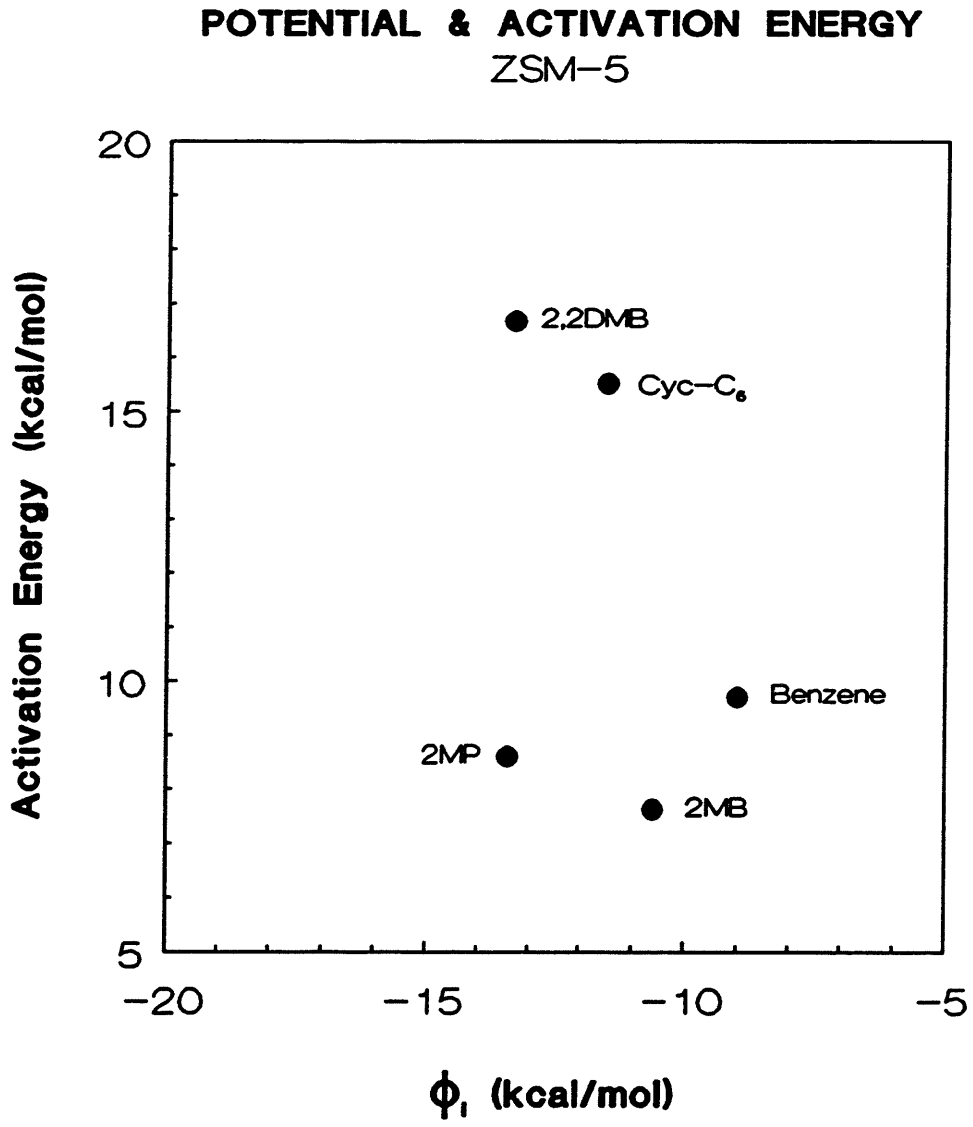

Figure 4.2 Potential & Activation Energy (ZSM-5): Effect of Intersection

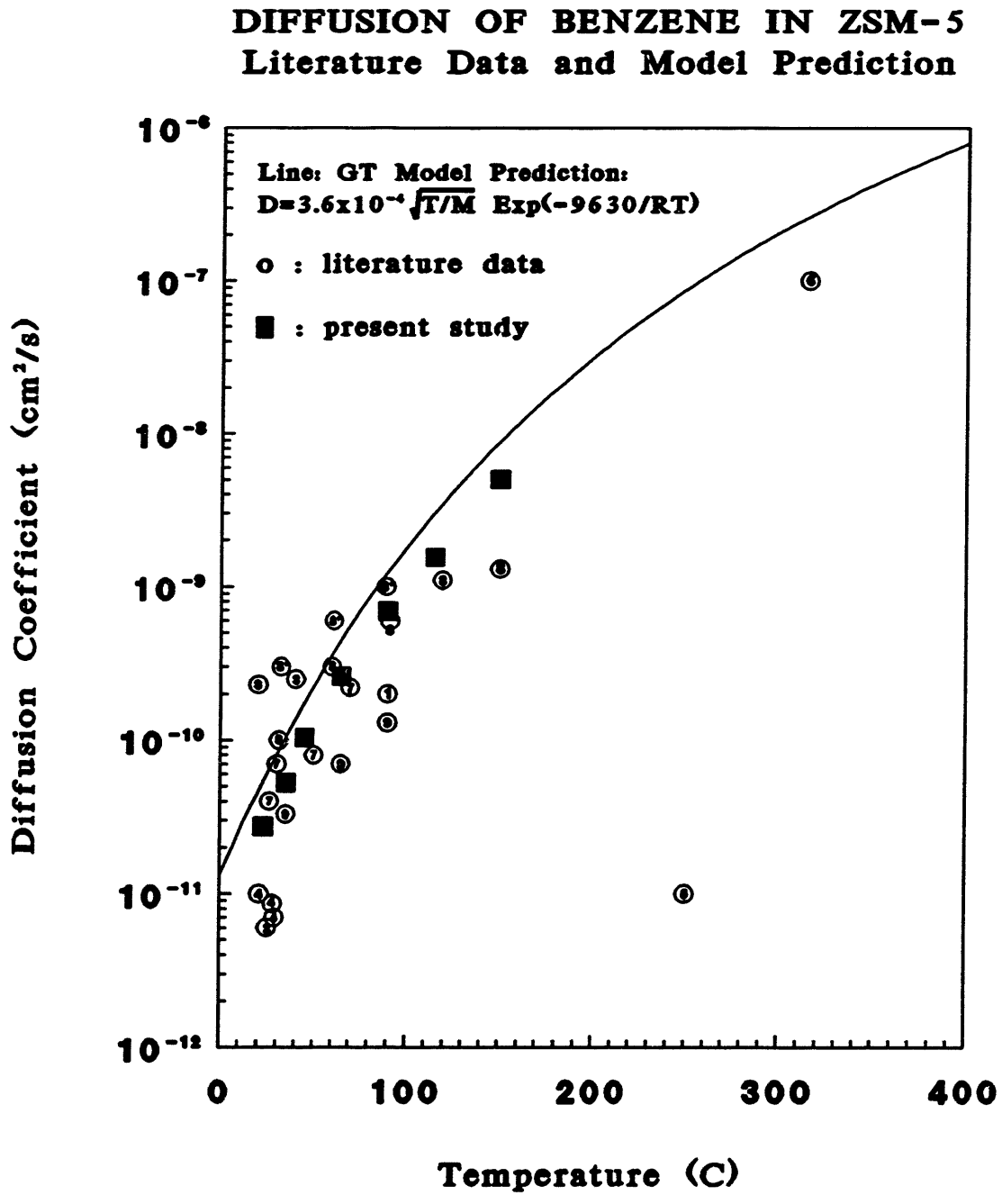

Figure 4.3 Diffusion of Benzene in ZSM-5: Comparison

reexamination of some sorption data. Many of the early uptake-rate studies had been carried out with small commercial zeolite crystal and, in some cases, with pelleted materials. It was revealed that, at least for some systems, the effects of external heat and mass-transfer resistances in limiting the adsorption/desorption rates were far greater than originally assumed (Kärger and Ruthven, 1989). In recent studies, measurements were carried out with much larger unaggregated crystals, in which the uptake rates were slower and more accurately measurable. In several instances, reasonable agreement between uptake rate and NMR data was observed. We will use these results in our analysis.

In Table 4.2, the pre-exponential terms of the diffusivities for CH_4, CF_4, C_3H_8, and nC_4 at specified temperatures are listed, together with the experimental values of the activation energy for these four molecules. These data are adapted from literature (Kärger and Ruthven, 1989). The pre-exponential terms were calculated from the reported values of the diffusivity and the activation energies at given temperatures. The GT model was used to estimated the pre-exponential terms and the activation energies were estimated by the Lennard-Jones potential method. For roughly spherical molecules, CH_4 and CF_4, the pre-exponential term is of about the order of $3x10^{-4}(T/M)^{1/2}$ according to the model. In the cases of C_3H_8 and nC_4, the intracrystalline partitioning were estimated according to the method suggested in section 2.3.3. The moment of inertia, I, was estimated by assuming that the mass center is at the middle of the molecule. The distances from the methyl groups to the mass center was then calculated according to the bond lengths and bond angles. The symmetry number, ζ, is the external symmetry number since we assume that the molecules only lose their "head to tail" rotational degrees of freedom. For both C_3H_8 and nC_4, the value of ζ is then 2. The effect of the intracrystalline partitioning thus calculated is about $8x10^{-3}$ for C_3H_8, and about $3x10^{-3}$ for nC_4. For these two

Table 4.2 Comparison Between the GT Model & Experimental Results

(5A)

	Literature Data (Kärger & Ruthven, 1989)			the GT model	
	T(K)	pre-expo. term	E	pre-expo. term	E
CH_4	300	$5x10^{-5}$	1.0	$1x10^{-3}$	1.0
CF_4	473	$3x10^{-5}$	6.6	$7x10^{-4}$	8.0
C_3H_8	273	$1x10^{-6}$	3.5	$6x10^{-6}$*	3.6
nC_4	400	$9x10^{-7}$	4.0	$2x10^{-6}$*	5.0

* intracrystalline partitioning included

** pre-exponential term: cm^2/s; E: kcal/mol

molecules in 5A, the intracrystalline partitioning is, therefore, very important. The potential at the channel (window) was estimated by

$$\Phi_c = 8 \times 4\epsilon \times [(\frac{\sigma_c}{r_c})^{12} - (\frac{\sigma_c}{r_c})^{6}] \qquad (4.3)$$

for the 8-membered ring, where σ_c=½(d_m+2.8), and r_c=3.5(=½(4.2+2.8)). The potential in the intersection (cage) was calculated according to

$$\Phi_i = 72 \times 4\epsilon \times [(\frac{\sigma_i}{r_i})^{12} - (\frac{\sigma_i}{r_i})^{6}] \qquad (4.4)$$

where σ_i=½(σ_m+2.8), and r_i=7.1(=½(11.4+2.8)). The activation energies were calculated by $E=\Phi_{max}-\Phi_{min}$, where Φ_{max} = max { Φ_c, Φ_i} and Φ_{min} = { Φ_c, Φ_i}. The estimated pre-exponential terms given in Table 4.2 are within about one order of magnitude as those reported in the literature. The estimated activation energies are also in good agreement with the experimental values.

Three of four experimental pre-exponential terms in Table 4.2 are smaller than the corresponding theoretical values. The discrepancy might be caused by the model assumptions. In the GT model, we assumed that an activated molecule would make a jump attempt at the channel. Since the large-cage-small-channel structure of 5A, it is possible for an activated molecule not to make the jump successful simply because this molecule bumps into the impermeable wall instead of trying to passing through the channel. It means that only portion of the spherical surface of the cage is accessible to the molecules: the channels. For a sphere of 11.4 Å in diameter with six channels of 4.2 Å in diameter, the ratio of accessible surface area to the total surface area of the sphere is about 0.2. For the first-order approximation, we can therefore assume that the probability of a successful jump would decrease by a factor

of 0.2 due to this structure constraint. The discrepancy between the predicted diffusivities and the experimental values would be nearly diminished if the theoretical values are multiplied by a factor of 0.2.

Ruthven and co-workers have extensively studied the diffusion of n-paraffins in 5A. In Figure 4.4, the values of the activation energies for the diffusion of CH_4, C_2H_6, C_3H_8, nC_4, nC_5, nC_7, nC_8, and C_{10} in 5A (Ruthven, 1984) are plotted against the values of $(-\Phi_i)$, absolute values of the attraction potential in the cage. The values of Φ_i were calculated by Eq. (4.4). Once again, we observe an approximate correlation between the activation energies for the diffusion and the potentials in the cage: The stronger the attraction, the higher the activation energy.

Therefore, the activation energy difference for the molecule/ZSM-5 systems we investigated is caused mainly by the difference in the potential at the channel. For n-paraffins/5A, it is mainly caused by the difference in the strength of the attraction molecules experience in the cage. Those are the reasons that when one correlates the diffusivities, an apparent increase in the activation energy is observed in ZSM-5 as d_m increases, and in 5A, the activation energy increases with an increase in σ_m.

The above observations are consistent with the structures of ZSM-5 and 5A. In ZSM-5, there is no large cage in the lattice. The channel size is close to the intersection size. In the diffusion measurements, the zeolite channel discriminates molecules mainly according to their minimum kinetic diameters. The pore size of 5A, however, is relatively small (about 4.2 Å), and the cage is much larger in size (about 11.4 Å). The pores of 5A only admit molecules of small diameter, such as n-paraffins, and exclude larger molecules, such as branched paraffins or aromatics.

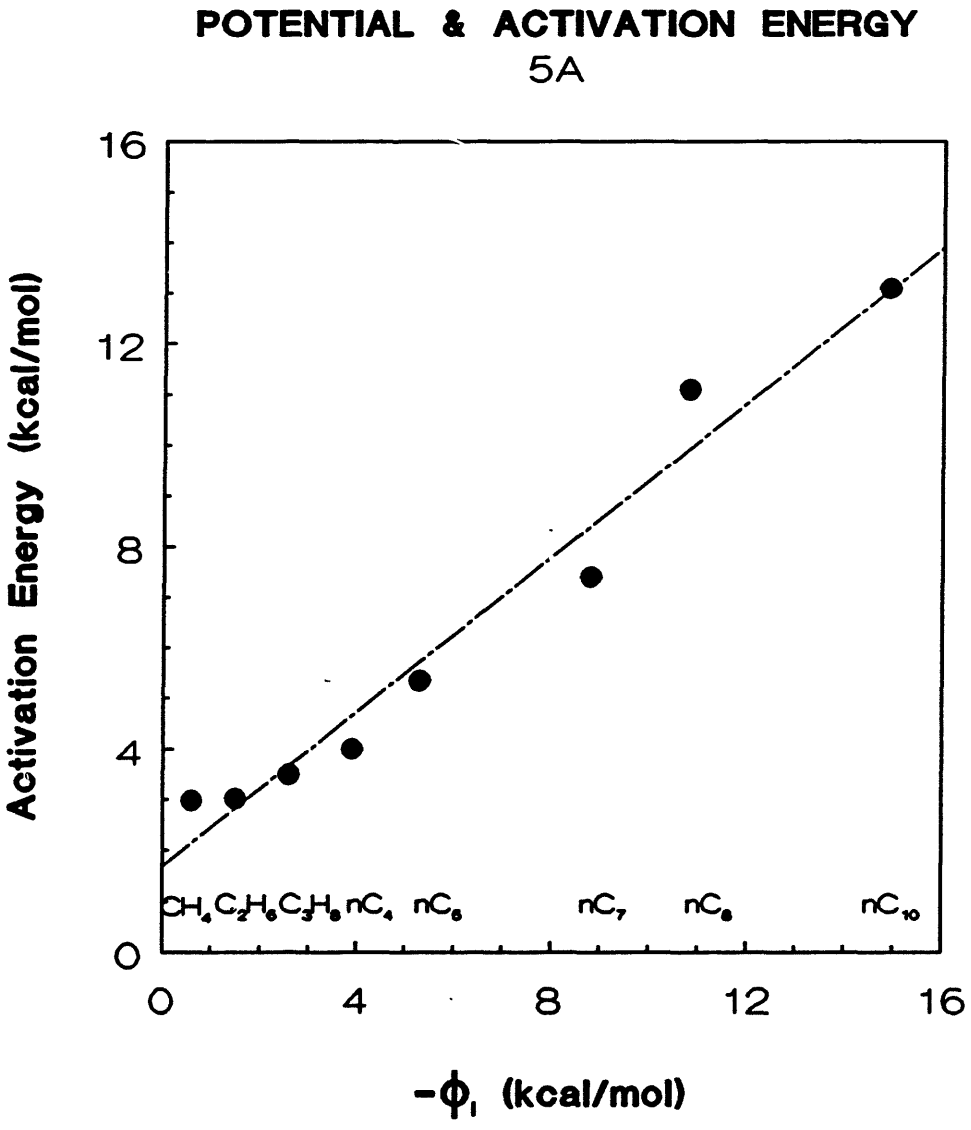

Figure 4.4 Potential & Activation Energy (5A): Effect of Cage

The effect of d_m on the diffusivity in 5A was not systematically investigated since the range of d_m for the accessible molecules is not wide enough. The family of normal paraffins all have about the same minimum diameter. The difficulty in passing through the channel is comparable. The difference in the activation energies is, therefore, mainly caused the difference in their interactions with the cage due to the different values of molecular length.

In the above discussions, the GT model has been used successfully in predicting the diffusivities, and in analyzing the characteristics of the molecule-lattice interactions for some molecules in ZSM-5 and 5A. The significance of the model success is two-fold.

First, this model can be therefore served as the first-order approximation for the more detailed predictive model(s). The improvement on the model could be made mainly on the activation energy estimations by identifying the contributions of each functional groups of the molecules instead of lumping molecules as a single mass center. This functional-group method is more flexible and more accurate on describing molecules. We can take toluene as an example. Experimentally, it was observed that toluene is more strongly adsorbed in ZSM-5 than benzene (see Chapter 3). Therefore, the potential at the intersection for toluene is lower than that for benzene. On the other hand, the diffusion for toluene in ZSM-5 is faster than that of benzene by about a factor of two. Thus, the potential at the channel for toluene should also be lower than that for benzene so as to make the a little smaller activation energy for toluene, which would result in the faster toluene diffusivity. By the Lennard-Jones potential method proposed in Chapter 2, the potentials at the channel for both molecules would be, however, the same since their minimum diameters are the same. By using the functional-group method, the effect of methyl

group of toluene molecule on the potential could be possibly evaluated. On the other hand, the functional-group method is not as complicated as the atom-atom interaction model, which exclusively considers each atom of the molecule. The successful of the GT model and the Lennard-Jones method, although limited, might suggest that such detailed atomic descriptions is probably not necessary for the purpose of diffusivity estimation.

Secondly, since the pre-exponential term can be easily determined by the GT model or its modified form, the only parameter in the model to be determined is the activation energy. Its value can be estimated. Or for a practitioner, this single parameter can be easily obtained by performing an experiment at one temperature without worrying the compensation effect between the pre-exponential term and the activation energy.

In this thesis, we have only used the GT model in predicting and analyzing the diffusivity. As shown in Section 2.1.2 of Characterization of Molecules Inside Zeolites, some molecules inside the zeolites behave indeed as described by the GT model (we call these molecules at the GT mode), and some behave as described by the SV model (we call these molecules at the SV mode). For the same molecule, one of these two modes would become predominant, depending on temperature. For the system we discussed, molecules are at the GT mode, verified by the characterization and the good agreement between the GT model predictions and the experimental data. In applying either the GT model or the SV model, it is important first to verify the mode of the molecule inside the lattice. This could be done by either experimental characterizations or theoretical calculations. In the calculations, one could investigate whether the molecule-oxygen interaction or the molecule-cation specific interaction is more important, and then determine to choose one of the

models.

Since one molecule can has two different modes, the GT mode and the SV mode inside the zeolite, we should be very careful in comparing the diffusion results by different techniques with different time scales, such as the NMR method and the uptake method. It is possible that the techniques with different time scale monitor different modes of molecular motion inside the lattice. The occurrence of the disagreement between the diffusivities obtained by these different techniques should not be viewed as a surprise.

The difference between the diffusivities for the apparently same molecule/zeolite system could be caused by the difference in the definitions of the diffusivity as discussed in Chapter 1, or the difference on the time scale of the measurements as discussed above. Another possibility for the discrepancy is the unintentional experimental errors. As shown in the Chapter 3, a possibly little contaminants on the surface could lower the diffusivity by one order of magnitude. In theory one should be able to distinguish the rate limiting step of a diffusion process by comparing the uptake curve with the different models. For example, the "surface barrier" model should give the uptake curve an exponential form of time dependence, whereas the intracrystalline diffusion model gives initially a square root of time dependence and, when the uptake is more than about 70%, then a exponential time dependence. In practice, however, this kind of model comparison is often not sensitive enough to identify the nature of the diffusion process. For example, when we performed the diffusion measurements on the surface-coated ZSM-5, the rate limiting step for the diffusion should be diffusion through the surface layer. The uptake curves, however, showed good fitting with the solutions of Fick's diffusion law. The good fitting of the Fick's law solution is, therefore, not a sensitive

indication about the rate limiting step.

4.2 On the Concentration Dependence

According to the Non-Interacting Lattice model, a constant diffusivity should be observed if one site can only host one molecule and the interactions between the molecules at the different sites are negligible. The isotherm under this condition is of Langmuir type. The Interacting Lattice model, on the other hand, predicts a rising trend of the diffusivity for the lattice where one site can host two molecules and there is repulsive interaction between these two molecules. A decrease trend of Langmuir parameter should be observed.

One pair of the ideal molecule/zeolite systems for testing these two model are: Benzene/ZSM-5 and Heptane/5A. For the concentration less than 4 benzene molecules/unit cell, or 1 benzene molecule/intersection, in ZSM-5, molecules would preferentially reside at the channel intersections, as demonstrated by the characterization of benzene molecule inside the ZSM-5 (Mentzen, 1987). The average distance between the intersection is about 10 - 12 Å (Richards and Rees, 1987). Figure 4.5 is the Lennard-Jones potential plot of interaction between two benzene molecules based on the values of potential constants given in Table 1.1. As shown in the figure, for a distance of 10 to 12 Å, the interactions between two molecules are negligibly small (less than about -0.05 kcal/mol) compared to the activation energy of about 10 kcal/mol. We indeed observed a nearly constant trend of diffusivities for the concentration less than 4 molecules/unit cell, and a Langmiur type isotherm, which are in good agreement with the predictions of the Non-Interacting Lattice model.

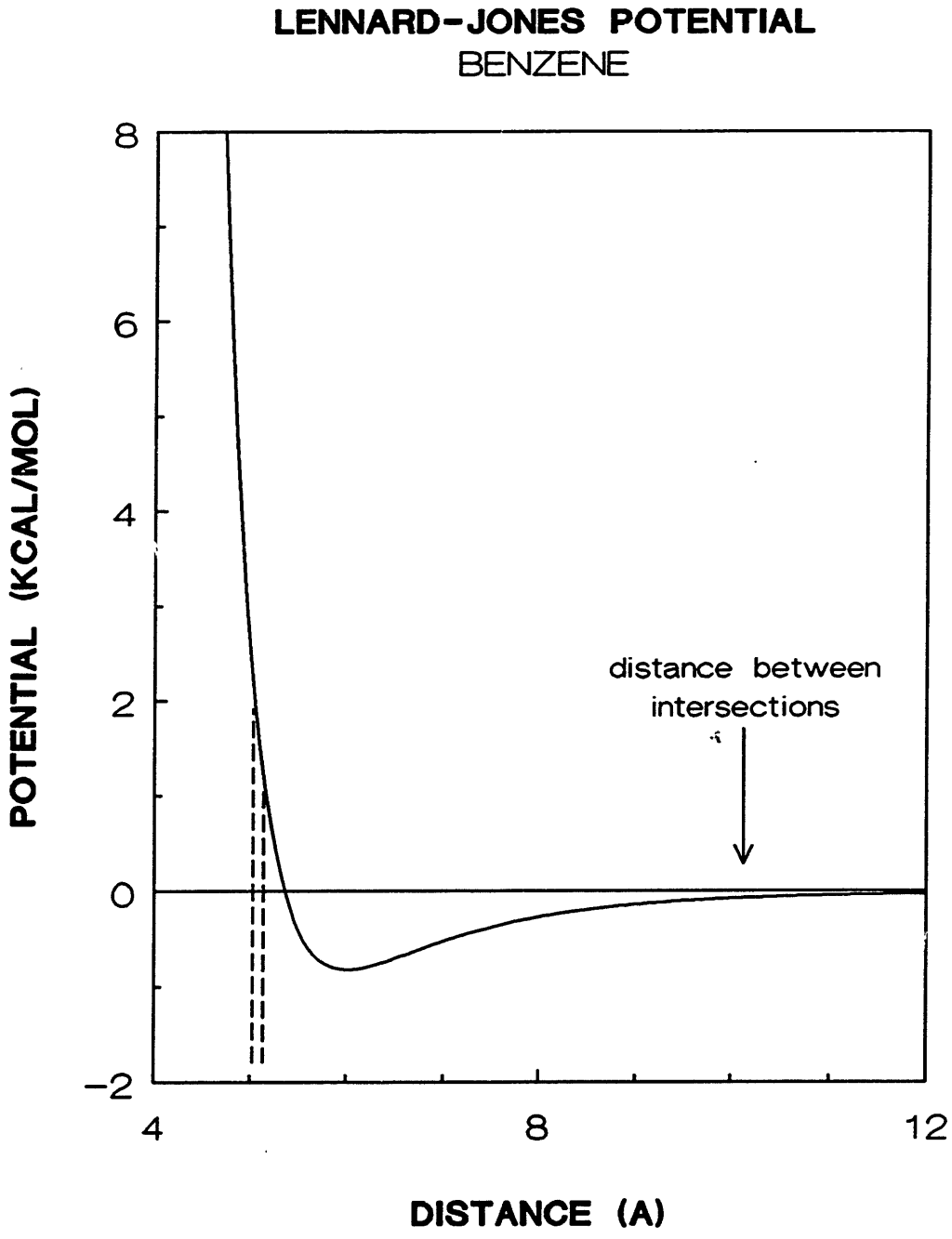

Figure 4.5 Lennard-Jones Potential of Benzene

For heptane in 5A, both the experimental results and theoretical calculation showed that the sorption capacity was roughly 2 molecules/cage (Doetch et al, 1974). Figure 4.6 showed that if two molecules are put into one cage it is possible to result in a repulsive potential of about 1.7 kcal/mol between these two molecules. Figure 4.7 presents the predictions of the Interacting Lattice model based on this potential value (w=2). The trend agrees with the experimentally observed one. According to the calculations in Chapter 2, the Langmuir parameter should decrease by about a factor of 2 as concentration increases. The experimental results by Doetsch et al (1974) showed a more dramatic decrease in this parameter.

The same analysis could be done for the diffusion of benzene at concentration higher than 4 molecules/unit cell. The distance between molecules could be about 5 Å since molecules begin to reside at the channels. Figure 4.5 shows such a distance could result in a repulsive potential about 0.7 kcal/mol, which could cause a diffusivity increase as shown in Figure 4.8. In the figure, the concentration was normalized by 8 molecules/ unit cell.

The Non-Interacting Lattice model and the Interacting Lattice model, although very crude and oversimplified, give us a kinetic explanation of the concentration dependence of the diffusivity. These two models are capable of predicting when this concentration dependence should be expected. An approximate estimation on the change of the diffusivity is also possible to be made based on the information of the molecule-molecule interaction. However, the interaction potential between two molecules is very sensitive to the distance chosen to do the estimation. The exact location of the molecules inside the lattice and their relative position are too difficult to be exactly quantified, which makes the estimation on the interaction potential even more uncertain. Furthermore, in the Interacting Lattice model, the

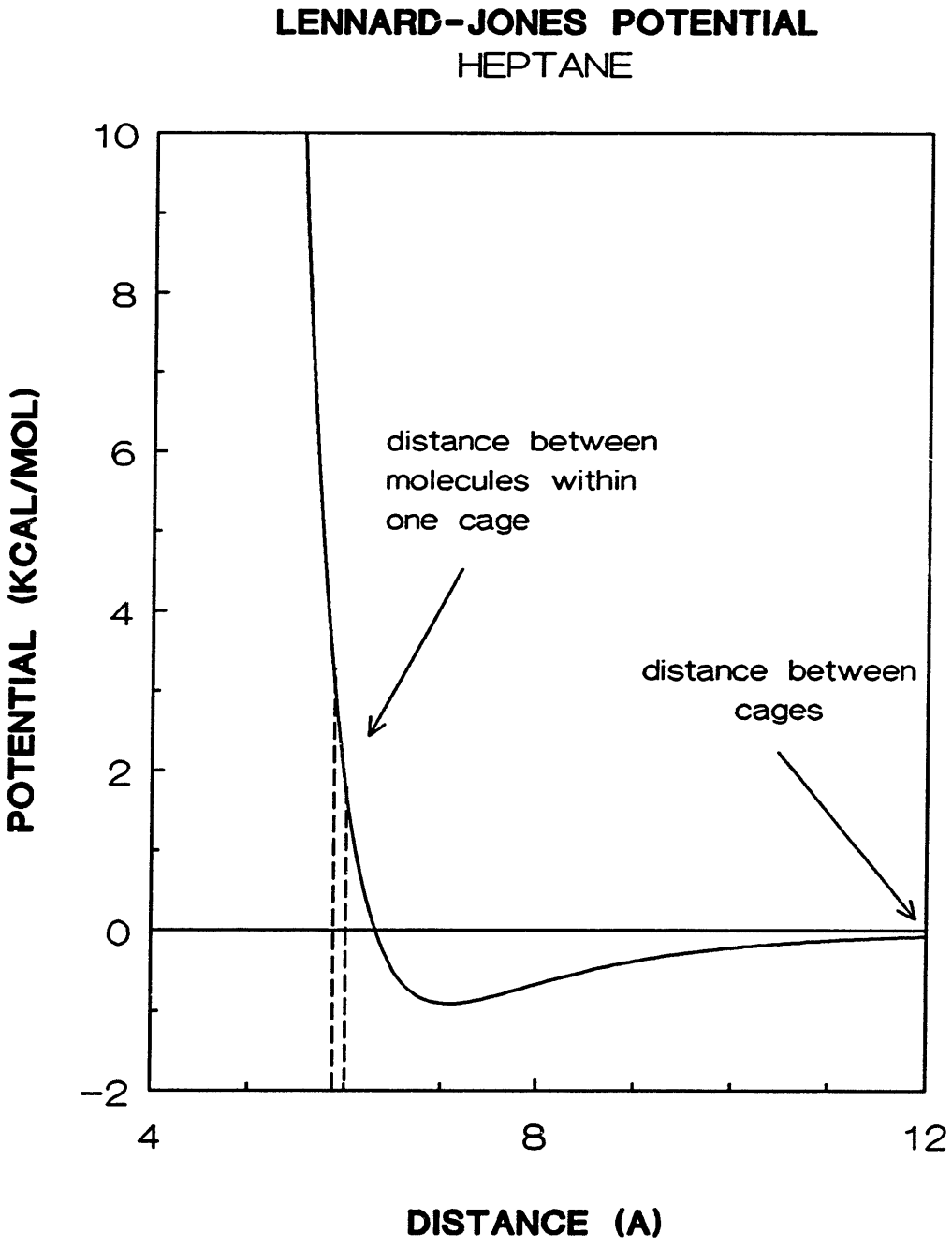

Figure 4.6 Lennard-Jones Potential of Heptane

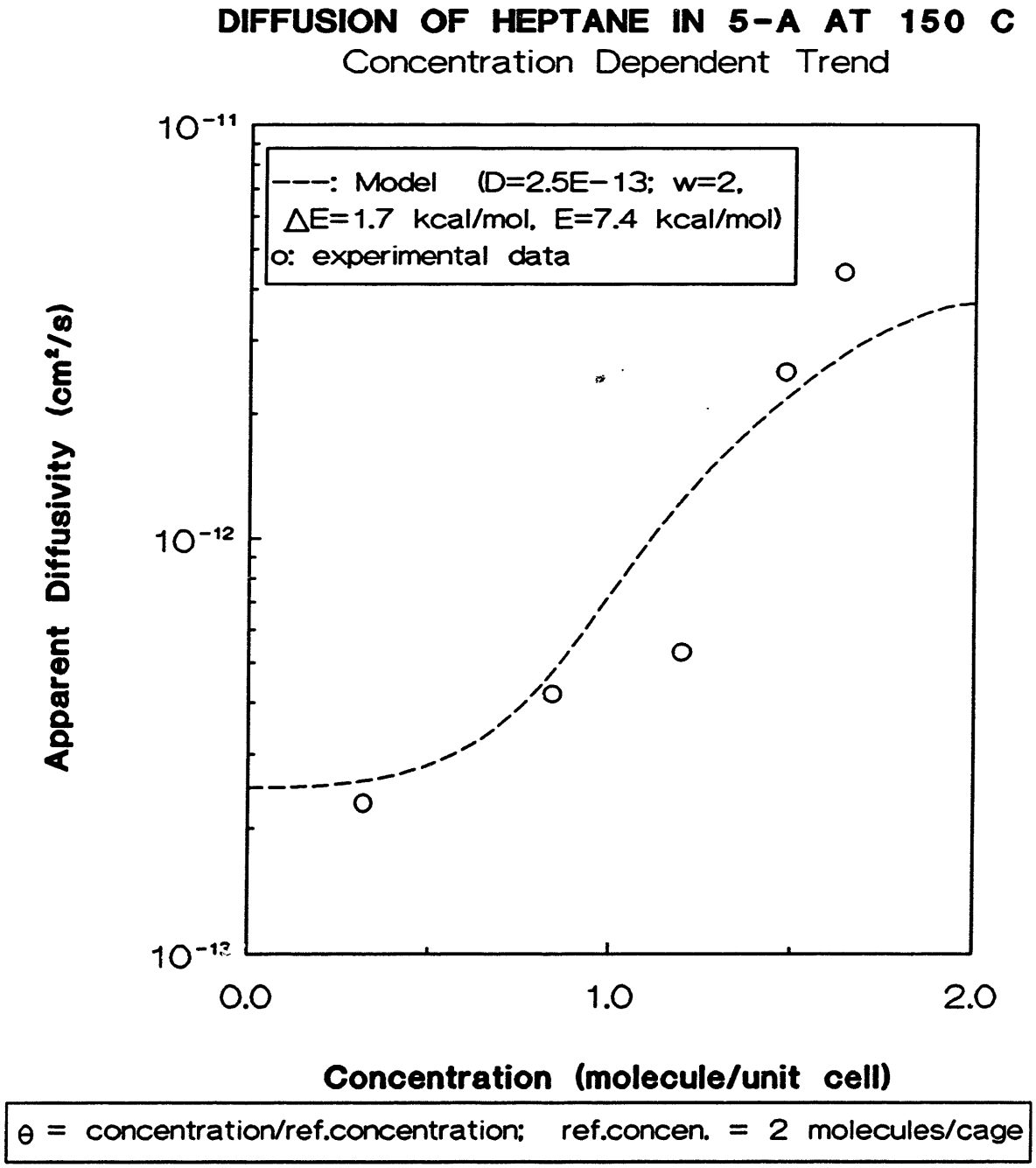

Figure 4.7 Diffusion of Heptane in 5A: Concentration Dependence

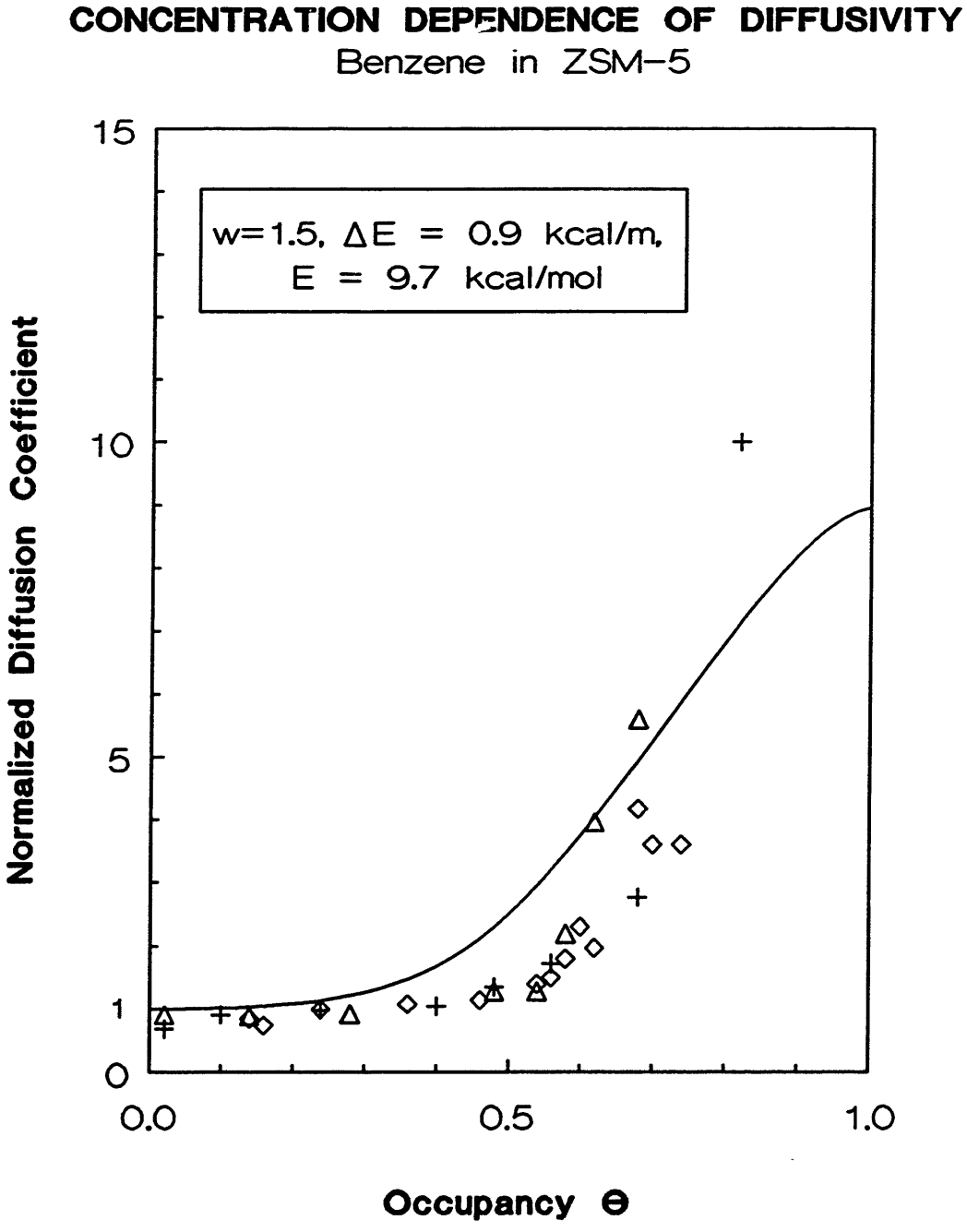

Figure 4.8 Diffusion of Benzene in ZSM-5: Concentration Dependence

effect of the molecule-molecule interaction on the molecule-lattice interaction, the interactions between molecules at the different sites were not considered in the model formulation. The latter one might be very important at the high concentration, which might be one of the reasons that the model predictions on the concentration dependence of the diffusivity and of the Langmuir parameter are less dramatic than the experimental observations. In the modeling, we also assumed that the correlation between neighboring sites are neglected so that the joint probability can be written as the product of two first-order correlation functions (see, e.g., Eqs. (2.62) and (2.63)). This assumption is, rigorously speaking, only valid if the interaction between molecules does not disturb the randomness of the molecular distribution.

Since the isotherm is of Langmuir type for benzene in ZSM-5 at the concentrations less than 4 molecules/unit cell, the Darken's equation (Eq. (1.15)) predicts an increase in the apparent diffusivity as $1/(1-\theta)$ with a constant D_c. Our experimental observations showed, however, that there is no dramatic concentration effect on the diffusivity within this concentration range. There is no reason why it happens. For the most of n-paraffins in 5A, the Darken's equation appears to be a good correlation on the concentration dependence of the diffusivity as shown by Ruthven and co-workers through the years. The reason is not clear on why for these two zeolite systems, Darken's equation with a constant diffusivity works for one and not for the other. The kinetic theory we proposed can at least predict and explain, to certain extent, the occupance of the diffusivity dependence.

5. CONCLUSIONS

Two significant, previously unreported results have been achieved:

1. A theory for the diffusion of hydrocarbons in zeolites is proposed based on the understanding of the molecule-interactions and the molecule-molecule interactions. The proposed models are self-consistent, capable of predicting not only the order of magnitude of the diffusivity, but also its concentration dependence.

2. The results of the diffusion measurements by this study have been directly and satisfactorily compared with the model predictions on both their orders of magnitude and the concentration dependence.

The molecule-lattice interaction is the dominant factor in determining the diffusion characteristics of molecules in zeolites. The activation energy for the diffusion can be caused predominantly either by the structural constraints of the lattice, or by the specific attraction between the adsorption site and the molecule. The corresponding modes of the molecular translational motion are termed as the "gaseous translation" (GT) mode and the "solid vibration" (SV) mode. The GT model assumes that the diffusion of the molecules inside the zeolites are restricted by the potential field of lattice structure whereas the molecules retain their gaseous entity. The SV model assumes that the attachment of molecules to the lattice is so strong that the molecules vibrate with the host lattice before accumulating enough energy to jump. The GT model applies to non-polar molecules at temperatures above room temperature, according to the characterization of molecular motion inside the lattice. The SV model might be applicable to polar molecules or the

molecules at temperatures much lower than room temperature.

The pre-exponential term of the diffusivity of molecules for ZSM-5 is of the order of about $10^{-4}(T/M)^{1/2}$, according to the GT model. The experimental results of six hydrocarbons (branched paraffins, benzene, and cyclohexane) support the theoretical predictions. The activation energy for the diffusion in the lattice increases with the increase in the minimum diameter of the molecule, and is mainly responsible for the difference in the diffusivities for the different molecules. The values of the activation energy can be estimated by the proposed Lennard-Jones potential method based on the zeolite structural and molecular properties. For 5A, the pre-exponential term of the diffusivity is of the same order of magnitude as that for ZSM-5 if a molecule is roughly spherical. The GT_{ip} model should be used for the diffusion of rod shape molecules, such as n-paraffins, in 5A, in which the effect of intracrystalline partitioning is superimposed on the pre-exponential term. The intracrystalline partitioning could reduce the pre-exponential term by as many as three or more orders of magnitude. Literature data agree with the model predictions.

The interactions among molecules inside the lattice could alter the concentration dependence of the diffusivity. If the interaction between molecules inside the lattice is negligible and double-occupancy of a site is excluded, a constant Fick's law diffusivity is predicted by the Non-Interacting Lattice model. The equilibrium isotherm is of Langmuir type. Diffusivities of benzene/ZSM-5(PJ), toluene/ZSM-5(WQ), and 2-methylbutane/ZSM-5(PJ) for the concentration less than 4 molecules/unit cell exhibited experimentally a relatively flat trend. The Langmuir models can describe the equilibrium isotherms. The interacting model predicts a rising trend of apparent diffusivity, and a decreasing trend of Langmuir

parameter at the high concentration where the interaction between molecules is significant and the interaction is repulsive. Only the interaction between the molecules at the same site is considered. The interactions between molecules at the different sites are excluded. The concentration dependent trends of benzene/ZSM-5(PJ), 2-methylbutane/ZSM-5(PJ) for the concentration higher than 4 molecules/unit cell, and the concentration trend of heptane/5A were observed to be rising dramatically. The Langmiur parameters decrease significantly at the same concentration.

The orders of magnitude of the diffusivity of hydrocarbons are strongly affected by molecule shapes. For ZSM-5, the larger the molecular diameter, the more pronounced the decrease in the diffusivity. The effect of the molecular length diminishes once the molecular length exceeds about 8-9 Å. For n-paraffins/5A, the longer the molecular length, the higher the activation energy due to the stronger attractions of molecules at the cage. The equilibrium capacities for ZSM-5 depends mainly on the molecular length. The diffusivity results are not sensitive to the Si/Al ratio of ZSM-5, and to whether adsorption or desorption is performed. The results are, however, very sensitive to the contaminant on the crystals. Surface-coated Mg not only decreases the diffusivity but also change the concentration dependent trend.

NOMENCLATURE

English

B	mobility
c	concentration inside zeolite
c_g	concentration in gas phase
c_s	saturation concentration inside zeolite
D	diffusivity
D_{app}	apparent diffusivity
D_c	corrected diffusivity
D_g	diffusivity defined by concentration gradient in gaseous phase
d_c	channel diameter
d_i	intersection diameter
d_m	minimum kinetic diameter of molecule
d_o	oxygen diameter
d_p	pore diameter
E	activation energy
f	"equilibrium constant" for the molecular distribution in a interacting lattice
f_c	partition function at the channel
f_i	partition function at the intersection/cage
g	geometry constant
H	Hooke's law constant
h	Planck's constant
I	moment of inertia
J	diffusive molar flux with respect to stationary axes
J_x	diffusive molar flux in x-direction

j_A	diffusive mass flux of species A with respect to stationary axes
K	Langmuir parameter
K_H	Henry's law constant
K_H^o	pre-exponential term of Henry's law constant
k	Boltzmann constant
L	diffusional length
$\bar{L}$	mean free path of gaseous molecule
L_{ij}	proportional constant in irreversible thermodynamics
M	molecular weight
M_t/M_∞	fractional approach to equilibrium
m	molecular mass
m_n	nth atom of the molecule
n_A	mass flux of species A with respect to stationary axes
P	pressure
p	bombardment rate of molecule from gas phase into the lattice
q	the rate parameter of the Poisson distribution, the jump frequency from one site to a particular adjacent site at the level of the first-order correlation function
q_r	rotational partition function
R	gas constant
r_c	distance from the center of the channel to the nuclei of the oxygen on the channel perimeter
r_i	distance from the center of the intersection to the nuclei of the oxygen on the surface of the intersection sphere
r_n	distance from the nth atom to the center of the molecule
r_p	crystal radius
T	temperature
T_b	normal boiling point

t	time coordinate
t_b	time a molecule spends at the bottom of the potential well
t_t	time a molecule spends at the top of the potential well
u	molecular velocity
u_m	mass average velocity of a mixture of A and B
u_a	average molecular velocity in the lattice
u_i	velocity of species i relative to stationary coordinate (i=A,B)
V	vacancy (Figure 2.1)
V_b	Le Bas volume of molecule
V_{cage}	cage volume of 5A
$V(x)$	potential field
V_w	van der Waals interacting volume defined in Section 3.2.3
w	nondimensionalized activation energy, $\Delta E/kT$
X_j	thermodynamics force
x	space coordinate
z	coordination number

Greek

α	distance between the adjacent sites
α_T	thermal expansion coefficient
ϵ	pairwise Lennard-Jones energy constant
ϵ_m	Lennard-Jones energy constant for molecule
ϵ_o	Lennard-Jones energy constant for oxygen
ζ	external symmetry number
θ	occupancy, short-handed form of $\theta(S_i, X;t)$
$\theta(S_i, X; t)$	the first-order occupancy function, the probability of finding a molecule, X, at a site, S_i, at time, t, for a specified initial condition
$\theta(Si, 0; t)$	the probability of finding no molecule

$\theta(0)$	empty site probability, short-handed form of $\theta(S_i, 0; t)$
$\theta(S_i, 1; t)$	the probability of finding one and only one molecule
$\theta(1)$	single-occupancy probability, short-handed from of $\theta(S_i, 1; t)$
$\theta(Si, 2; t)$	the probability of finding two and only two molecules
$\theta(2)$	double-occupancy probability, short-handed form of $\theta(S_i, 2; t)$
$\theta(S_i, X; S_j, 0; t)$	the second-order occupancy function, the joint probability of finding a molecule at a site, S_i, and no molecule at its neighboring site, S_j, at time t, with the same initial condition for $\theta(S_i, X; t)$
$\theta(S_i, X; S_j, \underline{2}; t)$	the joint probability of finding molecule(s) at site S_i and not two molecules at site S_j at time t
θ_p	porosity
λ	ratio of the minimum kinetic diameter of the molecule and the channel size of the zeolite
ν	vibrational frequency of the solid lattice
ν_e	effect vibrational frequency of molecule inside zeolite
ν_{rc}	vibrational frequency along the reaction coordinate
ρ_i	mass concentration of species i (i=A,B)
σ_c	pairwise Lennard-Jones length constant for each molecule-oxygen at the channel
σ_i	pairwise Lennard-Jones length constant for each molecule-oxygen at the intersection/cage
σ_m	Lennard-Jones length constant for molecule
σ_o	van der Waals diameter ($=2^{1/2}\sigma_m$)
τ	tortuosity
Φ_c	potential at the channel
Φ_i	potential at the intersection/cage
Φ_{i1}	potential at the intersection/cage for one molecule
Φ_{i2}	potential at the intersection/cage for two molecule

Φ_{max}	maximum potential of potential field
Φ_{min}	minimum potential of potential field
ω_i	mass fraction of species i (=A,B) in a mixture of A and B

REFERENCES

Argauer, R. J., and G. R. Landolt, "Crystalline Zeolite ZSM-5 and Method of Preparing the Same", U.S. Patent 3702886, (1972).

Aronson, M. T., R. J. Gorte, and W. E. Farneth, " An infrared Spectroscopy Study of Simple Alcohols Adsorbed on ZSM-5", J. Catal., 105, 455 (1987).

Ash, R., and R. M. Barrer, "Mechanism of Surface Flow", Surface Science, 8, 461 (1967).

Aust, E., K. Dahlke, and G. Emig, "Simulation of Transport and Self-Diffusion in Zeolites with the Monte Carlo Method", J. Catal., 115, 86 (1989).

Barrer, R. M., "Migration in Crystal Lattices", Trans. Faraday Soc., 37, 590 (1941).

Barrer, R. M., and D. A. Ibbitson, "Kinetics of Formation of Zeolitic Solid Solutions", Trans. Faraday Soc., 40, 206 (1944).

Barrer, R. M., and D. W. Riley, "Sorptive and Molecular-sieve Properties of a New Zeolitic Mineral", J. Chem. Soc., 133 (1948).

Barrer, R. M., and W. Jost, " A Note on Interstitial Diffusion", Trans. Faraday. Soc. 45, 928 (1949).

Barrer, R. M., and D. W. Brook, "Molecular Diffusion in Chabazite, Mordenite and Levynite", Trans. Faraday Soc., 49, 1049 (1953).

Barrer, R. M., and B. E. F. Fender, "The Diffusion and Sorption of Water in Zeolites - II. Intrinsic and Self-Diffusion', J. Phys. Chem. Solids, 21, 12 (1961).

Barrer, R. M., and J. A. Davies, "Sorption in Decationated Zeolites II. Simple Paraffins in H-forms of Chabazite and Zeolite L", Proc. Roy. Soc. London. A., 332, 1 (1971).

Barrer, R. M. and D. J. Clarke, "Diffusion of Some n-Paraffins in Zeolite A", J.C.S. Faraday Trans. I, 70, 535 (1974).

Barrer, R. M., Zeolite and Clay Minerals as Sorbents and Molecular Sieves, Academic Press (1978).

Barrow, G. M., Physical Chemistry, 3rd Ed., McGraw-Hill, (1973).

Benson, S. W., Thermochemical Kinetics, 2nd Ed., John Wiley & Sons, (1976)

Bird, R. B., W. E. Stewart, and E. N. Lightfoot, Transport Phenomena, John Wiley & Son, (1960).

Breck, D. W., W. R. Eversole, R. M. Milton, T. B. Reed, T. L. Thomas, "Crystalline Zeolites. I. The Properties of a New Synthetic Zeolite, Type A", J. Amer. Chem. Soc., 78, 5963 (1956).

Breck, D. W., US Patent 3,130,007 (1964).

Breck, D. W., Zeolite Molecular Sieves, John Wiley & Sons, New York (1974).

Bülow, M., P. Struve, G. Finger, C. Redszus, K. Ehrhardt, W. Schirmer and J. Kärger, "Sorption Kinetics of n-Hexane on MgA Zeolites of Different Crystal Sizes", J.C.S. Faraday I, 76, 597 (1980).

Bülow, M., P. Struve, and S. Pikus, "Influence of Hydrothermal Pretreatment on Zeolitic Diffusivity Detected by Comparative Sorption Kinetics and Small-

Angle X-ray Scattering Investigations", Zeolites, 2, 267 (1982).

Bülow, M., H. Schlodder, L. V. C. Rees, and R. E. Richards, "Molecular Mobility of Hydrocarbon ZSM-5/Silicalite Systems Studied by Sorption Uptake and Frequency Response Methods", Proc. of the Seventh International Zeolite Conference, Y. Murakami, A. Iijima, and J. W. Ward, editors, Elsevier, p579 (1986).

Casimir, H. B. G., " On Onsager's Principle of Microscopic Reversibility", Rev. Mod. Physics, 17, 343 (1945).

Chen, N. Y., and P. B. Weisz, "Molecular Engineering of Shape-Selective Catalysts", Chem. Eng. Prog. Symp. Ser., No. 73, Vol. 63, p86 (1967).

Chen, N. Y., and W. E. Garwood, "Industrial Application of Shape-Selective Catalysis", Catal. Rev. - Sci. Eng., 28(2&3), 185 (1986)

Chen, N. Y., and T. F. Degnan, "Industrial Catalytic Applications of Zeolites", Chem. Eng Prog., 84 (2), 32 (1988).

Chon, H., and D. H. Park, "Diffusion of Cyclohexanes in ZSM-5 Zeolites", J. Catal., 114, 1 (1988).

Choudhary, V. R., and K. R. Srinivasan, "Desorptive Diffusion of Benzene in H-ZSM-5 under Catalytic Conditions Using Dynamic Sorption/Desorption Technique", J. Catalysis, 102, 316 (1986).

Choudhary, V. R., and D. B. Akolekar, "Shuttlecock-Shuttlebox Model for Shape Selectivity of Medium-Pore Zeolites in Sorption and Diffusion", J. Catal., 117, 542 (1989).

Cohen De Lara, E., and R. Kahn, "Experimental and Theoretical Analysis of the Adsorption of Methane in A Zeolites. Infrared and Neutron Spectroscopy Studies", Proc. of Sixth Intern. Zeolite Conf., 172, Ed. David Olson and Attilio Bisio, Butterworth (1984).

Davis, M. E., C. Saldarriaga, C. Montes, J. Garces, and C. Crowder, "VPI-5: A Novel Large Pore Molecular Sieve", in Microstructure and Properties of Catalysts, M. M. J. Treacy, J. M. Thomas, and J. M. White, eds., 276, (1988).

Derouane, E. G., "Shape Selectivity in Catalysis by Zeolites: The Nest Effect", J. Catal., 100, 541 (1986).

Derouane, E. G., J. B. Nagy, C. Fernandez, Z. Gabelica, E. Laurent, and P. Maljean, "Diffusion of Alkanes in Molecular Sieves", Applied Catalysis, 40, L1 (1988).

Doelle, H. -J., J. Heering, and L. Riekert, "Sorption and Catalytic Reaction in Pentasil Zeolites. Influence of Preparation and Crystal Size on Equilibria and Kinetics", J. Catal., 71, 27 (1981).

Doetsch, I. H., D. M. Ruthven, and K. F. Loughlin, "Sorption and Diffusion of n-Heptane in 5A Zeolite", Can. J. Chem., 52, 2717 (1974).

Eagan, J. D., and R. B. Anderson, " Kinetics and Equilibrium of Adsorption on 4A Zeolite", J. Coll. I. S., 50(3), 419 (1975).

Eckman, R. R., and A. J. Vega, "Deuterium Solid-State NMR Study of the Dynamics of Molecules Sorbed by Zeolites", J. Phys. Chem., 90, 4679, (1986).

Egelstaff, P. A., J. S. Downes, and J. W. White, in "Molecular Sieves", Soc. Chem. Ind., London, p306 (1968).

Flanigen, E. M., J. M. Bennet, R. W. Grose, J. P. Cohen, R. L. Patton, and R. M. Kirchner, "Silicalite, a New Hydrophobic Crystalline Silica Molecular Sieve", Nature, 271, 512 (1978).

Flanigen, E. M., "Molecular Sieve Zeolite Technology: the First Twenty-Five Years", NATO ASI Ser., 80, 3 (1984).

Flanigen, E. M., B. M. Lok, R. L. Patton, and S. T. Wilson, "Aluminophosphate Molecular Sieves and the Periodic Table", in Proc. of 7th International Zeolite Conf., Y. Murakami, A. Iijima, and J. Ward, eds. 103, Elsevier, Amsterdam (1986).

Flanigen, E. M., R. L. Patton, and S. T. Wilson, "Structural, Synthetic and Physicochemical Concepts in Aluminophosphate-Based Molecular Sieves", Stud. Surf. Sci. Cat., 37, 13 (1988).

Fowler, R. H., and E. A. Guggenheim, Statistical Thermodynamics, Cambridge, (1960).

Fraissard, J., "NMR Study of ^{129}Xe Adsorbed on Zeolites and Metal-Zeolites", Zeitschrift für Physikalische Chemie Neue Folge, 152, S. 159 (1987).

Garcia, S. F., and P. Weisz, "Effective Diffusivities in Zeolites", J. Catal., 121, 294 (1990).

Girigalco, L. A., Statistical Physics of Materials, John Wiley & Sons (1973).

Gorring, R. L., "Diffusion of Normal Paraffins in Zeolite T: Occurrence of Window Effect", J. Catalysis, 31, 13 (1973).

de Groot, S. R., and P. Mazer, Nonequilibrium Thermodynamics, North-Holland

(1969).

Guo, C., O. Talu, and D. T. Hayhurst, "Phase Transition and Structural Heterogeneity; Benzene Adsorption on Silicalite", AIChE J., 35(4), 573 (1989).

Haag, W. O., R. M. Lago, and P. B. Weisz, "Transport and Reactivity of Hydrocarbon Molecules in a Shape-selective Zeolite", Faraday Discussion of the Chem. Soc., 72, 317 (1981).

Habgood, H. W., " The Kinetics of Molecular Sieve Action. Sorption of Nitrogen-Methane Mixtures by Linde Molecular Sieve 4A", Can. J. Chem., 36, 1384 (1958).

Hayhurst, D. T., and A. R. Paravar, "Diffusion of C_1 to C_5 Normal Paraffins in Silicalite", Zeolites, 8, 27 (1988).

Haynes, H. W., "THe Experimental Evaluation of Catalyst Effective Diffusivity", Catal. Rev. - Sci. Eng., 30(4), 563 (1988).

Hill, T. L., An Introduction to Statistical Thermodynamics", Addison-Welsley, (1960).

Hirschfelder, J. O., C. F. Curtiss, and R. B. Bird, Molecular Theory of Gases and Liquids, John Wiley & Sons, (1954).

Hoel, G. P., C. S. Port, and J. C. Stone, Intro. to Stochastic Processes, Houghton Mifflin (1972).

June, R. L., A. T. Bell, and D. N. Theodorou, "Prediction of Sorption and Diffusion in Zeolite Catalysts", presented at the Annual Meeting of the AIChE, Washington, D. C., (1988).

Kärger, J., "Some Remarks on the Straight and Cross-Coefficients in Irreversible Thermodynamics of Surface Flow and on the Relation Between Diffusion and Self-Diffusion", Surface Science, 36, 797 (1973).

Kärger, J., and M. Bülow, " Theoretical Prediction of Uptake Behaviour in Adsorption Kinetics of Binary Gas Mixtures Using Irreversible Thermodynamics", Chem. Eng. Sci., 30, 893 (1975).

Kärger, J., "On the Correlation between Diffusion and Self-Diffusion Processes of Adsorbed Molecules in a Simple Microkinetic Model", Surface Science, 59, 749 (1976).

Kärger, J., H. Pfeifer, and R. Haberlandt, "Application of Absolute Rate Theory to Intracrystalline Diffusion in Zeolites", J.C.S. Faraday I, 76, 1569 (1980).

Kärger, J., and H. Pfeifer, " N.m.r. Self-Diffusion Studies in Zeolite Science and Technology", Zeolites, 7, 90 (1987).

Kärger, J., and D. M. Ruthven, "On the Comparison Between Macroscopic and N.M.R. Measurements of Intracrystalline Diffusion in Zeolites", Zeolites, 9, 267 (1989).

Kirkaldy, J. S., and D. J. Young, Diffusion in the Condensed State, the Institute of Metal (1987).

Kiselev, A. V., and P. Q. Du, "Molecular Statistical Calculation of the Thermodynamic Adsorption Characteristics of Zeolites Using the Atom-Atom Approximation", J. C. S. Faraday Trans. II, 77, 1 & 17 (1981).

Kittle, C., Introduction to Solid State Physics, 5th Ed., John Wiley & Sons (1976).

Kokotailo, G. T., S. L. Lawton, D. H. Olson, and W. M. Meier, "Structure of Synthetic Zeolite ZSM-5", Nature, 272, 437 (1978).

Kustanovich, I., D. Fraenkel, Z. Luz, S. Vega, and H. Zimmermann, "Dynamic Properties of p-Xylene Adsorbed on Na-ZSM-5 Zeolite by Deuterium and Proton Magic-Angle Sample Spinning NMR', J. Phys. Chem, 92, 4134 (1988).

Kutner, R., "Chemical Diffusion in the Lattice Gas of Non-Interacting Particles", Physics Letter, 81A (4), 239 (1981).

Mentzen, B. F., "Characterization of Guest Molecules Adsorbed on Zeolites of Known Structure by Combined X-Ray Powder Profile Refinements and Conventional Difference-Fourier Techniques. Part I - Localization of the Benzene Molecule in A Pentasil Type Zeolite", Mat. Res. Bull., 22, 337 (1987a).

Mentzen, B. F., "Characterization of Guest Molecules Adsorbed on Zeolites of Known Structure by Combined X-Ray Powder Profile Refinements and Conventional Difference-Fourier Techniques. Part II - Localization of the N-Hexane, TPA, and P-Xylene Guests in A Pentasil Type Zeolite", Mat. Res. Bull, 22, 489 (1987b)

Mentzen, B. F., and F. Vigne-Maeder, "Caracterisation et Localisation de la Molecules de Para-Xylene dans une Zeolithe Pentasil: Cas des Complexes Formes par deux Boralites avec le Para-Xylene", Mat. Res. Bull., 22, 309 (1987c).

Mentzen, B. F., and F. Bosselet, "Characterization of Guest Molecules Adsorbed on Zeolites of Known Structure. Part III - Localization of the p-XYLI and p-XYLII Species Sorbed in A High Coverage B.ZSM-5/p-Xylene Complex", Mat. Res. Bull., 23, 227 (1988).

Milton, R. M., US Patent 2,882,244 (1959).

Nagy, J. B., E., G. Derouane, H. A. Resing, and G. R. Miller, "Motions of o- and p-Xylenes in ZSM-5 Catalyst. Carbon-13 Nuclear Magnetic Resonance", J. Phys. Chem. 87, 833 (1983).

Nayak, V. S., and L. Riekert, "Factors Influencing Sorption and Diffusion in Pentasil Zeolites", in Proc. of International Symp. on Zeolite Catalysis, Siofok, Hungary, 157 (1985).

Nowak, A. K., A. K. Cheetham, and S. D. Pickett, "A Computer Simulation of the Adsorption and Diffusion of Benzene and Toluene in Zeolites Theta-1 and Silicalite", Molecular Simulation, 1, 67 (1987).

Olson, D. H., G. T. Kokotailo, S. L. Lawton, and W. M. Meier, "Crystal Structure and Structure Related Properties of ZSM-5", J. Phys. Chem, 85, 2238 (1981).

Onsager, L., "Reciprocal Relations in Irreversible Process. I. & II.", Phys. Review, 37, 405 & 38, 2265 (1931).

Palekar, M. G., and R. A. Rajadhyaksha, "Sorption Accompanied by Chemical Reaction in Zeolite", Frontiers in Chemical Engineering Science, L. K. Doraiswamy and R. A. Mashelkar, ed., Wiley, New Delhi, 142 (1984).

Palekar, M. G., and R. A. Rajadhyaksha, "Sorption in Zeolites - I. Sorption of Single Component and Binary Sorbate Systems", Chem. Eng. Sci., 40, 1085(1985a).

Palekar, M. G., and R. A. Rajadhyaksha, "Sorption in Zeolites - II. Tracer Diffusion", Chem. Eng. Sci., 40, 663(1985b).

Palekar, M. G., and R. A. Rajadhyaksha, "Sorption in Zeolites - III. Binary

Adsorption", Chem. Eng. Sic., 41, 463 (1986a).

Palekar, M. G., and R. A. Rajadhyaksha, "Sorption Accompanied by Chemical Reaction on Zeolites", Catal. Rev. -Sci. Eng., 28, 371 (1986b).

Pope, C. G., "Sorption of Benzene, Toluene, and p-Xylene on ZSM-5", J. Phys. Chem., 88, 6312 (1984).

Post, M. F. M., J. van Amstel, and H. W. Kouwenhoven, "Diffusion and Catalytic Reaction of 2,2-Dimethylbutane in ZSM-5 Zeolite", in Proc. of the Sixth International Zeolite Conf., Edited by David Olson and Attilio Bisio, Butterworths, U. K., p517 (1984).

Prigogine, I., Introduction to Thermodynamics of Irreversible Processes, Wiley, NY (1967).

Prinz, D., and L. Riekert, "Observation of Rates of Sorption and Diffusion in Zeolite Crystals at Constant Temperature and Pressure", Ber. Bunsenges. Phys. Chem., 90, 413 (1986).

Quig, A., and L. V. Rees, "Self-Diffusion of n-Alkanes in Type A Zeolite", J.C.S. Faraday Trans. I, 72, 771 (1976).

Qureshi, W. R., and J. Wei, "Counter- and Co-Diffusion in Zeolite ZSM-5: An Experimental and Theoretical Study", AIChE Annual Meeting, paper No. 35b, Washington, DC (1988).

Qureshi, W. R., "The Mechanism of Diffusion in Zeolite ZSM-5: An Experimental and Theoretical Study of Counter-Diffusion and Co-Diffusion", Ph.D Thesis, Dept. of Chem. Eng., MIT (1989).

Ramdas, S., J. M. Thomas, P. W. Betteridge, A. K. Cheetham, E. K. Davis, " Modelling the Chemistry of Zeolites by Computer Graphics", Angew. Chem. Inte. Ed. Engl., 23, 671 (1984).

Reid, R., J. M. Prausnitz, T. K. Sherwood, The Properties of Gases and Liquids, McGraw-Hill (1977).

Richards, R. E., and L. V. C. Rees, "Sorption and Packing of n-Alkane Molecules in ZSM-5", Langmuir, 3, 335 (1987).

Riekert, L., "Sorption, Diffusion, and Catalytic Reaction in Zeolites", Adv. in Cataly., 21, 281 (1970)

Ross, J, and P. Mazur, "Some Deductions from a Formal Statistical Mechanical Theory of Chemical Kinetics", J. Chem. Phys., 35(1), 19 (1961).

Ruthven, D. M., K. F. Loughlin, "Correlation and Interpretation of Zeolitic Diffusion Coefficients", Faraday Soc. Trans., 67, 1661 (1971)a.

Ruthven, D. M., and K. F. Loughlin, "The Sorption and Diffusion of n-Butane in Linde 5A Molecular Sieve", Chem. Eng. Sci., 26, 1145 (1971)b.

Ruthven, D. M., and R. I. Derrah, "Transition State Theory of Zeolitic Diffusion: Diffusion of CH_4 and CF_4 in 5A Zeolite", J. C. S. Faraday I, 68, 2332 (1972).

Ruthven, D. M., R. I. Derrah, and K. F. Loughlin, "Diffusion of Light Hydrocarbons in 5A Zeolite", Can. J. Chem., 51, 2514 (1973)a.

Ruthven, D. M., K. F. Loughlin, and R. I. Derrah, "Sorption and Diffusion of Light Hydrocarbons and Other Simple Nonpolar Molecules in Type A Zeolites", Adv. Chem. Ser., 121, 330 (1973)b.

Ruthven, D. M., and R. I. Derrah, " Diffusion of Monatomic and Diatomic Gases in 4A and 5A Zeolites", J.C.S. Faraday Trans. I, 71, 2031 (1975)a.

Ruthven, D. M., and R. I. Derrah, "A Comparative Study of the Diffusion of C_2H_6, C_2H_4 and nC_5H_{12} in Erionite and in Type A Zeolite", J. Coll. I. S., 52(2), 379 (1975)b.

Ruthven, D. M., and I. H. Doetsch, "Diffusion of SF_6 in 13X Zeolite", J.C.S. Faraday I, 72, 1043 (1976)a.

Ruthven, D. M., and I. H. Doetsch, "Diffusion of Hydrocarbons in 13X Zeolite", AIChE J., 22(5), 882 (1976)b.

Ruthven, D. M., L. Lee, and H. Yucel, "Kinetics of Non-Isothermal Sorption in Molecular Sieve Crystals", AIChE J., 26, 16 (1980).

Ruthven, D. M., and L. Lee, "Kinetics of Nonisothermal Sorption: Systems with Bed Diffusion Control", AIChE J., 27, 654 (1981).

Ruthven, D. M., A. Vavlitis, and K. Loughlin, "Diffusion of n-Decane in 5A Zeolite Crystals", AIChE J., 28(5), 840 (1982).

Ruthven, D.M., Principles of Adsorption and Adsorption Processes, John Wiley and Sons (1984).

Satterfield, C. N., and J. R. Katzer, "Counterdiffusion of Liquid Hydrocarbons in Type Y Zeolites", Adv. in Chem. Ser., 102, 193 (1971).

Satterfield, C. N., and C. S. Cheng, "Liquid Counterdiffusion of Selected Aromatic and Naphthetic Hydrocarbons in Type Y Zeolites", AIChE J, 34, 1713 (1972).

Satterfield, C. N., Heterogeneous Catalysis in Practice, McGraw-Hill (1980).

Shah, d. B., D. T. Hayhurst, G. Evanina, and C. J. Guo, "Sorption and Diffusion of Benzene in HZSM-5 and Silicalite Crystals", AIChE J., 34, 1713 (1988).

Stach, H., H. Tham, J. Jänchen, K. Fiedler and W. Schirmer, "Experimental and Theoretical Investigations of the Adsorption of n-Paraffins, n-Olefins and Aromatics on Silicalite", Proc. of the Sixth International Zeolite Confe., Edited by D. Olson and A. Bisio, 225, Butterworths (1984).

Thamm, H., "Adsorption Site Heterogeneity in Silicalite: A Calorimetric Study", Zeolites, 7, 341 (1987).

Theodorou, D., and J. Wei, "Diffusion and Reaction in Blocked and High Occupancy Zeolite Catalysts", J. Catal, 83, 205 (1983).

Tsikoyiannis, J. G., "On the Equilibrium Sorption and Diffusion of Aromatic Hydrocarbons in ZSM-5 Catalysts: Experimental and Theoretical Considerations", Ph.D Thesis, Dept. of Chem. Eng., MIT (1986).

Vaughan, D. E. W., "The Synthesis and Manufacture of Zeolites", Chem. Eng. Prog. 84(2), 25 (1988).

Vavlitis, A. P., D. M. Ruthven, K. F. Loughlin, "Sorption of n-Pentane, n-Octane, and n-Decane in 5A Zeolite Crystals", J. Coll. I. S., 84(2), 526 (1981).

Vedrine, J. C., "Zeolite Chemistry in Catalysis", ACS Symp. Ser., 279, 257 (1985).

Walker, P. L., L. G. Austin, and S. P. Nandi, "Activated Diffusion of Gases in Molecular-Sieve Materials", in Chemistry & Physics of Carbons, P. L. Walker, Ed., Marcel Dekker Inc. NY (1966).

Wei, J., "A Mathematical Theory of Enhanced para-Xylene Selectivity in Molecular Sieve Catalysts", J. Catal., 76, 433 (1982).

Weisz, P. B., and V. J. Frilette, "Intracrystalline and Molecular-Shape-Selective Catalysis by Zeolite Salts", J. Phy. Chem., 64, 382 (1960).

Weisz, P. B., "Zeolites -- New Horizons in Catalysis", CHEMTECH, 3, 498 (1973).

Wu, P., A. Debebe, and Y. H. Ma, "Adsorption and Diffusion of C_6 and C_8 Hydrocarbons in Silicalite", Zeolites, 3, 118 (1983).

Wu, P., and Y. H. Ma, "The Effect of Cation on Adsorption and Diffusion in ZSM-5", in Proc. of Sixth International Zeolite Conf., Butterworths, U.K., p251 (1984).

Xiao, J., and J. Wei, "Diffusion Mechanism of Hydrocarbons in Zeolite ZSM-5", AIChE Annual Meeting, No. 53g, San Francisco (1989).

Xiao, J., and J. Wei, "Diffusion Mechanism of Hydrocarbons in Zeolites: I. Theory; II. Experiments and Discussions", to be submitted to J. Catal, (1990)

Zikanova, A., M. Bülow, and H. Schlodder, "Intracrystalline Diffusion of Benzene in ZSM-5 and Silicalite", Zeolites, 7, 115 (1987).